

Boiling Heat Transfer Phenomena  
During Rapid Decompression

by

Shin-Ping Kung

B.S. National Tsing Hua University, 1972

---

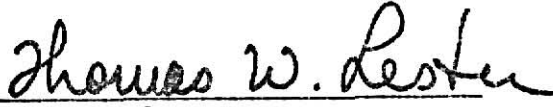
A MASTER'S THESIS

submitted in partial fulfillment of the  
requirement for the degree

Department of Nuclear Engineering  
Kansas State University  
Manhattan, Kansas 66506

1977

Approved by:

  
Major Professor

Docu-  
ment  
LD  
2668  
T4  
1977  
K85  
C.2

TABLE OF CONTENTS

109

	Page
NOMENCLATURE . . . . .	iii
LIST OF FIGURES . . . . .	vi
LIST OF TABLES . . . . .	vii
I. INTRODUCTION . . . . .	1
II. LITERATURE REVIEW . . . . .	4
A. The Mechanism and Current Theories of Steady-State Pool Boiling . . . . .	4
B. Steady-State Pool Boiling Critical Heat Flux (CHF) . . .	8
C. Boiling Heat Transfer in Transients . . . . .	17
1. Boiling Heat Transfer in Power Transients . . . . .	17
2. Boiling Heat Transfer in Pressure Transients . . . . .	21
III. EXPERIMENTAL EQUIPMENT AND PROCEDURES . . . . .	29
A. Experimental Equipment . . . . .	29
1. Test Assembly . . . . .	29
2. Electrical Circuit . . . . .	31
B. Experimental Procedures . . . . .	33
1. Steady-State Experiments . . . . .	33
2. Transient Experiments . . . . .	34
IV. RESULTS AND DISCUSSION . . . . .	36
A. Steady-State Experiments . . . . .	36
1. The Interpretation of Steady-State Experimental Data . . . . .	37
2. Discussion of Steady-State Results . . . . .	39
B. Boiling Heat Transfer During and Shortly After the Pressure Transient . . . . .	41
1. The Interpretation of Transient Experimental Data .	41
2. Discussion of the Results of Pressure Transient Experiments . . . . .	46
i. Subcooled Cases . . . . .	46
ii. Superheated Cases . . . . .	53
iii. Conclusions of Transient Experiments . . . . .	57
C. Suggestions for Future Research . . . . .	58

REFERENCES . . . . .	60
APPENDICES . . . . .	65
APPENDIX A -- Computer Program for Processing Steady-State Experimental Data . . . . .	66
APPENDIX B -- Computer Program for Processing Transient Experimental Data and Results . . . . .	99

# NOMENCLATURE

$A_L$	Area of liquid column
$A_T$	Total area of heat transfer surface
$A_v$	Area of vapor column
$c$	Wave velocity
CHF	Critical heat flux
$C_p$	Heat capacity at constant pressure
$D_{jet}$	Diameter of vapor jet flow
$f$	Frequency of bubble release from heater surface
$g$	Gravitational acceleration
$g_0$	Universal gravitation constant
$\bar{h}_1$	Convection heat transfer coefficient
$h_L$	Enthalpy per unit mass of saturated liquid
$h_v$	Enthalpy per unit mass of saturated vapor
$h_{Lv}$	$h_v - h_L$ or the latent heat of liquid
$I$	Electric current through heater element
$k_u$	Kutateladze empirical constant
$k$	Thermal conductivity
$M$	Molecular weight
$N$	Number of active nucleation sites on bubbling surface
$P_L$	Liquid pressure
$P_r$	Prandtl number
$\dot{Q}$	Heat generation rate per unit volume
$(Q/A)_b$	Heat flux from boiling
$(Q/A)_{CHF}$	Critical heat flux
$(Q/A)_{CHF,k}$	Critical heat flux after Kutateladze
$(Q/A)_{cond}$	Heat flux from conduction



$(Q/A)_{nc}$	Heat flux from natural convection
$(Q/A)_{op}$	Operating heat flux
$(Q/A)_{Total}$	Total heat flux
$R$	Universal gas constant
$R_b$	Bubble departure radius
$R_o$	Electrical resistance of heating wire at 0°C
$R_s$	Resistance of precise shunt resistor
$R_{sys}$	Resistance of heater element and connections
$R_{th}$	Theoretical resistance of the test wire
$R_w$	Resistance of the test wire
$r$	Radius of active site on heating surface
$r_b$	Bubble radius
$r_s$	The radius for which N would be one per unit area of heating surface
$T_L$	Liquid temperature
$T_s$	Saturation temperature
$T_v$	Vapor temperature
$T_w$	Heater element temperature
$V_L$	Liquid Velocity
$V_{ME}$	Average volume of microlayer evaporated
$V_P$	Voltage of the battery
$V_v$	Vapor velocity
$V_w$	Voltage across heater element and connections
$V_{pressure}$	Transient voltage signal from the pressure transducer
$\alpha$	Thermal diffusivity
$\beta$	Three phase contact angle in Table 1.
$\delta$	Bubble thermal boundary layer thickness

$\epsilon$	Accommodation coefficient, dimensionless
$\eta$	Wave amplitude
$\lambda$	Wave length
$\nu$	Viscosity
$\rho_L$	Liquid density
$\rho_v$	Vapor density
$\sigma$	Surface tension between liquid and its vapor

## LIST OF FIGURES

Figure	Page
1. A Typical Pool Boiling Curve . . . . .	5
2. Correlation of Critical Heat Flux in Pool Boiling. [After Zuber (56).] . . .	10
3. Effect of Power Transient on CHF. [After Tachibana (50).] . . . . .	19
4. Typical Temperature - Time Record for Platinum Ribbon in Sub-Cooled Water, during Power Transient. [After Rosenthal and Miller (47).] . . .	22
5. Ribbon Temperature Behavior during Transient Boiling in Decompression. [After Howell and Bell (23).] . . . . .	24
6. Relation Between Transient Events and the Pressure. [After Howell and Bell (23).] . . . . .	24
7. Ribbon Temperature Behavior during Transient Boiling in Rapid Decompression from Atmospheric Pressure. [After Aoki, et al. (3).] . .	26
8. Schematic Diagram of the Experimental Apparatus. . . . .	30
9. Circuitry for Steady-State and Transient Measurements. . . . .	32
10. Steady-State Boiling Curve at Atmospheric Pressure in a Saturated Pool of Water. . . . .	40
11. Steady-State CHF at Sub-Atmospheric Pressures. . . . .	42
12. Typical Pressure Transient Data. . . . .	45
13. Typical Sub-Cooled Data at Low Heat Flux. . . . .	48
14. Typical Sub-Cooled Data at Medium Heat Flux. . . . .	48
15. Typical Sub-Cooled Data at Medium Heat Flux. . . . .	49
16. Typical Sub-Cooled Data at High Heat Flux. . . . .	49
17. Typical Superheated Data at Low Heat Flux. . . . .	54
18. Typical Superheated Data at Medium Heat Flux. . . . .	54
19. Typical Superheated Data at High Heat Flux. . . . .	55
20. Typical Superheated Data at High Heat Flux. . . . .	55

## LIST OF TABLES

	Page
1. The Equations for the Prediction of the Steady-State Nucleate Boiling and Critical Heat Flux (CHF). . . . .	11
2. Summary of the Test Conditions of the Transient Experiments. . .	43
3. Summary of the Experimental Conditions and Oscilloscope Parameters for Figures 12-20. . . . .	47

## I. INTRODUCTION

New developments in engineering applications often require that heat be transferred under not only steady-state, but also transient conditions. For example, during the operation of light water nuclear reactors, heat generated in the fuel rods is increased exponentially as the reactor is started up or is required to change power levels within a short time. If the period is significantly shorter than that at which the coolant can transfer all the heat generated in the fuel rods, the fuel rod cladding may be exposed, for short periods, to nucleate or to film boiling and rapid temperature fluctuations. Rapid decompressions are potentially more serious. If a reactor primary coolant pipe ruptures, the high pressure inside the reactor vessel will be released to the atmosphere in seconds. The coolant becomes superheated rapidly which in turn induces flashing throughout the reactor core and alters the local heat transfer mechanisms. An accurate knowledge of the boiling behavior during pressure transients of varying periods is, therefore, necessary for the designer to estimate the worst possible heat transfer during normal operation or abnormal occurrences.

Boiling heat transfer has been studied comprehensively for several decades. The majority of previous analyses and experiments have been concerned with steady-state, pool boiling. Most conventional applications of boiling processes involve steady-state phenomena, in which the liquids are at a certain pressure and only slow, incremental changes in heat flux are encountered. As a result of this extensive research, there are numerous equations, either experimentally or theoretically derived, available for the prediction of steady-state nucleate boiling heat fluxes and critical heat fluxes under various thermodynamic conditions and with different solid/liquid combinations.

Boiling heat transfer during both power and pressure transients has been studied more recently. Most effort has been devoted to power transients because of their more frequent occurrence in light water reactors. Empirical correlations have been developed which predict the transition from nucleate to film boiling as a function of transient power period, initial heat flux, and thermodynamic conditions. Pressure transients, on the other hand, have been studied only recently because of the increasing concern about the Loss of Coolant Accident (LOCA). However, no systematic study has been performed.

Power transient studies to date have reported that if the transient time constant is longer than about 100 milliseconds, the peak heat flux during the transient can be predicted adequately by steady-state conditions. If, however, the time constant is shorter than 20 milliseconds, the heat flux during the transient may reach a higher value than that predicted by steady-state correlations before the boiling transits from nucleate to film boiling. It has been observed that even under a step increase in power, nucleate boiling always precedes the transition to film boiling. Pressure transients have been much less thoroughly studied. Investigations in rod bundles have been performed more to provide design information rather than fundamental knowledge. In view of the few studies of relatively slow pressure transients, it has been suggested that the critical heat flux can be predicted with no significant errors by steady-state correlations. But the results of recent and more basic research into the heat flux and transient bubble growth indicate that the heat transfer mechanisms may be quite different. Because of the paucity of data on this topic, no solid conclusions have been made about the actual effects of pressure transients on boiling heat transfer.

Accordingly, as a first step in a comprehensive research program the effect of very rapid pressure transients on boiling heat transfer has been studied. The effects of two parameters, temperature of bulk liquid and initial heat flux level, on the temporal variation of heat flux and wire temperature are investigated during the depressurization of water from 760 to 420 torr in approximately 10 milliseconds. The review of pertinent literature, design of experiments, and experimental results are discussed in turn in the following sections.

## II. LITERATURE REVIEW

In this section, steady-state boiling will be discussed briefly and applicable Critical Heat Flux correlations will be reviewed. Subsequently, critical heat flux during power transients and decompressions will be covered.

### A. The Mechanism and Current Theories of Steady-State Pool Boiling

Steady-state boiling heat transfer studies have shown conclusively that different levels of wall superheat, the wall temperature excess above the saturation temperature, result in very different heat transfer phenomena, which are fundamental to the understanding of the boiling mechanism. The existence of several regimes of boiling was first clearly discussed by Nukiyama (41) in 1934 and followed by many papers. A typical steady-state boiling curve is shown in Fig. 1. The entire curve is generally divided into four regions: free convection, nucleate boiling, transition, and stable film boiling regions followed by film boiling with radiation augmentation. Nucleate boiling is characterized by the formation, growth, and detachment of vapor bubbles in the liquid near the heater surface. It results in a sharp increase in heat flux, but only a moderate increase in surface temperature. At low values of wall superheat, bubbles are far apart and are nearly independent of one another. As the superheat increases, more nucleation sites appear and bubbles form more rapidly. At high superheats, no discrete bubbles can be seen as they interfere with one another and unite to form bigger vapor patches. As point B is approached, a further increase in wall superheat will cause the heat flux to decrease since all heat must be transferred through a vapor layer. This is called transition boiling.



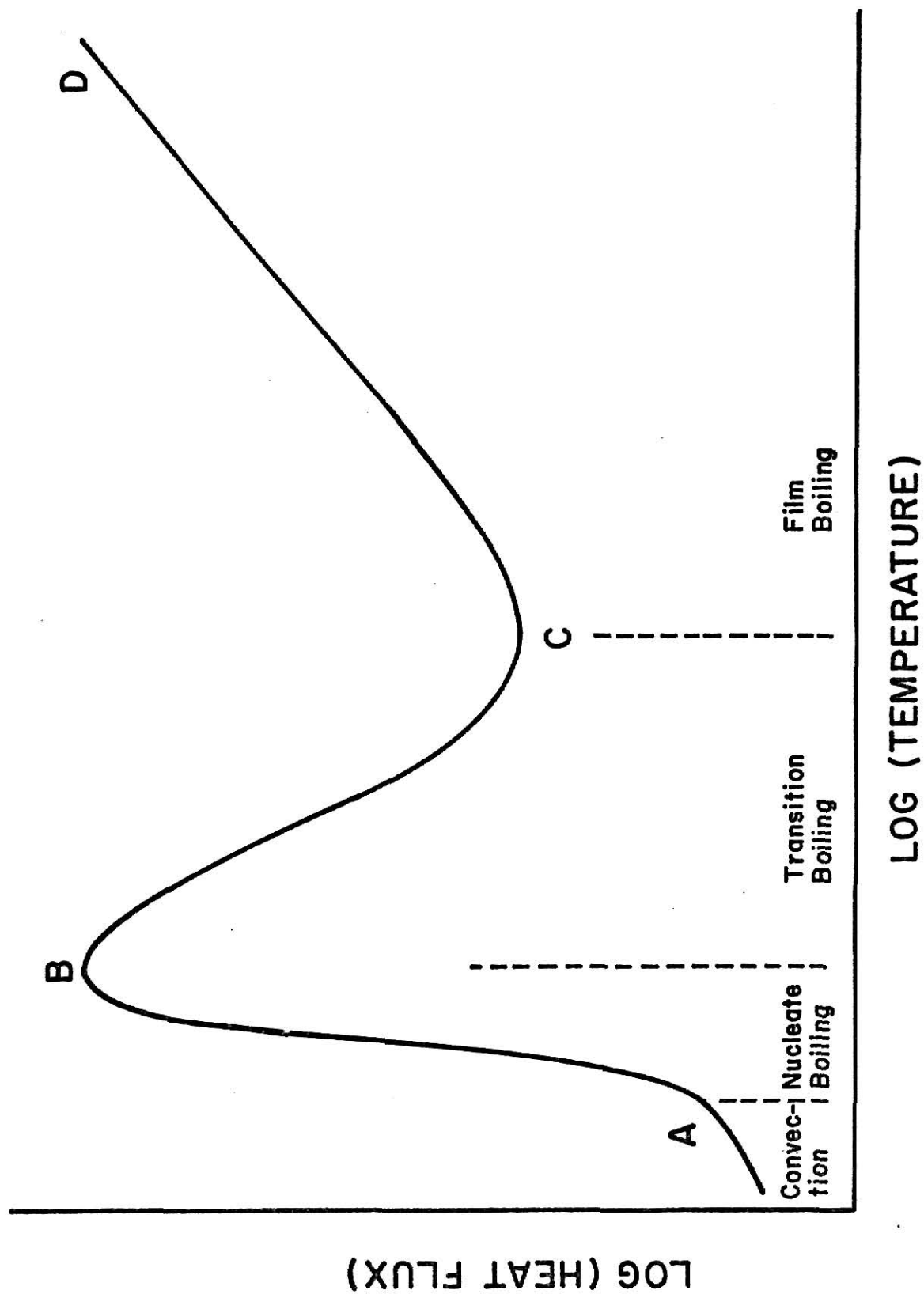


Fig. 1. A Typical Pool Boiling Curve.

Heat transfer during this region is unstable. Part of the surface is covered by vapor film, the rest is still undergoing stable nucleate boiling until the superheat is increased high enough to cause the coalesced bubbles to form a layer of vapor film covering the entire surface. This is called film boiling. The critical point B is known widely as DNB - departure from nucleate boiling, or the burnout point. Hereafter, this point will be referred to as the boiling transition and the heat flux at this point as the CHF - critical heat flux - as used most commonly in recent literature.

There are several plausible physical explanations for the high rate of heat transfer in nucleate boiling. Earlier researchers tended to focus on the agitation induced by the bubble formations on the heater surface. For example, Rohsenow and Clark (45) proposed that the bubbles behave as agitation agents which increase the heat transfer. This proposal has been studied by Robinson and Katz (43), by Grose et al. (19), and by Mixon et al. (38). These experiments showed that the bubble agitation does increase the heat transfer, but the heat fluxes in these studies were in the lower range of nucleate boiling. Other mechanisms which are not substantially different from the above include that of the "bubble action," whereby the bubbles are assumed to push the superheated liquid layer away from the heater surface (17), and the mechanisms which explain the high heat flux by the increased turbulence imparted to the boundary layer by the growing bubbles (21, 25).

More recently, latent heat transport mechanisms have been put forth by several investigators. Moore and Mesler (39), in a pioneering experiment, provided new data explaining the mechanism by which latent heat is transported away from the heated surface. A fast response thermocouple

was used during the nucleate boiling of water. Surface temperature drops of 11 °C to 16.7 °C within 2 milliseconds were observed indicating a rapid extraction of heat during a very short time. The authors suggested that there is a thin liquid layer underneath the growing bubbles and that the evaporation of this layer into the bubbles brings the surface temperature down during bubble growth. Further studies of this model have shown that it is insufficient to explain the very high heat flux (54). Most recently, Kirby and Westwater (32) and Katto and Yokoya (31) experimentally found that a thin liquid film exists beneath irregular vapor masses with the principal heat transfer mechanism at high heat flux being the evaporation from this liquid film. It appears that these different conceptual models reflect different stages of the boiling mechanism; consequently, no overall analytical solution or empirical correlation is available to accurately predict the CHF.

In a recent review of current nucleate boiling theory, Labuntsov (34) pointed out that future analyses should concentrate on the features and structure of a very thin, liquid-rich film directly on the heater surface which sustains the principal temperature drop. The existence of such a film over the entire range of nucleate boiling has been confirmed by probing local voids with micro thermocouples (7,26). Therefore, the bubble agitation model appears to be more satisfactory for lower heat fluxes in nucleate boiling, while the latent heat transfer model is more applicable at high heat fluxes. None of the models previously mentioned explains the results of the latter experiments. Hence present nucleate boiling models will have to be modified or a new model developed in order to describe the entire nucleate boiling regime adequately.

## B. Steady-State Pool Boiling Critical Heat Flux (CHF)

Tong (52) and Balzhiser (4) have given comprehensive reviews of pool boiling heat transfer. They concluded that although the problem has been approached from many different points of view, no overall analytical solution has been obtained, and the design equations for CHF predictions are strictly empirical. For instance, Gambill (18) has noted that approximately fifty equations have been developed for predicting CHF in pool and flow boiling situations. Only those generalized CHF correlations that apply to saturated pool boiling will be discussed here.

In boiling, bubbles appear to form repeatedly at nucleation sites (cavities) on the heating surface, thus forming a "column" of bubbles. As the surface heat flux increases, visual observations indicate that the number of active nucleation sites per unit area increases (44). In addition, observations suggest that, as the heat flux increases to just below the critical value, the successive bubbles coming from a nucleation site converge into each other to form an undulating column of vapor. Rohsenow and Griffith (46) formulated a semi-empirical relation for the critical heat flux by combining observations from experiments in organic liquid and water with the conceptual model noted above. Their relation,

$$(Q/A)_{CHF} = 143 \rho_v h_{Lv} g^{1/4} \left( \frac{\rho_L - \rho_v}{\rho_v} \right)^{0.6} \quad (2.1)$$

was derived by tacitly assuming that the heater surface is covered by vapor bubbles at CHF.

Addoms (2) proposed a dimensionless correlation:

$$(Q/A)_{CHF} = 2.5 \lambda \rho_v (g\alpha)^{1/3} \left( \frac{\rho_L - \rho_v}{\rho_v} \right)^{0.5} \quad (2.2)$$

which also agrees well with data from experiments in water and organic fluids.

Other researchers have developed semi-empirical correlations using a more universal approach. For instance, Zuber (55,56), basing his arguments on wave motion, postulated that the boiling crisis is due to a combination of Taylor's and Helmholtz's instabilities which deal with the instability of a plane interface and the relative velocity of the liquid and its vapor respectively. The resulting equation is:

$$(Q/A)_{CHF} = 0.18 \rho_v h_{Lv} \left[ \frac{g g_o (\rho_L - \rho_v)}{\rho_v^2} \right]^{1/4} \left[ \frac{\rho_L}{\rho_L + \rho_v} \right]^{1/2} \quad (2.3)$$

Here the constant, 0.18, was determined empirically from the data shown in Fig. 2.

Kutateladze (33), Chang and Snyder (12), and Cobb and Park (14), have also developed equations which are nearly the same as those of Zuber and Addoms. Their equations, Berenson's modification of Zuber's analysis, in addition to some other pertinent correlations are listed in Table 1.

The examination of the above correlations does not make the effects of different parameters on the critical heat flux entirely obvious. However, from a thermodynamic point of view, it is apparent that the system pressure will be a dominant factor since it determines the latent heat of vaporization, the saturated vapor density and affects the surface tension. In fact, its effect has been well documented by many authors (13,15,18,24). Yet the CHF is far more complicated than this.

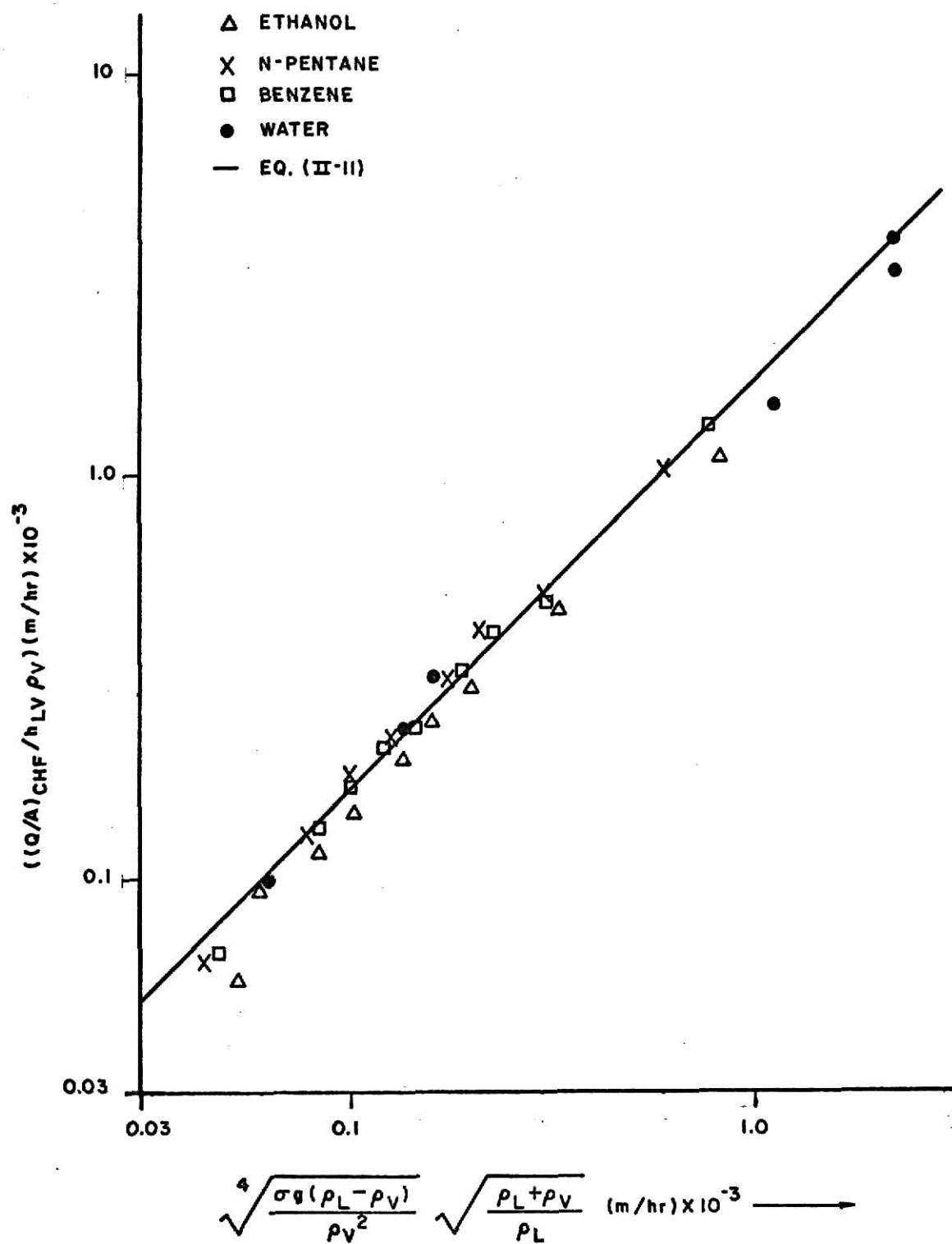


Fig. 2. Correlation of Critical Heat Flux in Pool Boiling.  
[After Zuber (56)].

TABLE 1-a. Equations for the Prediction of Nucleate Boiling Heat Flux

Equation	Theoretical Background	Validity	Author	Year
$(Q/A)_{\text{Total}} = \left( \frac{C_{PL}(T_w - T_s)}{h_{LV} Pr^{1.7}} \right)^3 \left( \frac{\mu_L h_{LV}}{C_{sg}^3} \right) \left[ \frac{g_O \gamma}{g(\rho_L - \rho_g)} \right]^{-1/2}$	Dimensional Analysis	It predicts the shape of the nucleate boiling regime with good accuracy.	W.M. Rohsenow (44)	1952
$\frac{A}{(Q/A)_{\text{Total}}} = \frac{n_c}{A_T} (Q/A)_{nc} + (Q/A)_b$ $\text{where } (Q/A)_b = C_1 \frac{C_2 C_3^{1/2} \mu_s}{\sqrt{\pi} 2^{m-1}} (k p_c)_L^{1/2} \cdot$ $\left( \frac{h_{LV} \rho_v}{T_s \sigma} \right)^m \cdot \left[ \frac{\sigma g_O g(\rho_L - \rho_v)}{\rho_L^2} \right]^{1/8}$ $\cdot \left[ \frac{\sigma g_O}{g(\rho_L - \rho_v)} \right]^{3/4} (Ja^*)^{15/8}$ $\cdot (T_w - T_s)^{m+1}$	Assumes the main mechanism of heat transfer in nucleate boiling is transient heat conduction to, and subsequent re-placement of, the superheated layer around boiling sites associated with bubble departure and considers effects of heat transfer surface characteristics.	For checking the equation, the required information about the boiling surface was found from $q/A$ versus $(T_w - T_s)$ data at one pressure and applied to all. The results are satisfactory.	Mikic and Rohsenow (37)	1969

TABLE 1-a. (Continued)

Equation	Theoretical Background	Validity	Author	Year
$c_1, c_2, c_3$ , and $m$ are constants. $Ja^* = \frac{\rho_L C_{pL} T}{\rho_v h_{Lv}}$ $(Q/A)_{nc} = 0.54 \rho_L C_{pL} \left[ \frac{rg(T_w - T_s)^5 \alpha^{3/4}}{\sqrt{A_T} \alpha} \right]$ for $10^5 < R_a < 2 \times 10^7$ $(Q/A)_{nc} = 0.14 \rho_L C_{pL} \left[ \frac{rg(T_w - T_s)^4 \alpha^{1/2}}{v} \right]$ for $2 \times 10^5 < R_a < 3 \times 10^{10}$				
$(Q/A)_{Total} = 4.35 \times 10^8 (N/A_t)^f \bar{V}_{ME}$ $+ 184 (T_w - T_L)^{4/3}$ $[1 - K\pi R_b^2 (N/A_T)]$ $+ 1543 kR_b^2 \sqrt{f}$ $(N/A_T) T_w - T_L$	Incorporation of microlayer evapo- ration, natural convection, and nucleate boiling mechanisms	Microlayer evaporation heat transfer is the prominent feature of this model. More data needed to support this equation.	R. L. Judd (29)	1976



TABLE 1-b. Equations for the Prediction of Critical Heat Flux

Equation	Theoretical Background	Validity	Author	Year
$(Q/A)_{CHF} = K_u \rho_v^{1/2} [g\sigma(\rho_L - \rho_v)]^{1/4}$ $ku: 0.14 \sim a/b$	Dimensional Analysis	Agrees well with large amount of data for water and organic liquids	Kutateladze (33)	1953
$(Q/A)_{CHF} = 2.5 \rho_v (g\alpha)^{1/4} \left( \frac{\rho_L - \rho_v}{\rho_v} \right)^{1/2}$	Hydrodynamic Analysis	Agrees well with data of water and organic liquids	Addoms and Ivey in 1961 (2)	1954
$(Q/A)_{CHF} = 0.18 \rho_v \left[ \frac{g(\rho_L - \rho_v)}{2 \rho_v} \right]^{1/4} \cdot \left[ \frac{\rho_L}{\rho_L + \rho_v} \right]^{1/2}$	Taylor and Helmholtz Instabilities	Agrees well with data of water and organic liquids.	Zuber (55,56)	1958
$(Q/A)_{CHF} = 0.145 \rho_v^{1/2} \left[ \frac{\rho_L + \rho_v}{\rho_L} \right]^{1/2} \cdot [g\sigma(\rho_L - \rho_v)]^{1/4}$	2-Dimensional interfacial stability analysis	Agrees with Zuber's and Kutateladze's equations	Chang and Snyder (12)	1960

TABLE 1-b. (Continued)

Equation	Theoretical Background	Validity	Author	Year
$(Q/A)_{CHF} = 0.16 \rho_v h_{Lv} \cdot \left( \frac{\rho_L + \rho_v}{\rho_L \rho_v} \right)^{1/2} \cdot \left[ gg_0 \sigma (\rho_L - \rho_v) \right]^{1/4} / \left[ 1 + \left( \frac{\rho_v}{\rho_L} \right)^{1/2} + \left( \frac{\rho_v}{\rho_L} \right)^{2/3} + \left( \frac{\rho_v}{\rho_L} \right) \right]$	A modification of Zuber's equation	Same as that of Zuber's but with more satisfactory theoretical consideration	Berenson (6)	1960
$(Q/A)_{CHF} = 143 \rho_v h_{Lv} g^{1/4} \left( \frac{\rho_L - \rho_v}{\rho_v} \right)^{0.6}$	Hydrodynamic Analysis	Good agreement with data of water and organic liquids	Rohsenow and Griffith (46)	1961
$(Q/A)_{CHF} = \frac{2570 \rho_v}{\left[ 1 + \left( \frac{\rho_v}{\rho_L} \right)^{1/2} \right]^2} (1 + 0.318 \frac{\rho_L}{\rho_v})^{1/2} \cdot \left[ \frac{gg_0 \sigma (\rho_L - \rho_v)}{\beta^2 \rho} \right]^{1/4}$	3-Dimensional analysis of a cylindrical vortex sheet	Limited because of the limited availability of data on the three phase contact angle for various combinations of fluids and solids	Adams (1)	1963

TABLE 1-b. (Continued)

Equation	Theoretical Background	Validity	Author	Year
$(Q/A)_{CHF} = 0.144 \rho_v \left[ \frac{\rho_L - \rho_v}{\rho_v} \right] \cdot$ $\frac{g g_o \sigma^{1/4}}{\left[ \frac{\rho_o}{\rho_L} \right]} Pr^{-0.245}$	A correction of Zuber's equation takes viscosity and conductivity of sodium into consideration	$0.003 \leq Pr \leq 11$	Noyes (40)	1963
$(Q/A)_{CHF} = 1.02 \times 10^6 \frac{\rho_v^k}{C_p \sigma} \cdot$ $\left[ \frac{\rho_L - \rho_v}{\rho_v} \right]^{0.65} Pr^{0.71}$	Dimensional Analysis	Agrees well with liquid metals, water, and organic liquids	Casell and Balzhiser (10)	1965
$(Q/A)_{CHF} = \frac{\pi}{24} \lambda \rho_v \left[ \frac{\sigma g (\rho_L - \rho_v)}{g_o \rho_v^2} \right]^{1/4} \cdot$ $\left( \frac{\rho_L}{\rho_L + \rho_v} \right)^{1/2}$ $+ \int_{-\lambda/4}^{\lambda/4} \frac{(T_w - T_s)}{\cos(\frac{2\pi x}{\lambda})} dx$ $\lambda = \frac{2\pi}{g_o \sigma} \left[ \frac{g_o \sigma}{g (\rho_L - \rho_v)} \right]^{1/2}$	Hydrodynamic Instability plus temperature profile model	Needs more supporting experiments	Balzhiser, et al. (4)	1971

TABLE 1-b. (Continued)

Equation	Theoretical Background	Validity	Author	Year
$(Q/A)_{CHF} = (Q/A)_{CHF,k} + 2(Q/A)_{cond}$ $= k_u h_u (\rho_v g)^{1/2} [\sigma(\rho_L - \rho_v)]^{1/4}$ $+ \frac{2(T_v - T_s)}{\frac{\delta}{k} + \frac{2\pi RT_v}{M} \left( \frac{T_s}{2\rho_v} \right) \epsilon h_{Lv}}$	Kutateladze equation condensing heat flux within bubbles	Needs to be proven experimentally	Bankoff, et al. (5)	1974

Many other variables can influence the CHF experimentally and confuse data interpretation. For instance, Tong (53), commenting on the effects of wetting agents and surface conditions on the CHF in pool boiling, noted that the maximum heat flux is practically independent of surface material, cleanliness, and roughness. Berenson (6) found that a smooth surface has a higher superheat at boiling crisis than a rough surface, although both have approximately the same CHF. On the other hand, other investigators have obtained different results. Costello and Frea (53) found that deposits on stainless steel heater surfaces result in at least a 50% increase in the CHF. Ivey and Morris (53) stated that oxidized surfaces appear to yield a higher CHF than that associated with a clean metallic surface. Other parameters such as the diameter, the surface orientation geometry and system acceleration all have small effects on the CHF (53).

### C. Boiling Heat Transfer in Transients

A clear interpretation of boiling behavior and CHF in both power and pressure transients remains elusive even though these phenomena have become of increasing importance. Because knowledge of the boiling behavior during power transients is required for nuclear reactor design and operation, basic studies of this phenomena are numerous while investigations of pressure transients have been more recent, relatively few, and unsystematic.

#### 1. Boiling Heat Transfer in Power Transients

Transient thermal behavior originally became of interest because of the possible effects of a prompt supercritical period on fuel cladding integrity in nuclear reactors. Many studies have been performed on

this topic (27,28,30,48,49,51,52,53). Notable early work was performed by Rosenthal and Miller (47) and Johnson and Schrock (28), who studied exponential increases in power to simulate transient conditions in light water reactors. The experimental results have, in general, been consistent and are reviewed by Tong (52). Transient CHF increases as the power impulse time decreases. In fact, when the impulse time is larger than 200 milliseconds, the transient CHF does not deviate significantly from the steady-state CHF for similar subcooling. According to the results of Rosenthal and Miller (47), the power excursion effect on CHF decreases as the initial exponential period increases and gradually becomes insignificant at periods greater than 14 to 30 milliseconds. When time constants are extremely short the transient heat flux can surpass the steady-state value before the boiling transitions to film boiling. These effects are shown clearly by the data of Tachibana, et al. (50) in Fig. 3. These authors have speculated that the CHF during rapid power transients may increase because of a corresponding increase in the number of surface nucleation sites. This supposition agrees with the observation of Hall and Harrison (20) who observed that in extremely rapid exponential power impulses with periods as short as 0.7 millisecond, film boiling was invariably preceded by a short burst of nucleate boiling. Furthermore, peak heat fluxes 5 to 10 times the steady-state CHF values under the same thermodynamic conditions were noted.

On the other hand, experiments of power transients with relatively long time constants have been conducted also. Fontana (16), for instance, studied transients with periods of up to 2 minutes, and Sakurai et al. (48) studied transients with periods up to 1 second. In both cases, the transient CHF was observed to be the same as the steady-state CHF for the same liquid temperature and pressure. Although Fontana found

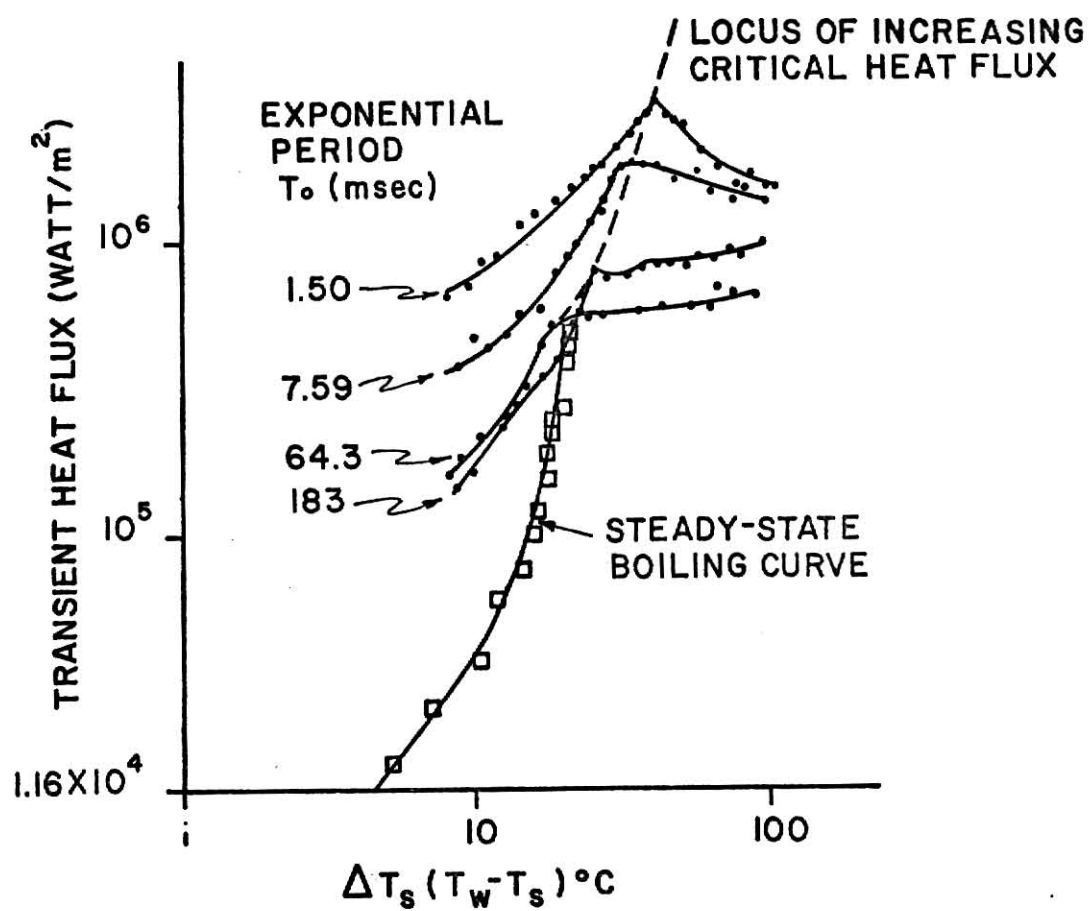


Fig. 3 Effect of Power Transient on CHF. [After Tachibana (50)].

this to be true only for periods greater than 10 seconds, Sakurai observed that transient values of CHF corresponded with steady state levels for periods down to 20 milliseconds. This agrees with earlier power transient experiments conducted by Rosenthal and Miller (47).

It is well known that nucleation and subsequent bubble growth, which are highly dependent on the thermodynamic conditions of the heater and the liquid in the vicinity of the heater surface, directly influence the heat flux. The effects of both power and pressure transients on the CHF may be discussed on these bases. Equation (2.4), which is derived from the surface tension of a spherical bubble and the Clausius - Clapeyron equation, gives an estimation of the surface superheat required to initiate nucleation,

$$T_v - T_s \approx 2 \left( \frac{R T_s^2 \sigma}{h_{Lv} P_L r_b} \right) . \quad (2.4)$$

After nucleation and a few milliseconds after growth has begun, i.e., the later part of the bubble's life, according to Tong's analysis (53), inertia of the surrounding liquid and the surface tension forces can probably be neglected. The pressure can be considered uniform throughout the bubble and liquid. At this stage, bubble growth is governed by the rate at which heat can be supplied from the superheated liquid to the bubble interface to facilitate the vapor formation associated with growth.

If the liquid in the vicinity of the heating surface is very subcooled initially, only a small amount of natural convection heat transfer occurs. During a subsequent power transient, the heater surface temperature will surge because the heat input is rapidly increasing, but the surrounding liquid, which remains cool, is not favorable to bubble growth.



However, the fluid temperature lags behind at a value below that necessary for incipient bubble growth. Nucleation may occur, however, on the heater surface due to rapid increase in surface temperature. Transition to film boiling results, as shown by the data of Rosenthal and Miller (49), Johnson and Schrock (28), in Fig. 4. The smaller the impulse power period, the more the temperature overshoot and the shorter the delay time.

If the heater is initially hot enough that the liquid layer surrounding it is close to the saturation temperature, the increasing power during the transient is more effectively transferred because of bubble nucleation and growth. In this case, the transient CHF is significantly different. The effect of the initial heat flux level on CHF is to lower the transient CHF considerably at low initial heat flux and to approach steady-state CHF at high initial heat flux (51).

## 2. Boiling Heat Transfer in Pressure Transients

The situation during a pressure transient is substantially more complex due to the changing thermodynamic conditions in the bulk fluid. As the pressure decay is initiated, the surface superheat increases due to the decrease of  $T_{sat}$ . The bulk coolant, instead of only the liquid layer in the vicinity of the heater, becomes warmer relative to the decreasing  $T_{sat}$ . The magnitude of the pressure decrease, of course, determines the corresponding decrease in  $T_{sat}$ . If the transient is sufficiently fast that it completes the depressurization before bubbles can detach from the heater surface, the heat transfer cannot increase until after the transient is completed. If the transient is slow, for example,  $7.07 \times 10^4$  pascal/sec, there is ample time for many generations of bubbles to grow on the surface and equilibrium may be reached. Therefore the heat flux can follow the pressure change, and in this limiting case, the CHF can be predicted by steady-state correlations.

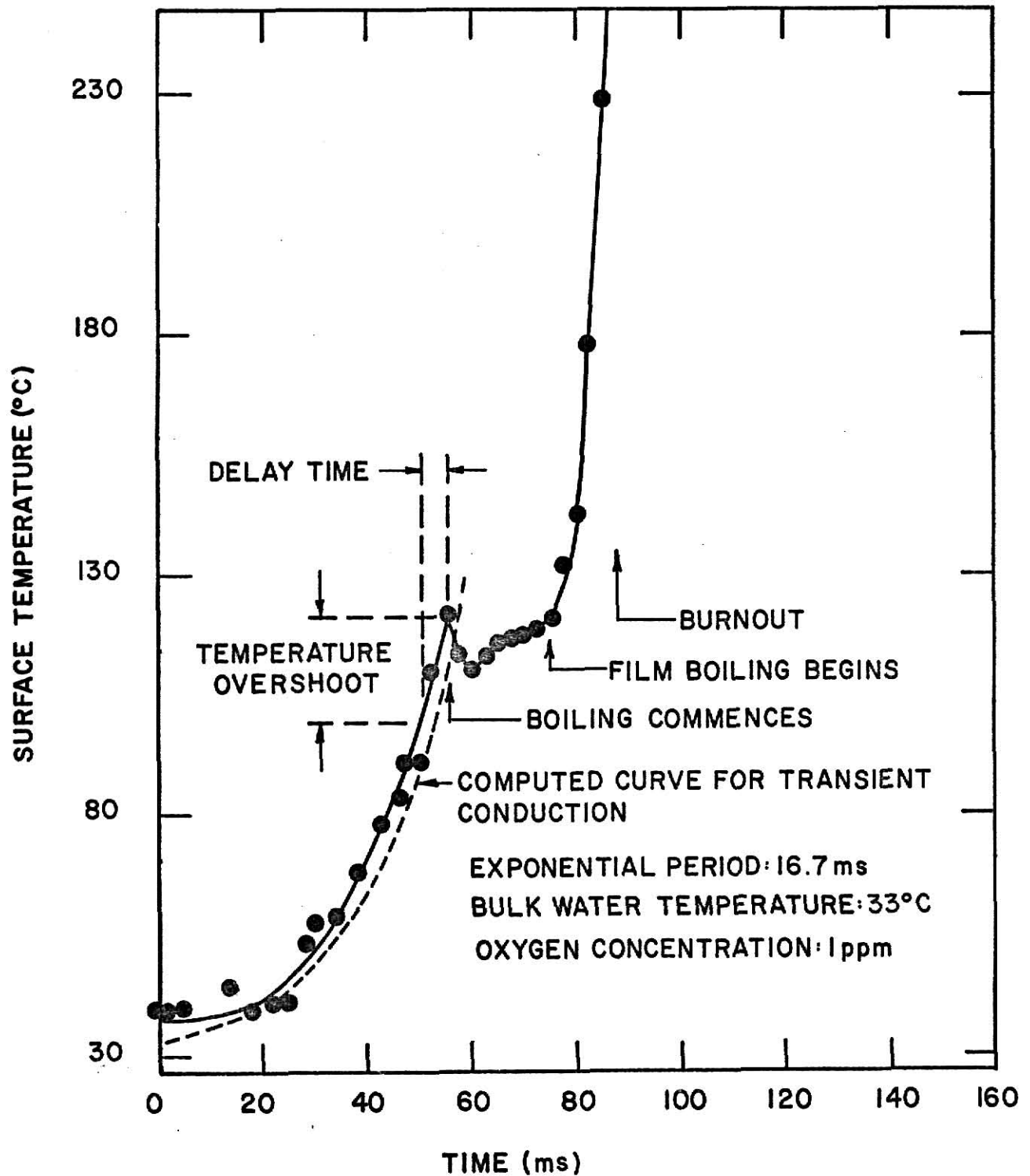


Fig. 4. Typical Temperature-Time Record for Platinum Ribbon in Sub-Cooled Water during Power Transient. [After Rosenthal and Miller (47)].

In practice, the pressure transient is more complicated because bulk flashing is often involved. The heater boundary will be disturbed by bubble agitation and heat transfer mechanisms observed in steady state circumstances may no longer apply shortly after the transient is triggered. No theoretical work has been done on this subject, and only a few experiments have been conducted toward increasing our understanding of this phenomena.

Howell and Bell (23) investigated the pressure transient effect in pool boiling experimentally. The pressurized saturated water was allowed to decay from moderate pressures to atmospheric via a quick-opening valve. Decompression was relatively slow. For example, it required 12 seconds to reach atmospheric pressure from  $4.2 \times 10^5$  pascal. Because of this slow pressure transient, a link between steady-state and transient cases was attempted. A typical heater temperature behavior during transient boiling is shown in Fig. 5. The relation between transient events and the transient pressure is shown in Fig. 6. The ribbon temperature started to decrease once the decompression began and continued until point c, the inception of film boiling, was reached. The heater temperature then increased until the burnout point was detected. The magnitude of transient CHF appears higher than steady-state CHF by about 20 to 30 percent but independent of the decompression rate. During this experiment, only the initial heat flux was measured; hence, the magnitude of the fluctuation of the heater temperature and the resulting variation in heat flux were not indicated. The time from the start of decompression to the burnout point was discussed more fully. Thus, knowing the initial conditions and the decay rate, the time from point A to point B on Fig. 10b can be calculated. The period between point B until film boiling begins (from

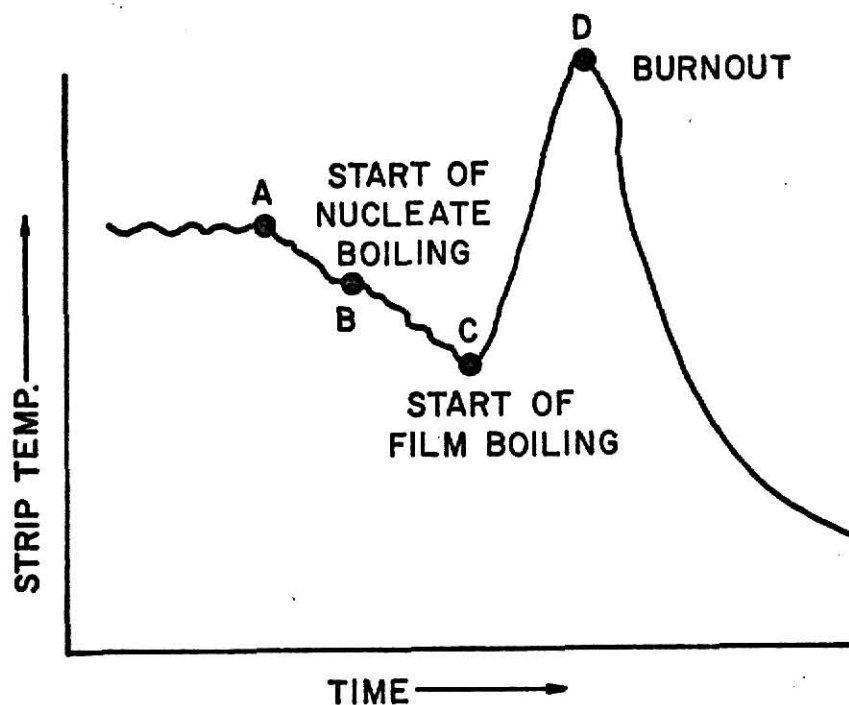


Fig. 5 Ribbon Temperature Behavior During Transient Boiling in Decompression ( $P_o \approx 4$  atm). [After Howell and Bell (23)].

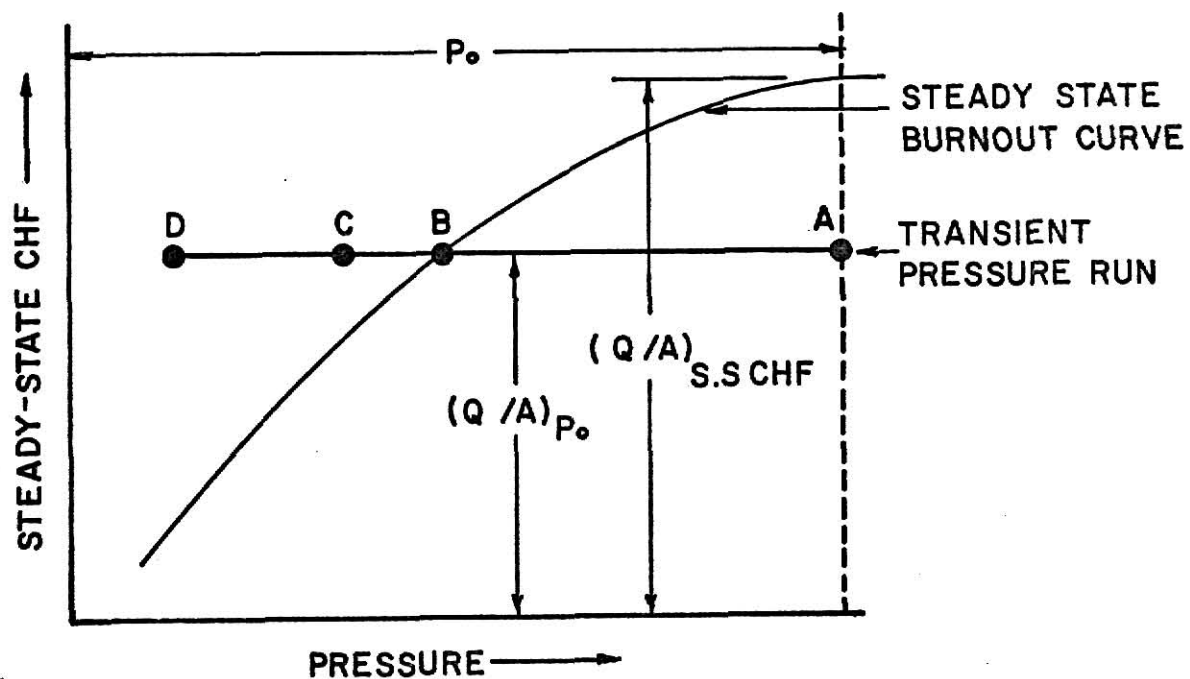


Fig. 6 Relation Between Transient Events and the Pressure. [After Howell and Bell (23)].

point B to point C) is then found from a corrected experimental curve. The final time segment, between the inception of film boiling and actual burnout (point C to point D) can then be found analytically by assuming complete insulation of the heating surface and calculating the time required to reach the temperature of material failure. The time to burnout was observed to increase with decreasing rate of pressure release. Flashing, encountered in these experiments, was deemed responsible for the delay of the boiling transition corresponding to the steady-state prediction.

Cermak, et al. (11) examined the effect of pressure blowdown on flow CHF in rod bundles. It was observed that for pressures of  $6.3 \times 10^5$  to  $10.5 \times 10^5$  pascal and relatively short time constants of 1 second, steady-state CHF agreed with the observed transient CHF values to about 5 percent.

Studies of fast pressure transients are very few. Aoki, et al. (3) investigated the boiling and burnout phenomena during very fast pressure transients of time periods of approximately 25 milliseconds from atmospheric pressure down to at most  $7.3 \times 10^4$  pascal or higher. Heater surface temperature behaviors for different initial heat flux levels were studied. According to their results, the initial heat flux level determines the overall transient behavior, as shown in Fig. 7. The most interesting findings are for type B behavior (see Fig. 7). Specifically, the investigators noted a spike characteristic of heat fluxes slightly lower than the steady-state CHF of the final equilibrium state, a secondary boiling during which boiling transition occurred, (see Fig. 7), and an initial temperature drop for all levels of heat flux. The third observation was also reported by Howell and Bell, but the first two findings are

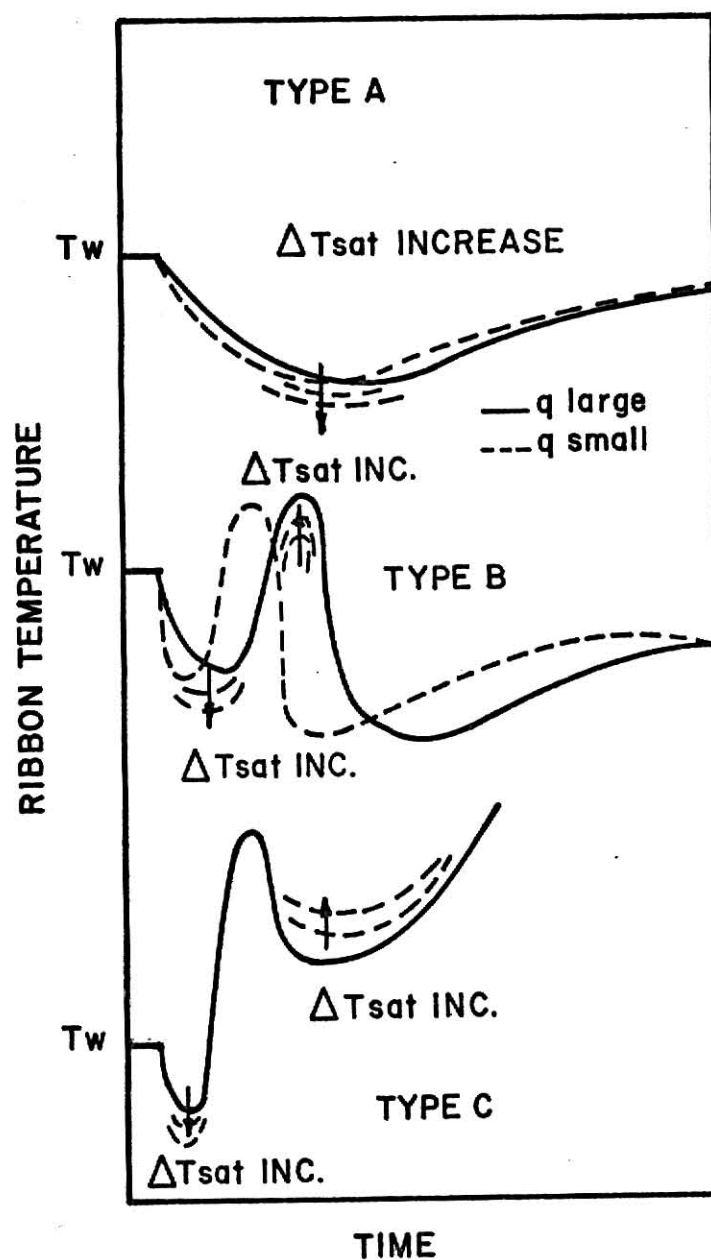


Fig. 7. Ribbon Temperature Behavior during Transient Boiling in Rapid Decompression from Atmospheric Pressure. [After Aoki, et al. (3)].

unique. By the use of high speed photography, Aoki, et al. were able to explain the bubble growth behavior in more depth than Howell and Bell. Thus, at medium heat flux level, the temperature falls during the initial sudden decompression but its drop ceases when the generated bubbles near the wall begin to coalesce. After the heater wall is covered with a large single coalesced bubble, the wall dries out and the temperature increases steeply. However, as the large bubble is removed from the surface by buoyancy, the temperature begins to drop and stable nucleate boiling insues.

When the initial heat flux was higher than the steady-state CHF, boiling transition and subsequent stable film boiling were observed. The transition, however, did not occur during the pressure drop but during the secondary boiling instead. By incorporating the thin liquid layer model for the bubble generation and detachment at high heat flux in nucleate boiling with their observations, the authors contend that boiling transition occurs when a second generation of bubbles is formed inside the thin liquid layer underlying the bubble layer from the primary boiling.

Summarizing previous decompression work, the following points should be noted. Howell and Bell tried to predict transient boiling transition on the basis of the initial conditions, i.e., operating heat flux, pressure decay rate, and range. And perhaps more importantly, they attempted to answer, if boiling transient occurs, at what stage in the decompression will it happen? Aoki, et al. (3), on the other hand, were interested in determining whether the boiling transition occurs during or after the pressure transient. The small time constant and comprehensive recording of heater temperatures accompanied by photographic studies of bubble growth made their investigation more fundamental.

In steady-state boiling, the CHF is defined at the critical point as indicated in the beginning of this chapter. In power transients, the CHF is similarly defined as the point at which the heat flux decreases with further increase in heater temperature. Following the same line of thought and considering that the variation of the heat flux during the transient event is not controllable, perhaps the best definition of the CHF in pressure transients is that minimum initial heat flux which is sufficient to cause boiling transition during or shortly after the pressure transient event. Howell and Bell obtained some data for this purpose, but more data are necessary to establish a comprehensive relation. Aoki, et al. were unable to provide a comprehensive data set since the degree of superheat in their apparatus also affected the rate of decompression and the transient pressure behavior. Their observation of different temperature behaviors is of potential importance in the better understanding of pressure transient boiling phenomena.

The research reported herein is the initial stage in a comprehensive study of boiling transition under decompression. As an extension to the work described above, subcooled as well as saturated decompressions were studied to better elucidate the effect of flashing on the wire temperature behavior and boiling transition. In subsequent chapters, the experimental apparatus, technique, results, and conclusions are covered.



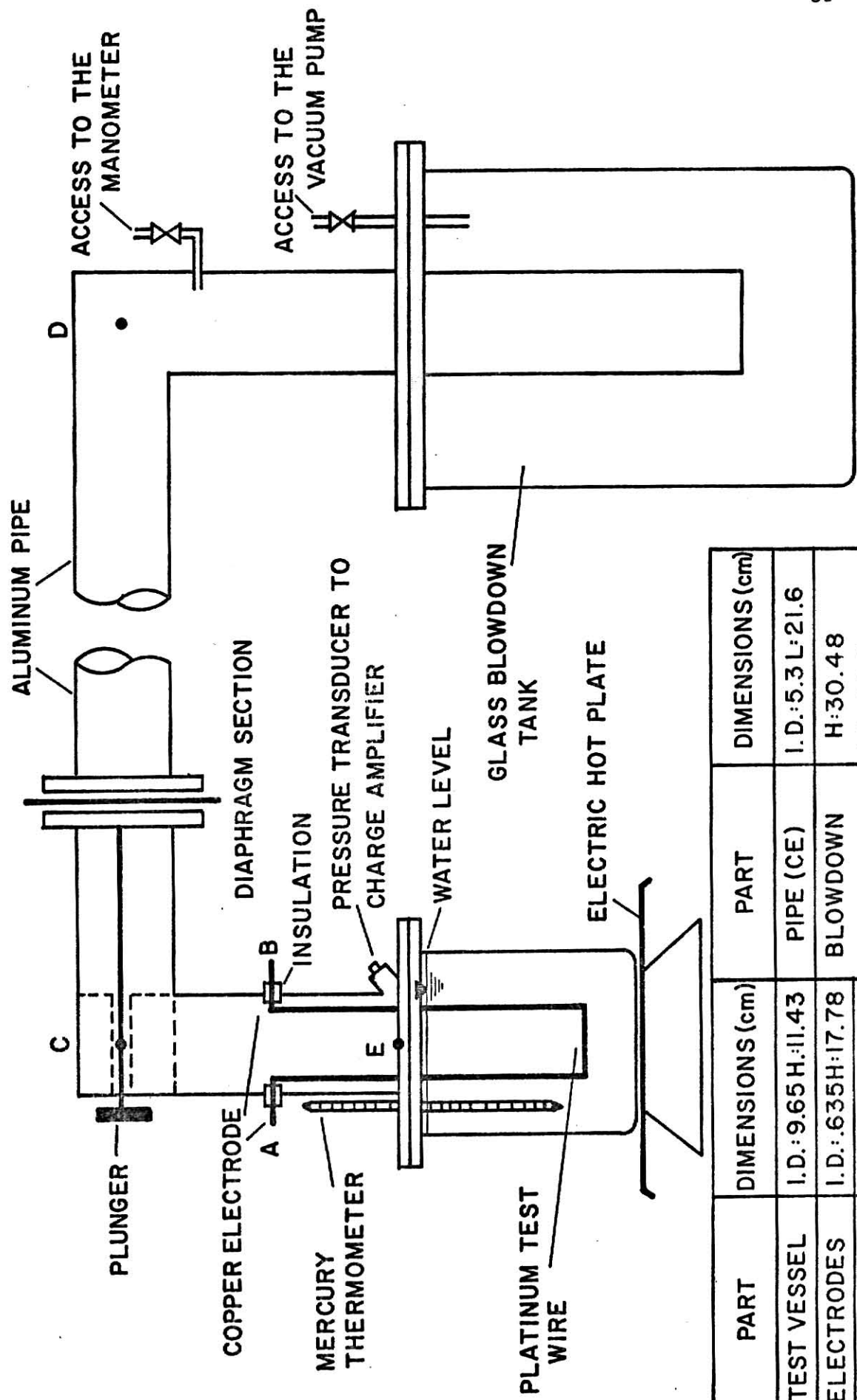
### III. EXPERIMENTAL EQUIPMENT AND PROCEDURES

#### A. Experimental Equipment

Because only low liquid temperatures (less than 100 °C) and low pressures (less than atmospheric) were involved in this experiment, pyrex glass and aluminum were used to construct the entire apparatus. In order to produce very fast transients, a diaphragm bursting technique was used instead of a quick opening valve. When burst by a spring-loaded plunger, this method has yielded consistent results. A fast response temperature sensor, in the form of a platinum wire, was used for following the transient temperature history for a period of up to 500 milliseconds. The platinum wire was also used as the heater. Details of the test assembly and the measuring circuit are described in the following sections.

##### 1. Test Assembly

A schematic diagram of the test assembly is shown in Fig. 8. The test section was composed of an 800 ml Pyrex glass beaker that was fitted with an aluminum flange. The reduced pressure, or blow-down tank, was made of an eleven - liter glass vessel which has an aluminum flange and valving to provide access to a vacuum pump. Aluminum pipe, 5.08 cm I.D., was used to connect the two sections through a diaphragm section. Prior to each transient run, an aluminum foil was clamped between the two flanges of the diaphragm section, and the pressure in the dump tank was reduced to sub-atmospheric, in most experiments to 400 torr. An aluminum tank was built originally to provide a constant temperature environment for the test section during steady-state boiling experiments. This was found to be unnecessary, and later experiments were performed



PART	DIMENSIONS (cm)	PART	DIMENSIONS (cm)
TEST VESSEL	I.D.: 9.65 H.: 11.43	PIPE (CE)	I.D.: 5.3 L: 21.6
ELECTRODES	I.D.: .635 H.: 17.78	BLOWDOWN TANK	H: 30.48 I.D.: 20.3
PIPE (CD)	I.D.: 5.3 L: 55.3		

Fig. 8. Schematic Diagram of the Experimental Apparatus.

using a hot plate with a magnetic stirrer as the bath temperature control. Distilled and deionized water was used in the experimentation. No further filtration or purification was performed.

## 2. Electrical Circuit

The circuitry used in making steady-state and transient measurements is shown in Fig. 9. Resistors  $R_1$ ,  $R_2$ , and  $R_3$  are one 500 ohm and two-1 ohm high wattage resistors respectively for the control of current through the test wire. Resistor  $R_s$  is a 0.226 ohm precision shunt resistor. Current through the test wire is proportional to the voltage across  $R_s$ . Resistor  $R_w$  is the test wire resistance. The test specimen consisted of a 0.0127 cm-dia platinum wire approximately 2.0 cm in length. It was soldered on the ends of two copper electrodes and immersed in the water bath in the test vessel.

In steady-state measurements, as shown in 9a, the test wire was kept 8 cm below the water level to avoid surface effects as suggested by Aoki (3). The steady-state boiling curves for various pressures have been obtained by the use of a digital voltmeter to read wire voltage across A-B and current during operation up to the burnout point. Two 12-volt lead batteries provided stable wire current during each test run. Bulk water temperature was monitored by a mercury thermometer inserted inside the test vessel. Static pressure was read directly on a u-tube mercury manometer. Steady state resistances were measured by a Leeds and Northrup Type S bridge circuit.

For the transient experiments, a Tektronix type 551 dual-beam oscilloscope with a four-trace preamplifier was used to record the voltage variation across and the current through the test wire, in addition to the output signal from a Kistler type 603 piezoelectric

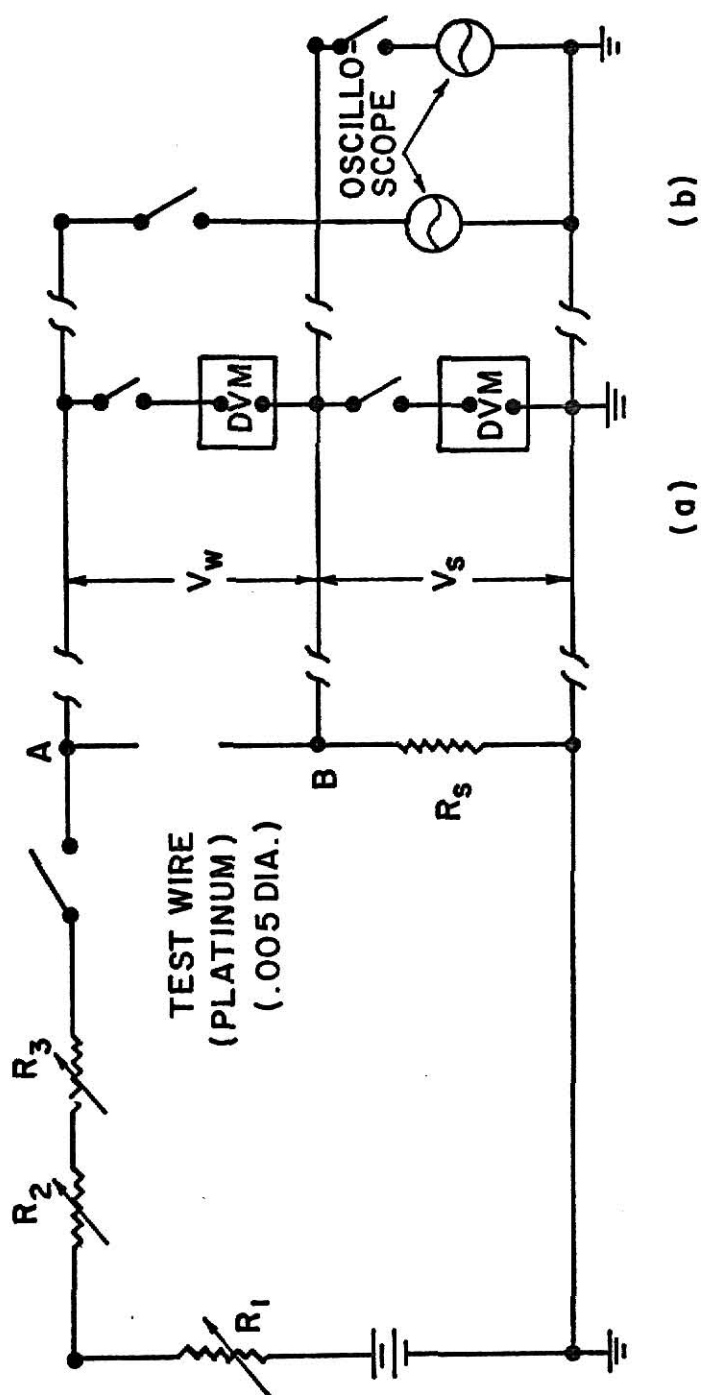


Fig. 9. Circuitry for Steady-State and Transient Measurements.

transducer with Kistler type 503 charge amplifier. The transient sweep on the oscilloscope was recorded by a Polaroid scope camera.

## B. Experimental Procedures

### 1. Steady-State Experiments

The following procedures were followed to produce steady-state boiling curves at different pressures:

- (1) The test vessel was cleaned and filled with deionized water which had been boiled for at least one hour. The test vessel was then placed in the constant temperature tank which had been previously brought up to the desired temperature. Later experiments were performed using a hot plate as the bath temperature control.
- (2) The test wire was inspected by a 50X optical microscope and cleaned with benzene. The wire was heated in air with a two amp. current for twenty minutes after it was soldered to the ends of the electrodes. The length of the wire was measured to  $\pm 0.05$  cm.
- (3) The electrical test assembly was inserted into the beaker. The system was closed and brought to the desired temperature at which time the resistance between points A and B on Fig. 8 was recorded. A vacuum pump was used to lower the pressure to the desired level.
- (4) Power was applied to the test wire, and the wire voltage,  $V_w$ , the voltage across the precision resistor,  $V_s$ , and the voltage across the power supply,  $V_p$ , were recorded.
- (5) The power level was raised incrementally in order that at least 10 data points were taken prior to boiling transition.
- (6) Information in the steady film boiling region was obtained by increasing the power until the wire burned out physically.

## 2. Transient Experiments

The following procedures were followed in recording the wire temperature behavior during and shortly after the pressure transient.

- (1) The test assembly was prepared prior to each run in accordance with steps 1 and 2 from section 1 above.
- (2) The test assembly was inserted into the test vessel and the whole system was brought to the desired temperature. The resistance between A and B in Fig. 8 was then recorded.
- (3) The aluminum was inserted in the diaphragm section and clamped. The pressure in the blow-down tank was reduced to 400 torr by the use of a mechanical vacuum pump.
- (4) The DC power supply was turned on and the current through the test wire was brought up gradually to a pre-planned value by adjusting the variable resistors.
- (5) The oscilloscope was DC balanced and proper sweep speed and sensitivity were selected.
- (6) The triggering level on the oscilloscope was pre-set. The triggering level adjustment was the determining factor in the system sensitivity. The beginning of the transient was not recorded, since the scope was triggered by the pressure response. The voltage traces actually represent the transient behavior after several milliseconds into the transient.
- (7) The voltage across the wire,  $V_w$ , the voltage across the precision resistor,  $V_s$ , and the voltage across the battery,  $V_p$  were recorded. Final adjustment of the system pressure was made.
- (8) The shutter control line of the scope camera was pressed. The plunger was released, breaking the diaphragm and then the shutter control was released.

- (9) DC power supply was turned off and the access valve was opened.
- (10) The Polaroid picture was developed.

#### IV. RESULTS AND DISCUSSION

A relatively straightforward but carefully controlled series of experiments have been performed. It was confirmed that the boiling mechanism is affected significantly during and shortly after fast transients. For instance, if flashing occurs in the bulk coolant, the mechanism of bubble formation and growth may be quite different than that expected when only local boiling around the wire is present. It is surprising, therefore, to observe that even when there was no bulk flashing, i.e., in the subcooled blowdown case, wire temperature behavior was similar to that in the presence of flashing. The understanding and the explanation of these boiling phenomena must be based in part, on a clear understanding of the steady state nucleate boiling mechanism, especially at high heat fluxes near the CHF. Unfortunately, as indicated in Chapter 2, this region is not yet understood fully. In this chapter, the results of both steady-state and transient boiling studies will be covered. Discussion is based on currently accepted boiling models, due to the lack of high speed photographic data in these first experiments.

##### A. Steady-State Experiments

In order to gain operating experience and to assure the consistency of the apparatus, steady-state boiling experiments were performed as a preliminary test. Data were collected under pressures from atmospheric to 200 torr in a nearly saturated pool of water to construct steady-state boiling curves. The circuitry used for steady-state measurements has been shown previously in Fig. 9a.



### 1. Interpretation of Steady-State Data

To calculate the temperature of the test wire from its resistance, the resistance-temperature relation of pure platinum wire was used:

$$R_w(T_w) = R_w(0^\circ\text{C})(1 + \alpha T_w + \beta T_w^2), \quad (4.1)$$

where

$$\alpha = 3.95 \times 10^{-3} \text{ deg}^{-1} \text{ }^\circ\text{K},$$

$$\beta = 5.85 \times 10^{-7} \text{ deg}^{-1} \text{ }^\circ\text{K} \quad (\text{Ref. 9}),$$

$T_w$  = the temperature of test wire in degrees of Celsius,

$R_w(T_w)$  = the resistance of test wire at  $T_w$  in ohms.

$R_w(T_w)$  can be calculated from the experimentally obtained values of  $V_I$  and  $V_w$  as shown below. Due to the existence of a connection resistance and the small resistance of the copper electrodes,  $V_w$  must be corrected by an amount  $V_{\text{stray}}$

where

$$V_{\text{stray}} = I R_{\text{stray}}, \quad (4.2)$$

and

$$I = V_I / R_s. \quad (4.3)$$

The stray resistance,  $R_{\text{stray}}$ , is assumed to be equal to the difference between the system resistance,  $R_{\text{sys}}$ , and the theoretical resistance,  $R_{\text{th}}$ ,

$$R_{\text{stray}} = R_{\text{sys}} - R_{\text{th}}, \quad (4.4)$$

The resistance of the wire under operating conditions is then calculated as

$$R_w = V'_w / I = (V_w - V_{\text{stray}}) / I. \quad (4.5)$$

By solving Eq. IV.1, it is obtained:

$$T_w = \frac{-\alpha \pm \sqrt{\alpha^2 - 4\beta\gamma}}{2\beta}, \quad (4.6)$$

where

$$\gamma = 1 - \frac{R_w(T_w)}{R_w(0^\circ\text{C})}. \quad (4.7)$$

The operating heat flux  $(Q/A)_{op}$ , can be calculated by the formula

$$(Q/A)_{op} = IV'_w/A, \quad (4.8)$$

where A is the surface area of the test wire.

The wire temperature was assumed uniform both axially and radially. The radial temperature distribution in a long cylindrical rod with internal heat generation is

$$\frac{T_w(r)}{T_{\max}} = 1 - \frac{\dot{Q} r_o^2}{4kT_{\max}} \left(\frac{r}{r_o}\right)^2. \quad (4.9)$$

where r is the radial distance from the centerline.

Because  $r_o$  is only 0.0635 cm, and the thermal conductivity of platinum, k, is 0.722 (Watt/cm °K) at 27 °C or 0.775 (Watt/cm °K) at 927 °C, the right hand side of Eq. IV.9 is not far from unity, i.e.,  $T_w \approx T_{\max}$ . Thus, the temperature distribution from the centerline to the surface is nearly uniform. However, neglecting any end effects may be an invalid assumption in the case of short wires, e.g. length of 1 cm or less. In this experiment, because the length of test wire is close to 2.5 cm and the temperature behavior of the entire wire was measured instead of the local temperature, the end effects were not considered. However, if the temperature distribution along the wire is known, the constant which relates the maximum temperature and the mean temperature of the wire can be calculated.

## 2. Discussion of Steady-State Results

The data were processed by a short computer program listed in Appendix A. All the results are presented in Appendix B. The boiling curve under atmospheric pressure was plotted along with Peterson's (42) and McAdom's (36) data and is shown in Fig. 10. Rohsenow's equation in Table I was also used and the calculated results are presented in the same figure for comparison.

The free convection region of the boiling curve in the present study deviated slightly from the previous results. This may indicate that an error was introduced because of uncertainty in wire length. For low heat fluxes, the heater temperature is very close to the bulk fluid temperature; therefore, the errors made in the measurement of the length and end effects, will be substantially more important than in the boiling region. One other factor that may have contributed to the uncertainty is the possible influence of augmented free convection on the heat transfer. Since the pool was held at constant temperature by a bottom hot plate, the resulting free convection may increase the heat transfer over that normally present from that induced only by the thermal boundary layer in the near-wire region.

The boiling mechanism becomes very unstable as the boiling transition is approached. Because the controlled variable in this experiment was the heat flux (as in most other studies except Peterson's (42)), it was impossible to precisely detect the critical point. As the point of transition was passed, the physical appearance of the wire changed noticeably. At one location, the wire began to grow red. This local behavior subsequently spread over the wire's entire surface except near

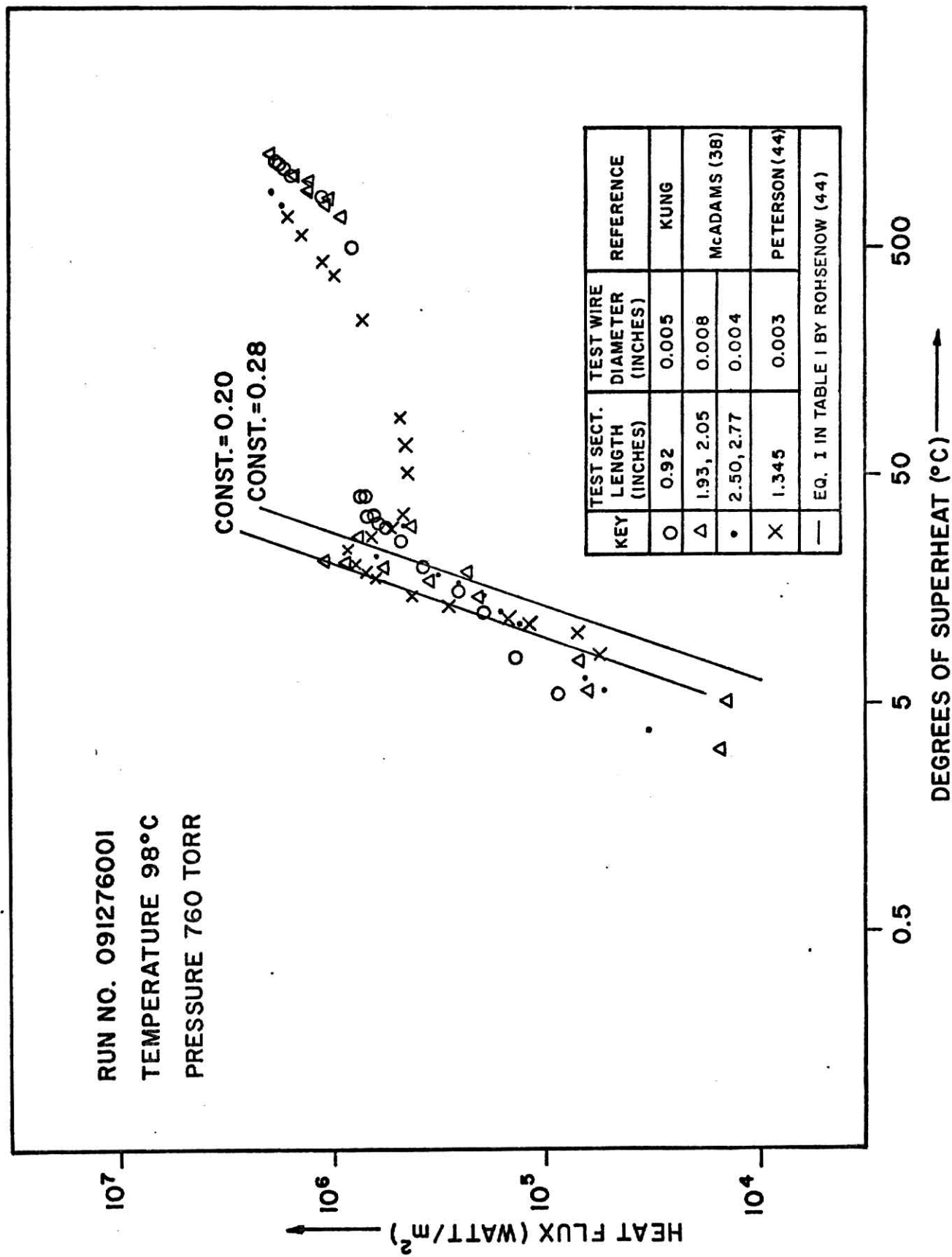


Fig. 10. Steady-State Boiling Curve at Atmospheric Pressure in a Saturated Pool of Water.

the ends where the surface temperature was lower. This phenomena corresponds to the case where the wire becomes engulfed in vapor and the boiling shifts to position D on the boiling curve (see Fig. 1), film boiling with radiation augmentation. The heat flux, as this transition was observed, was taken as the CHF. The results, shown in Fig. 11, are in good agreement with Aoki's data for a similar apparatus.

Frequently, the boiling transition was passed through without a clear indication of nucleate boiling. This behavior has been observed also by Aoki, et al. (3).

The steady-state experimentation described above gave confidence that the measurement system was reliable. Following this, transient data were gathered.

## B. Boiling Heat Transfer During and Shortly after the Pressure Transient

### 1. The Interpretation of Transient Experimental Data

During decompression testing, the pressure decayed to 420 torr from atmospheric. If the water reached its saturation pressure during the run (as determined by the initial bulk fluid temperature), the final pressure was at most 30 torr higher than 420 torr. All the transient data were recorded by Polaroid pictures of oscilloscope traces. The test conditions examined during the experimentation are shown in Table 2. Four levels of heat fluxes were tested. At low heat flux, no bubbles appeared before or after the pressure transient. The ratio of the initial heat flux,  $(Q/A)_{op}$ , to the CHF corresponding to the final state,  $(Q/A)_{CHF}$ , was about .6. Medium heat flux level was when  $(Q/A)_{op}/(Q/A)_{CHF}$  was about .8. High initial heat flux levels were close to the  $Q_{CHF}$ , and very high initial heat flux was higher than  $Q_{CHF}$ . For each level of heat flux, runs of different superheats and subcoolings were tested as recorded in Table 2.

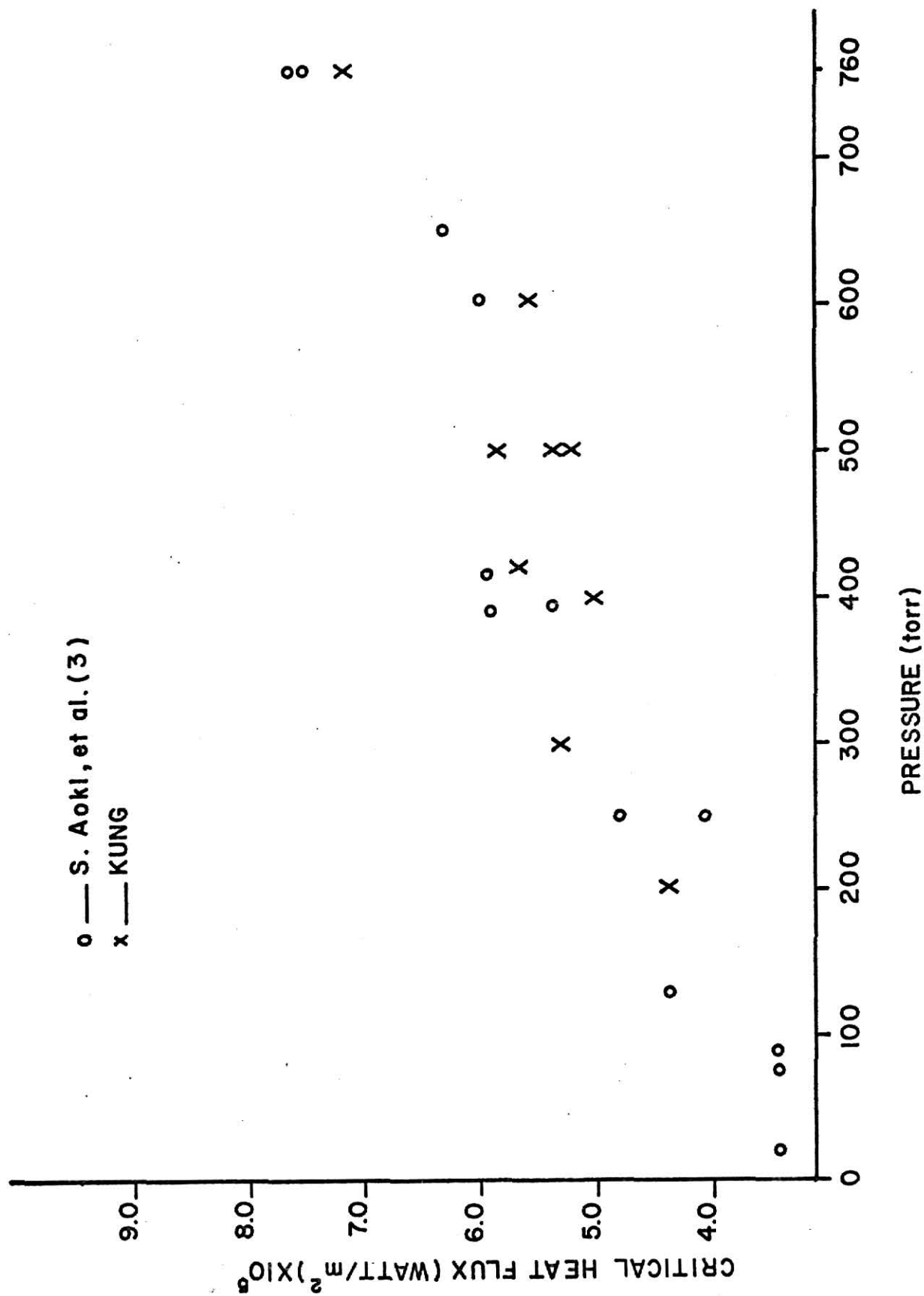


Fig. 11. Steady-State CHF at Sub-Atmospheric Pressures.

TABLE 2. Summary of the Test Conditions of the Transient Experiments

Initial Heat Flux Level [ $(Q/A)_{op}/(Q/A)_{CHF}$ ]	Number of Runs	Initial Water Temp. $T_L$ ( $^{\circ}\text{C}$ )	Note
$\sim 0.5$	10		Water became superheated after the transient was initiated. Degrees of superheat ranged from $\sim 0$ to $7^{\circ}\text{C}$ . [ $(Q/A)_{op}/(Q/A)_{CHF}$ ] was approximately 0.5, 0.8, 1.0, and greater than 1.0. Corresponding levels are defined as low, medium, high, and very high heat fluxes respectively.
$\sim 0.8$	7		
$\sim 1.0$	21	$< 84$	
$> 1.0$	12		
$\sim 0.5$	7		Water remained subcooled after transient was initiated. Degrees of subcooling ranged from 1 to $34^{\circ}\text{C}$ .
$\sim 0.8$	5		
$\sim 1.0$	8	$< 84$	
$> 1.0$	9		

NOTE:  $(Q/A)_{CHA}$  in saturated water under 420 torr is approximately  $5.7 \times 10^6 \text{ W/m}^2$  according to Figure 11.

It was assumed that the power supply provided a constant current source throughout the run; therefore, the voltage across the test wire,  $V_w$ , is proportional to the wire resistance,  $R_w$ ,

$$V_w \approx I R_w . \quad (4.10)$$

The time dependence of the current,  $I$ , introduces significant errors only at the end of the run, i.e. at the incidence of film boiling and later, and its neglect is therefore justified. From Eq. 4.10 it is apparent that

$$\Delta V_w \approx I \Delta R_w \quad (4.11)$$

Differentiating Eq. IV.1, it is obtained,

$$\frac{\Delta R_w}{R_o} = \alpha \Delta T_w + 2\beta T_w \Delta T_w \approx \alpha \Delta T_w \quad (4.12)$$

Therefore,

$$\Delta R \approx k \Delta T_w \quad \text{since } \alpha \gg \beta , \quad (4.13)$$

where

$$k = \alpha R_o = \alpha R_w(0^\circ \text{C}) . \quad (4.14)$$

Hence the voltage trace of the wire during the pressure transient gives a direct indication of the heater temperature variation. A typical oscilloscope trace is shown in Fig. 12. The top trace is the pressure transient behavior and indicates that the transient from 760 torr to 420 torr was complete within 10 milliseconds of initiation. The middle curve is the voltage across the test wire with respect to time. The lowest is the current trace which demonstrates that the current was constant during the time frame of interest. The small fluctuations are typical of medium and high heat flux levels because of nucleation and



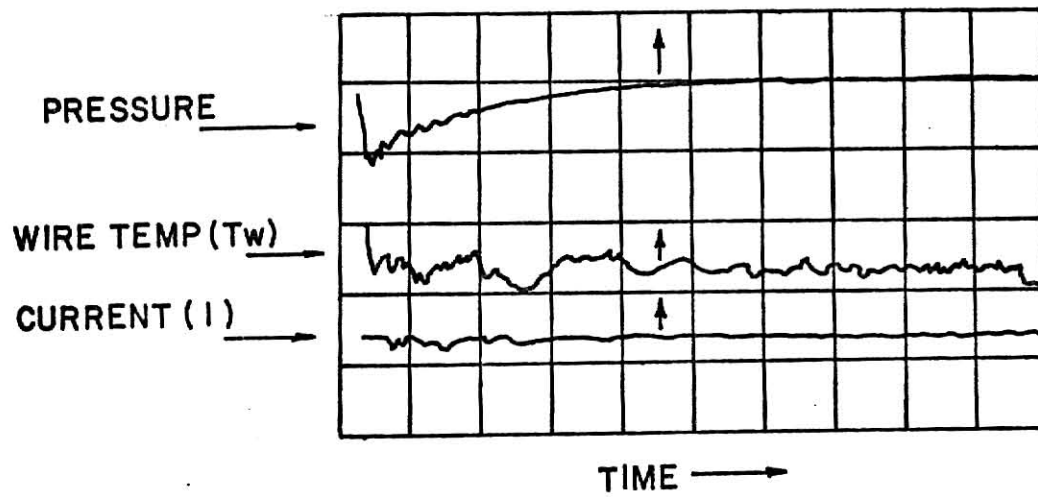


Fig. 12. Typical Pressure Transient Data.

Note: Arrows in the picture indicates positive increase direction.

subsequent bubble detachments altering the surface temperature at high frequency (39). In superheated experiments, the response of the pressure transducer becomes unstable. The oscilloscope trace indicated that after the first decompression, the pressure would decay further and went beyond the zero pressure level which is impossible. Hence, the pressure in superheated cases is assumed similar to that in subcooled cases. A summary of the experimental conditions and oscilloscope parameters for all the polaroid pictures cited here and after are listed in Table 3.

During the transient part of the experiment, 119 pictures were taken. The first 25 pictures were not useful for analysis because of the immature experimental technique. Out of the 94 following pictures, only 64 proved useful. Examples of these runs are shown and discussed in the following sections. Reduction of transient data is covered in Appendix C.

## 2. Discussion of the Results of Pressure Transient Experiments

### 1. Subcooled Case

When the bulk water remained subcooled during and after the pressure transient, no bulk flashing was induced. Typical results at different heat flux level are shown in Fig. 13, 14, and 15.

For low heat fluxes, no bubbles were generated on the heater surface before or after the transient. The heater temperature,  $T_w$ , was observed to drop almost 10 °C immediately after the transient. In this case, because natural convection was not affected significantly by the pressure,  $T_w$  always drifted back toward its original value at the end of the transient period.

TABLE 3. Summary of the Experimental Conditions and Oscilloscope Parameters for Fig. 12-20.

No. of Figure	$\frac{(Q/A)_{op}}{[(Q/A)_{CHF}]}$	$T_L$ ( $\pm 0.2^\circ\text{C}$ )	Sweep Speed (msec/Div.)	Voltage Sensitivity (Volts/Div.)			Observed Initial Voltage Drop of $V_w$ (volts)	Estimated Initial Temp. Drop of $T_w$ ( $^\circ\text{C}$ )
				$V_w$	$V_I$	$V_{\text{pressure}}$		
12	$\sim 0.8$	77	50	0.05 (DC)	0.05 (DC)	0.5 (AC)	0.035	7
13	$\sim 0.6$	70	50	0.05 (DC)	0.02 (DC)	0.5 (DC)	0.03	8.5
14	$\sim 0.8$	79	50	0.05 (DC)	0.05 (DC)	0.5 (AC)	0.04	8.2
15	$\sim 0.8$	82	50	0.05 (DC)	0.05 (DC)	0.5 (AC)	0.058	10.13
16	$\sim 1.1$	69	20	0.1 (DC)	0.05 (DC)	0.5 (DC)	0.060	11.9
17	$\sim 0.8$	90	50	0.05 (DC)	0.05 (DC)	0.05 (DC)	0.065	15.7
18	$\sim 0.8$	90	50	0.05 (DC)	0.05 (DC)	0.05 (AC)	0.064	12.9
19	$\sim 1.0$	92	20	0.1 (DC)	0.05 (DC)	0.5 (AC)	0.03	6.5
20	$\sim 1.0$	90	20	0.1 (DC)	0.05 (DC)	0.5 (DC)	0.05	11.8

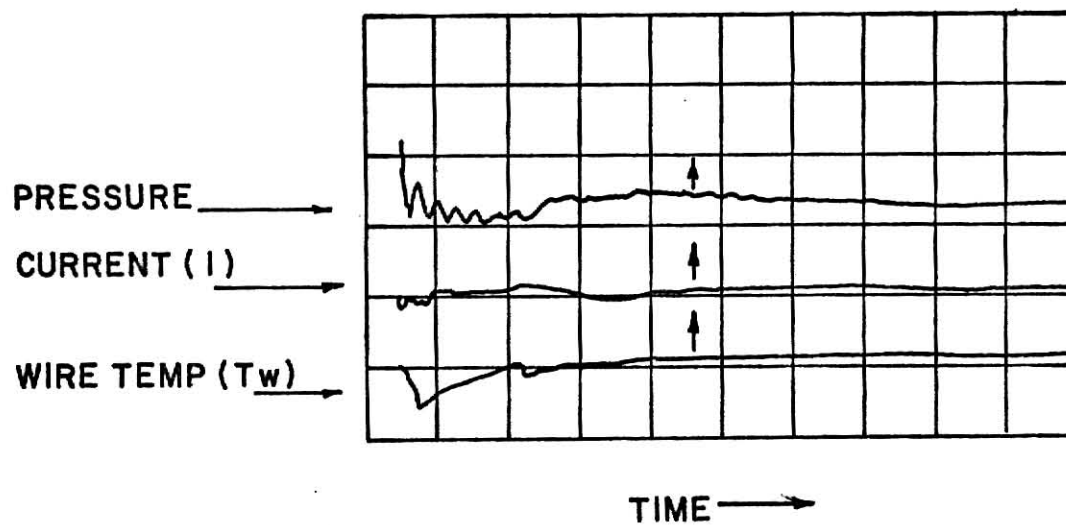


Figure 17.

Typical Sub-Cooled Data at Low Heat Flux.

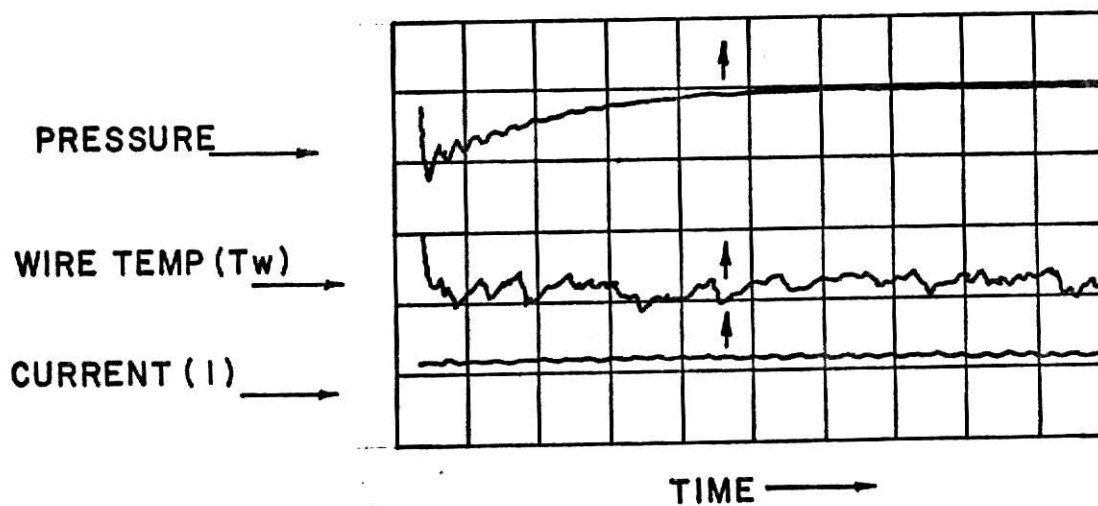


Figure 18.

Typical Sub-Cooled Data at Medium Heat Flux.

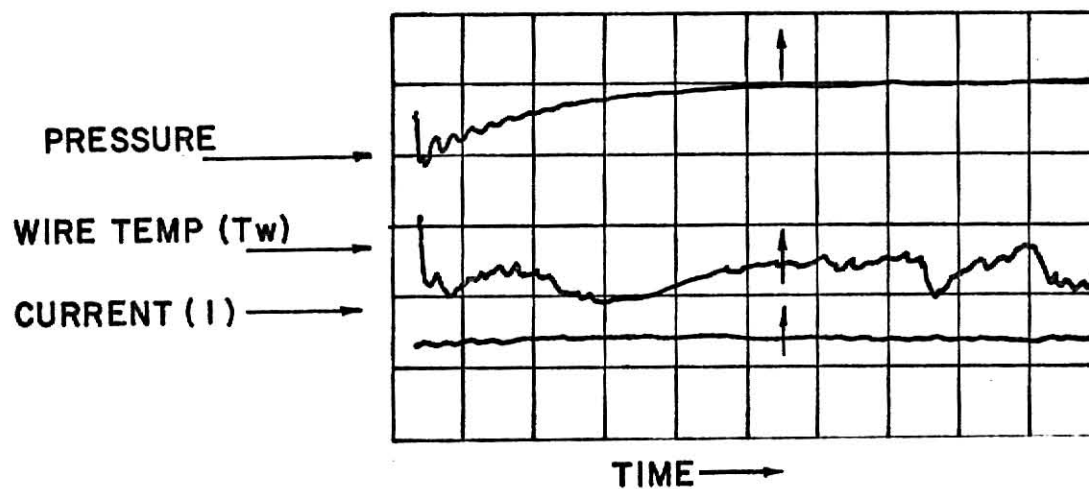


Fig. 15. Typical Sub-Cooled Data at Medium Heat Flux.

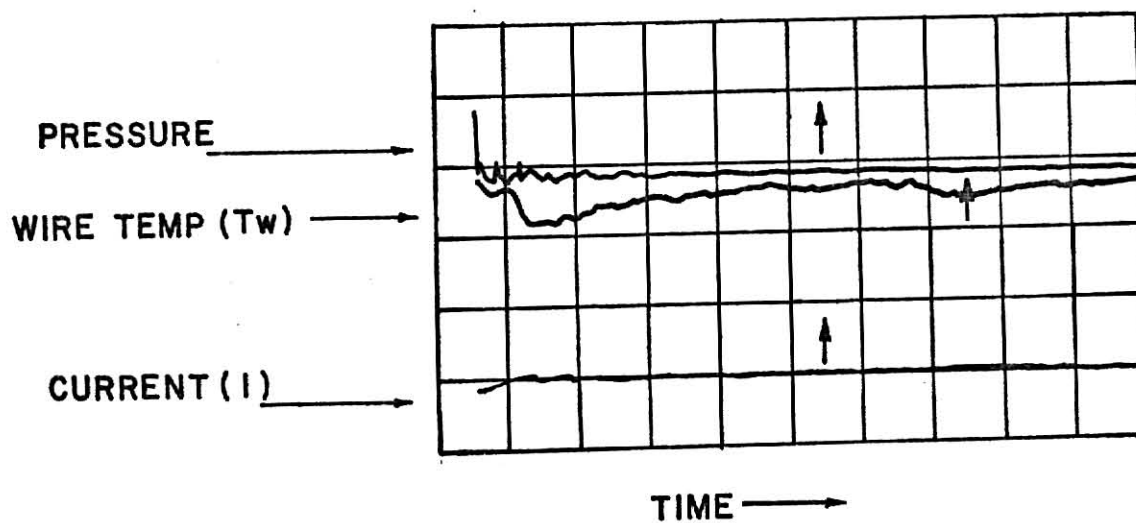


Fig. 16. Typical Sub-Cooled Data at High Heat Flux.

At medium levels of initial heat flux, nucleation was observed on the heater surface before the pressure transient. This bubble formation was enhanced by the reduced pressure during and after the decompression. Therefore, the heater temperature, which dropped initially during the decompression, remained at the reduced level due to the more vigorous nucleate boiling. The same result was obtained when another series of experiments with large initial subcoolings was conducted. In this case, a higher heat flux was applied. Consequently, even though the bulk fluid was well below the saturation temperature initially, nucleation on the wire was still present.  $T_w$  then stayed at the new reduced level of temperature after the transient. However, if the degree of initial subcooling was greatly increased, only natural convection contributed to the heat transfer. Therefore even if the applied heat flux was relatively high,  $T_w$ , in this case, drifted back to its original level. These results were shown in Fig. 15.

At high and very high heat flux levels, although  $T_w$  tended to drop initially as in the former cases, the boiling transitioned to film boiling and  $T_w$  increased due to reduced heat transfer. However, the delay from the start of the transient to the time of boiling transition was found to be very random. It ranged from 20 milliseconds to several hundred milliseconds. No boiling transition occurred during the decompression under any condition.

Two important results of subcooled depressurization deserve special emphasis. The first is the initial temperature drop under all conditions, even the most subcooled test in which no bubble mechanism existed during the entire event. This can be explained, perhaps, by turbulence in the surrounding liquid caused by the pressure wave. The rate of heat transfer

by convection between a solid boundary and a fluid is generally evaluated by means of Newton's Law of Cooling:

$$q_{\text{surface to fluid}} = A \bar{h}_c (T_w - T_\infty) , \quad (4.15)$$

where

$A$  = heat transfer surface

$\bar{h}_c$  = the convection coefficient,

$T_\infty$  = the water temperature,

$T_w$  = the temperature of test wire.

Once the pressure transient was initiated, the heat balance between the heat generation, which follows Ohm's law as

$$q_{\text{generated}} = I^2 R_w (T_w) , \quad (4.16)$$

and the convection heat flux was disturbed. The convection coefficient was increased because of the turbulence, and the wire temperature started to drop. This forced convection heat flux continued to be larger than the heat generation; therefore, the wire temperature continued to drop until thermal equilibrium was reestablished. In order to evaluate the magnitude of the change in  $\bar{h}_c$ , the condition prior to the pressure transient is referred to as 1, and 2 is the state of the reestablished equilibrium. If the following equations are used:

$$I^2 R_w (T_1) = (T_1 - T_L) \bar{h}_{c1} A , \quad (4.17)$$

$$I^2 R_w (T_2) = (T_2 - T_L) \bar{h}_{c2} A , \quad (4.18)$$

or

$$\bar{h}_{c1} = \frac{I^2 R_w (T_2)}{A (T_1 - T_L)} , \quad (4.19)$$

$$\bar{h}_{c2} = \frac{I^2}{A} \frac{R_w(T_2)}{(T_2 - T_L)} , \quad (4.20)$$

where current,  $I$ , is assumed constant, then from Eq. IV.1,

$$R_w(T_1) \approx R_o(1 + \alpha T_1) , \quad (4.21)$$

$$R_w(T_2) \approx R_o(1 + \alpha T_2) . \quad (4.22)$$

It may be easily found that the ratio of the heat transfer coefficients is:

$$\frac{\bar{h}_{c2}}{\bar{h}_{c1}} = \left( \frac{1 + \alpha T_2}{1 + \alpha T_1} \right) \left( \frac{T_1 - T_L}{T_2 - T_L} \right) . \quad (4.23)$$

As an example, for run #64,  $T_1$  was 170.5 °C,  $T_2 - T_1 = -10$  °C, and  $T_L = 82$  °C; therefore,

$$\begin{aligned} \frac{\bar{h}_{c2}}{\bar{h}_{c1}} &= \frac{1 + 0.00395 \times 165}{1 + 0.00395 \times 175} \frac{88.5}{78.5} , \\ &= 1.10 . \end{aligned}$$

The convection heat transfer caused by turbulence is estimated, in this case, to have been increased by 10%. Of course, further studies of the velocity field next to the wire are necessary to investigate this phenomena more completely. But, it can be seen that violent agitation by bubbles is not necessary to promote a heater surface temperature drops.

The second point of importance is the wire temperature behavior after the transient. It remained at a depressed level at high heat fluxes, but drifted back to its initial value at low heat fluxes. The explanation given in the first part of this section, which notes the presence of nucleate boiling for medium or high heat fluxes after the transient is applicable. But further study is needed because the heat transfer



immediately after the pressure transient is of special importance to the understanding of the effect of flashing, which will be discussed in the next section.

## ii. Superheated Cases

Superheated blowdown is much more complex than the preceeding subcooled cases, since bulk flashing is generated which influences the wire heat transfer. In this series, water in the test vessel was slightly subcooled initially so that vapor bubbles were generated throughout the bulk volume once the decompression was initiated. Hence, the objective was to determine the direct effect of the pressure transient and the indirect effect of the flashing on the heat transfer and boiling transition.

When the initial heat flux was low,  $T_w$  dropped during the pressure transient and remained at the lower level. By increasing the heat flux, the effect of flashing could be seen by comparing the transient wall temperature behavior with the subcooled cases. Instead of aiding the heat transfer, the flashing actually caused the heat transfer from the wire to deteriorate which resulted in the temperature peaks shown in Fig. 17.

As the initial heat flux was increased, the results, shown in Fig. 18, became unpredictable, because during some runs nucleate boiling persisted during and after the transient while during others, the boiling transitioned to film boiling with radiation augmentation. The characteristic fluctuation observed by Aoki, et al. as shown in Fig. 7, however, was not duplicated in these runs.

High initial heat fluxes were also studied. In all cases, film boiling was evidenced by the rapid temperature rise, as shown in Fig. 19, 20.

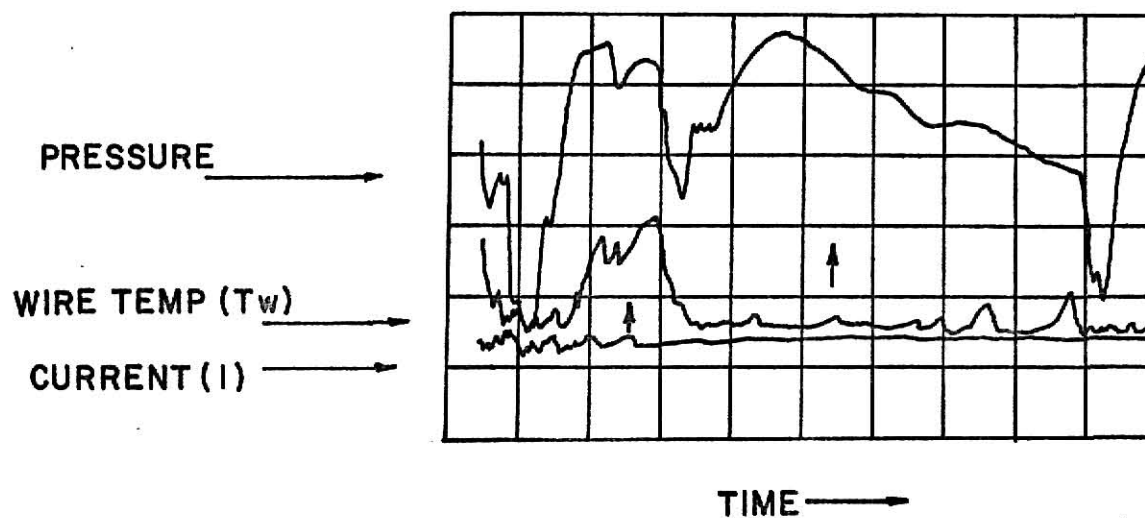


Fig. 17. Typical Superheated Data at Low Heat Flux.

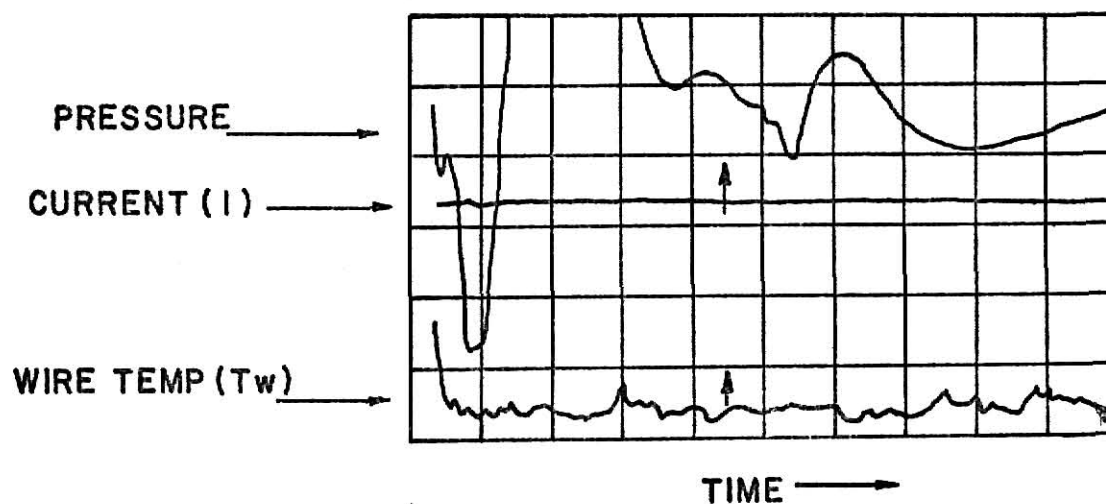


Fig. 18. Typical Superheated Data at Medium Heat Flux.

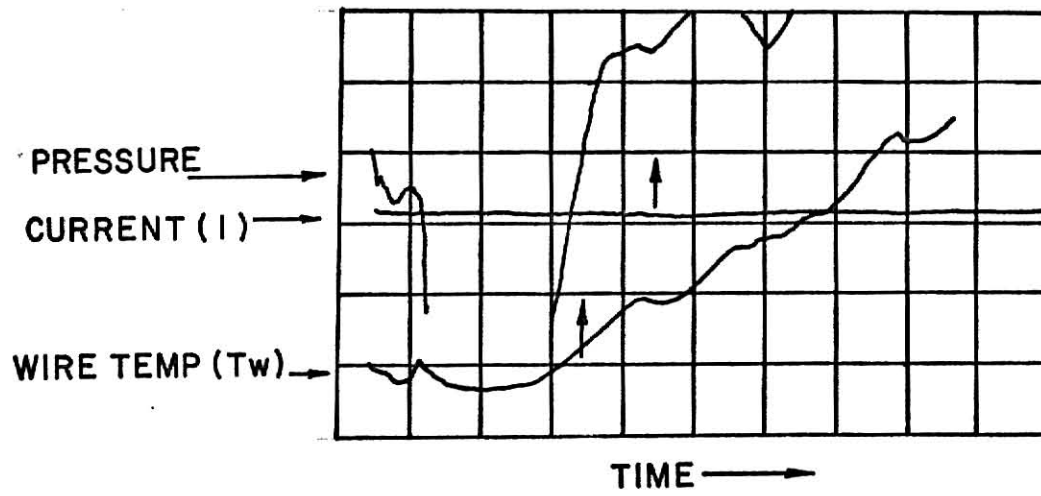


Fig. 19. Typical Superheated Data at High Heat Flux.

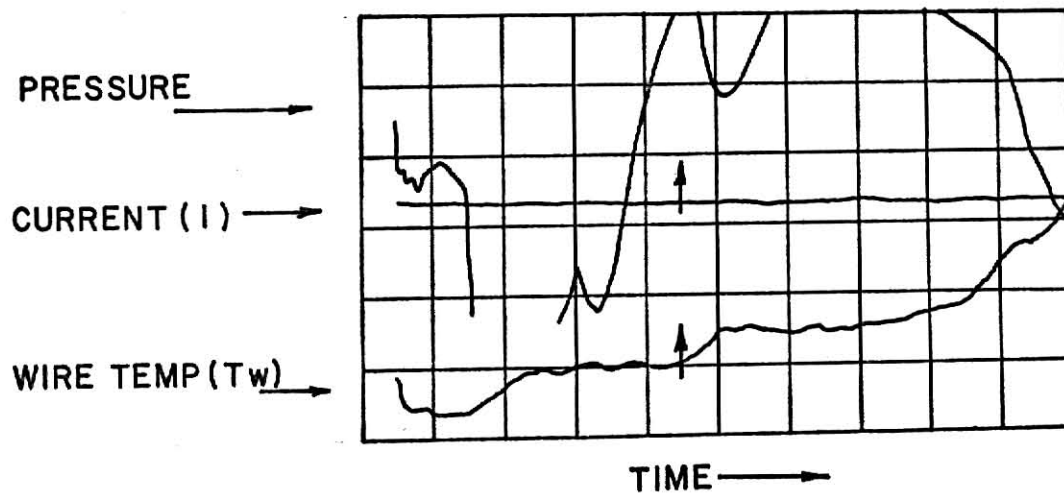


Fig. 20. Typical Superheated Data at High Heat Flux.

In all the runs,  $T_w$  dropped during the decompression, and rose rapidly as film boiling began. The secondary boiling reported in Aoki's work (3) could not be clearly identified. However, there was a delay time to boiling transition under all conditions, a result that should be regarded as one of the most important findings of the present study.

It has been explained previously, see for instance Howell and Bell (23), that the drop in wire temperature during the decompression is due to the violent flashing accompanying the decompression. That this is not the case is shown clearly by comparing the present subcooled blowdown results. The wire temperature drop during the transient was observed to be remarkably insensitive to not only flashing, but also the bulk water temperature. No significant dependence on the bulk water temperature can be found. This is contrary to what Aoki, et al. had reported, wherein the drop of  $T_w$  increased with increasing superheat as shown in Fig. 7. These results were generated, however, from a limited amount of data from saturated decompression only. Hence it must be concluded that  $\Delta T_w$ , the initial temperature drop, is a result of the pressure transient and not unique to flashing. Flashing, which only occurred in the superheated experiments, probably did not become significant during the rapid pressure decay and, therefore, could have had little effect on  $\Delta T_w$ . Hopper and Abdelmessih's investigation (22) supports this supposition. For decompression times of 5 milliseconds, they observed no bubble nucleation with less than 4 milliseconds delay beyond the termination of the decompression period. Moreover, it was found that several milliseconds were required for bubbles to grow to a significant size.

### iii. Conclusions of Transient Experiments

There are several interesting findings from this experiment, some of which had not been reported before. Among these are:

- (1) Boiling transition occurred after the completion of the pressure transient. This observation, as shown in Fig. 19 and 20 was also noted by Aoki, et al (3). But the "secondary boiling" postulated by them to explain this phenomenon was not identified in the current series of experiments. The time to the boiling transition after transient initiation and the characteristic behavior of the heater need to be studied further in order to make a definitive conclusion about the importance of "secondary boiling" and the pressure transient on transition.
- (2) The heater temperature dropped immediately after the pressure transient was initiated in both superheated and subcooled cases. The temperature depression in the superheated case was expected, but the temperature drop in subcooled transients has not been reported before. Furthermore, the amount of drop in the subcooled case was comparable to that in superheated depressurization. This, perhaps, indicates the importance of the convection current induced by the pressure wave propagation.
- (3) The amount of the initial heater temperature drop was found to be insensitive to the initial heat flux level and the surrounding coolant temperature. This is different from what Aoki, et al (3) had observed (see Fig. 7). However, the decompression rate in this experiment is approximately twice as fast as that used in the previous work. Since neither bubble nucleation in the bulk liquid nor that on the heating

surface is instantaneous, a critical decompression rate may exist which significantly alters the bubble growth history and, therefore, affects the heat transfer. This obviously places considerable importance on the study of bubble growth phenomena under pressure transients of varying time periods in future research.

- (4) The flashing may inhibit rather than enhance the heat transfer. Temperature peaks, observed only in the superheated cases, may imply that the heater surface experienced partial vapor insulation for a short period of time. The large amount of vapor generated during the process of flashing provides favorable conditions for the formation of a temporary vapor film on the heating surface.

#### C. Suggestions for Future Research

Since part of the purpose of this study was to be a first step in a comprehensive program, suggestions for future apparatus and areas of future interest are:

- (1) Since the input heat flux dominates the temporal behavior of the heater, as discussed in previous sections, a constant heat flux is desirable during and after the pressure transient. Therefore, a heating source isolated from the heat transfer surface is suggested.
- (2) At high heat fluxes in the nucleate boiling region, high frequency detachments from heating surface cause rapid fluctuations in both local and overall surface temperatures. Efficient averaging methods need to be developed to obtain reliable temperature measurements.
- (3) For rapid decompression work, the pressure history at the location of the heat transfer surface needs to be precisely recorded. A

pressure transducer for transient hydraulic pressure measurement mounted close to the heat transfer surface is recommended.

- (4) The pressure range needs to be extended, and a variable decompression rate is required to determine the actual effect of pressure transients on boiling heat transfer and transition.
- (5) Fast photography is recommended to investigate transient bubble growth. Such data, in turn, provides part of the information necessary for fundamental qualitative and quantitative analysis of the boiling process.

## REFERENCES

1. Adams, J. M., "An Investigation of Heat Transfer to Pool Boiling Mechanism," ASME paper 65-HT-49, Presented at 8th National Heat Transfer Conference, L.A., California, August 10, 1965.
2. Addoms, J. N., "Heat Transfer at High Rates to Water Boiling Outside Cylinders," D.Sc. Thesis, Chemical Engg. Department, M.I.T. (June, 1948).
3. Aoki, S., A. Inoue, and A. Mimura, "Boiling and Burnout Phenomena During Pressure Transient," Bulletin of the Tokyo Institute of Technology, No. 121, 1974.
4. Balzhiser, R. E., R. E. Barry, B. F. Caswell, R. L. Gahman, K. Y. Kim, and W. B. Lamber, "Critical Heat Flux Studies in Pool Boiling and Forced Convection," COO-1723-F.
5. Bankoff, S. G., and H. K. Fauske, "Improved Prediction of Critical Heat Flux in Liquid Metal Pool Boiling," Int. Heat Transfer Conference, 1974, Tokyo, Japan.
6. Berenson, P. J., "Experiments on Pool Boiling Heat Transfer," Int. J. Heat Mass Transfer, Vol. 5, pp. 985-99, (1962).
7. Bobst, R. W., and C. P. Colver, "Temperature Profiles Up to Burnout Adjacent to a Horizontal Heating Surface in Nucleate Pool-Boiling Water," CEP, Sympos. Ser., No. 64, Vol. 82, (1968).
8. Bonilla, C. F., "Nuclear Engineering," pp. 399-431, Chap. 9, McGraw-Hill, N.Y. (1957).
9. Butusov, I. V., "Automatic Control Measuring and Regulating Devices," Int. Ser. of Monographs on Automation and Automatic Control, Vol. 4, The Macmillan Co., N. Y. (1965).
10. Caswell, B. F. and R. E. Balzhiser, "The Critical Heat Flux for Boiling Liquid Metal System," 8th National Heat Transfer Conf., L.A., California, August 10, (1965).
11. Cermak, J. O., R. F. Farman, L. S. Tong, J. E. Casterline, S. Kokolis, and B. Matzmer, "The Departure from Nucleate Boiling in Rod Bundles During Pressure Blowdown," Trans. ASME, J. Heat Transfer, 92, (4), pp. 621-627, (1970).
12. Chang, Y. and N. W. Snyder, "Heat Transfer in Saturated Boiling," CEP, Sympos. Ser., No. 30, Vol. 56, (1960).
13. Cichelli, M. T. and C. F. Bonilla, Transactions A.I.Ch.E., 41, pp. 755-787, (1945).
14. Cobb, C. B. and E. L. Park, "Nucleate Boiling: A Maximum Heat Flux Correlation for Corresponding States of Liquids," CEP Sympos. Ser. No. 92, Vol. 65, p. 188, (1969).



16. Farber, E. A. and R. L. Scorah, "Heat Transfer to Water Boiling Under Pressure," Transaction of ASME, Vol. 70, pp. 369-82, May, 1948.
17. Forster, H. K. and R. Grief, "Heat Transfer to a Boiling Liquid Mechanisms and Correlations," Trans. ASME, J. Heat Transfer, Vol. 81 43 (1959).
18. Gambill, R. W., "A Survey of Boiling Burnout," Brit. Chem. Engg., Vol. 8, No. 2, pp. 93-98, Feb. 1963.
19. Gose, E. E., E. E. Perterson, and A. Acrivos, "On the Rate of Heat Transfer in Liquids with Gas Injection Through the Boundary Layer," J. Appl. Phys. Vol. 28, p. 1509 (1957).
20. Hall, W. B. and W. C. Harrison, "Transient Boiling of Water at Atmospheric Pressure," Int. Heat Transfer Conf., Chicago (1966).
21. Han, C. Y. and P. Griffith, "The Mechanism of Heat Transfer in Nucleate Boiling-Part I," Int. J. Heat Mass Transfer, Vol. 8, p. 887, (1965).
22. Hooper, F. C. And A. H. Abdelmessih, "The Flashing of Liquids of Higher Superheats," 3rd Int. Heat Transfer Conf., Chicago (1966).
23. Howell, J. R. and K. J. Bell, "An Experimental Investigation of the Effect of Pressure Transients on Pool Boiling Burnout," CEP Sympos. Ser., No. 41, Vol. 59, p. 88 (1963).
24. Hsu, Y. Y., "On the Size Range of Active Nucleation Cavities on a Heating Surface," Trans. of ASME, J. Heat Transfer, pp. 207-16, (1972).
25. Hsu, Y. Y. and R. W. Grahman, "Thermal Boundary Layer and Ebullition Cycle in Nucleate Boiling," NASA TN D-594 (1961).
26. Iida, Y. and K. Kobayasi, "An Experimental Investigation on the Mechanism of Pool Boiling Phenomena by a Probe Method," Fourth International Heat Transfer Conf., 1970, Vol. V, Paper B 1.2.
27. Johnson, H. A., "Transient Boiling Heat Transfer," Fourth Int. Heat Transfer Conf., 1970, Vol. V, Paper B 3.1.
28. Johnson, H. A., V. E. Schrock, F. B. Selph, et al., USAEC Report SAN-1001.
29. Judd, R. L. and K. S. Hwang, "A Comprehensive Model for Nucleate Pool Boiling Heat Transfer Including Microlayer Evaporation," Trans. of ASME, J. Heat Transfer, Vol. 98, pp. 623-29, November, 1976.
30. Kawamura, Hiroshi, F. Tachibana, and M. Akiyama, "Heat Transfer and DNB Heat Flux in Transient Boiling," Fourth Int. Heat Transfer Conf., 1970, Vol. V, Paper B 3.3.
31. Katto, Y. and S. Kokoya, "Principle Mechanism of Boiling Crisis in Pool Boiling," Int. J. Heat Mass Transfer Vol. 11, pp. 993-1002.
32. Kirby, D. B. and J. W. Westwafer, "Bubble and Vapor Behaviors on a Heated H. Plate During Pool Boiling Near Burnout," CEP, Symp. Ser., No. 57, Vol. 61, p. 238 (1965).

33. Kutateladze, S. S., "A Hydrodynamic Theory of Changes in the Boiling Process Under Free Convection Conditions," AEC-TR-1441, 1951.
34. Labuntsov, D. A., "Current Theories of Nucleate Boiling of Liquids," Heat Transfer--Soviet Research, Vol. 7, No. 3, May-June, 1975.
35. Lamb, H., Hydrodynamics, Dover Publications, Inc., New York, Chapter XI, (1954).
36. Mcadams, W. H., J. N. Addoms, P. M. Rinaldo, and R. S. Day, "Heat Transfer From Single Horizontal Wires to Boiling Water," CEP, No. 8, Vol. 44, pp. 639-46, (1948).
37. Mikic, B. B. and W. M. Rohsenow, "A New Correlation of Pool Boiling Data Including the Effect of Heating Surface Characteristics," Trans. of ASME, J. Heat Transfer, Vol. 91, pp. 245-50, May 1969.
38. Mixon, F. O., W. Y. Chon, and K. O. Beatty, "The Effect of Electrolytic Gas Evolution on Heat Transfer," CEP, No. 10, Vol. 55, p. 49 (1959).
39. Moore, F. D. and R. B. Mesler, "The Measurement of Rapid Surface Temperature Fluctuations During Nucleate Boiling of Water," AIChE. Vol. 7, No. 4, J., Vol. 7, pp. 620-24, (1961).
40. Noyes, N., "Boiling Sodium Heat Transfer," Proceedings of the Third Int. Heat Transfer Conference, Vol. 5, pp. 92-100, 1966.
41. Nukiyama, S., "Maximum and Minimum Values of Heat Transmission from Metal to Boiling Water Under Atmospheric Pressure," Journal of the Society of Mechanical Engineers, Japan, Vol. 36, pp. 367-74, June, 1934.
42. Peterson, W. C. and M. G. Zaalouk, "Boiling-Curve Measurements from a Controlled Heat-Transfer Process," Trans. of ASME, J. Heat Transfer, Vol. 93, pp. 408-12, Nov., 1971.
43. Robinson, D. B. and D. L. Katz, "Effect of Vapor Agitation on Boiling Coefficient," CEP, No. 6, Vol. 47, p. 317, (1951).
44. Rohsenow, W. M., "Developments in Heat Transfer," p. 225, MIT Press, 1964.
45. Rohsenow, W. M. and J. A. Clark, "Study of Mechanism of Boiling Heat Transfer," Trans. ASME, J. Heat Transfer, Vol. 73, p. 609 (1951).
46. Rohsenow, W. M. and P. Griffith, "Correlation of Maximum Heat Flux Data for Boiling of Saturated Liquids," Heat, Mass, and Momentum Transfer, Chap. 9, Prentice-Hill, N.Y., (1961).
47. Rosenthal, M. W. and R. L. Miller, "An Experimental Study of Transient Boiling," ORNL-2294, (1957).
48. Sakurai, A, K. Mizukami, and M. Shiotsu, "Experimental Studies on Transient Boiling Heat Transfer and Burnout," Int. Heat Transfer Conf., Vol. V, Paper No. B3.4, (1970).
49. Schrock, V. E., H. A. Johnson, A. Gopalakrishnan, K. E. Lavezzo, and S. M. Cho, USAEC Report SAN-1013.

50. Tachibana, F., M. Akiyama and H. Kawamura, "Heat Transfer and Critical Heat Flux in Transient Boiling--An Experimental Study in Saturated Pool Boiling," J. of Nuclear Science and Technology, Vol. 5, No. 3, pp. 117-26, March, (1968).
51. Tolubinskiy, V. I., Y. N. Ostrovskiy, and V. Y. Pisarev, "Effect of the Initial Heat Flux Level on the Transient Critical Heat Flux," Heat Transfer--Soviet Research, Vol. 8, No. 1, Jan.-Feb., (1976).
52. Tong, L. S., "Boiling Crisis and Critical Heat Flux," TID-25887, (1972).
53. Tong, L. S., Boiling Heat Transfer and Two-Phase Flow, John Wiley and Sons, Chap. 1, (1956).
54. Yu, Chi-Liang, "Nucleate Boiling Mechanism," Ph.D. Thesis, Dept. of Chem. Engg., University of Kansas, (1976).
55. Zuber, N., "Further Remarks on the Stability of Boiling Heat Transfer," AECU-3631, Jan., 1958.
56. Zuber, N., "On the Stability of Boiling Heat Transfer," Trans. ASME, Vol. 80, pp. 711-20, April, 1958.

## ACKNOWLEDGEMENT

The author wishes to express his gratitude to Dr. T. W. Lester for his guidance and help throughout this experiment. This is extended to Dr. J. O. Mingle, and Dr. F. Merklin, Department of Nuclear Engineering, and Dr. J. Kipp, Department of Mechanical Engineering for their very helpful advice. The technical assistance provided by Bill Starr, Patrick Gardner and Murry Roseberry is highly appreciated.

Finally, the author would like to thank Brenda Carney for her patience and excellent typing.

## APPENDICES

## Appendix A Computer Program for Processing Steady-State Experimental Data

PAGE 0001

10/48/18

DATE = 77175

MAIN

FORTRAN IV G LEVEL 21

```

0001 REAL IS(100),LENTH
0002 DIMENSION XARRAY(100),YARRAY(100)
0003 DIMENSION VS(100),VW(100),RW(100),H1(100),H2(100),H3(100),T(100),
1 DT(100)
0004 DIMENSION IBSUF(20000),IXNAME(30),IYNAME(30)
0005 DIMENSION TITLE(10)
0006 DIMENSION TITL(10),TIT(10)
0007 DIMENSION NN(3)

```

```

C THIS PROGRAM IS FOR PROCESSING STEADY-STATE DATA AND PLOTTING
C BOILING CURVE AT DIFFERENT PRESSURES

```

```

C WHERE LENTH: LENGTH OF THE TEST WIRE
C TEMP: WATER TEMPERATURE
C RSYS: RESISTANCE OF THE TEST WIRE INCLUDING THE
C ELECTRODES AND THE CONNECTIONS
C PRES: SYSTEM PRESSURE
C VS: VOLTAGE ACROSS THE SHUNT RESISTOR
C VW: VOLTAGE ACROSS THE TEST WIRE
C DT: WALL SUPERHEAT
C T: CALCULATED WIRE TEMPERATURE
C AREA: SURFACE AREA OF THE WIRE
C RTHED: THEORETICAL RESISTANCE OF THE TEST WIRE AT
C OPERATING TEMPERATURE

```

```

C SET UP PLOTTING PARAMETERS

```

```

0009 YFIRS=10**3
0010 YCYPIN=4./6.*0
0011 YLEN=6.0
0012 XFIRS=0.1
0013 XLIN=8.
0014 XCYPIN=5.0/8.*0
0015 READ(5,6000)(IXNAME(I),I=1,7)
0016 READ(5,6000)(IYNAME(I),I=1,7)
0017 READ(5,7000)IN
0018 CC 400 IN=1./IN
0019 READ(5,8000)(NN(I),I=1,3)
0020 READ(5,10000)(TITLE(I),I=1,5)
0021 READ(5,10000)(TITL(I),I=1,5)
0022 READ(5,10000)(TIT(I),I=1,5)
0023 READ(5,1100)RSYS
0024 1 FORMAT(2F6.4)
0025 READ(5,2)LENTH,TEMP,RSYS,PRES,RTI20,M
2 FORMAT(F5.3,F5.2,F5.4,F5.1,F8.6,I3)

```

```

C READ INPUT DATA

```

```

0026 READ(5,3)(VS(I),VW(I),I=1,M)
0027 WRITE(6,9000)NN
0028 WRITE(6,16000)TEMP
0029 WRITE(6,17000)PRES
0030 WRITE(6,18000)LENTH
0031 WRITE(6,19000)RSYS
0032 WRITE(6,15000)
0033 WRITE(6,14000)(I,VS(I),VW(I),I=1,M)
0034 FCPPAT(12F6.4)

```

## Appendix A (continued)

PAGE 0002

10/48/18

DATE = 77175

MAIN

FORTAN IV G LEVEL 21

```

0035 WRITE(6,20000)
0036 WRITE(6,30000)
0037 WRITE(6,40000)
0038 XARRAY(M+1)=-1.0
0039 XARRAY(M+2)=5.0/XLEN
0040 YARRAY(M+1)=3.0
0041 YARRAY(M+2)=4.0/YLEN
0042 NUMY=28
0043 NUMX=28

      C
      C
      C      CALCULATION
0044 A=0.00392
0045 B=-0.00000588
0046 RTI=1+A*TEMP+B*TEMP**2.0
0047 RTI=RTI/RTI20
0048 RTHEC=LENTH#R20*RTI
0049 SR=PSYS-RTHEC
0050 AREA=LENTH*3.1416*.005*2.54*2.54
0051 DC 100 I=1,M
0052 IS(I)=VS(I)/RS
0053 PW(I)=VM(I)/IS(I)-SR
0054 H1(I)=PW(I)*IS(I)**2.0/AREA
0055 H2(I)=H1(I)*3170.2
0056 H3(I)=H2(I)*2.7126
0057 T(I)=(-A*(A*2.0-4.0*B*(1.0-RTI*RTI20*PW(I)/RTHEC))**0.5)/(2.0*B)
0058 DT(I)=(T(I)-TEMP)
0059 WRITE(6,50001),IS(I),H2(I),H3(I),DT(I),RW(I),T(I)
0060 CONTINUE
0061 WRITE(6,11000)
0062 DC 300 I=1,M
0063 XARRAY(I)=ALOG10(DT(I))
0064 YARRAY(I)=ALOG10(H2(I))
0065 CONTINUE
0066 IF(MM-1)10,10,20

      C
      C
      C      PLCT
10 CALL LIMITS(150.,11.0,25.6,-3)
0067 CALL PLOTS(180,20000)
0068 CALL PLCT(0.,-11.,-3)
0069 CALL PLCT(12.,1.5,-3)
0070 CALL DLOGAX(0.,0.,XLEN,XCYPIN,0.,-1)
0071 CALL SLOGAX(XFIRS,+1,-1,IXNAME,-NUMX)
0072 CALL DLOGAX(0.,0.,YLEN,YCYPIN,90.,+1)
0073 CALL SLOGAX(YFIRS,+3,+1,IYNAME,-NUMY)
0074 CALL DLOGAX(0.,YLEN,XLEN,XCYPIN,0.,+1)
0075 CALL SLOGAX(XLEN,0.,YLEN,YCYPIN,90.,-1)
0076 CALL LINE(XARRAY,YARRAY,M,1,-1,1)
0077 CALL SYMBCL(0.5,0.0,0.125,TITLE,0.0,20)
0078 CALL SYMBCL(0.5,4.5,0.125,TITLE,0.0,20)
0079 CALL SYMBCL(0.5,4.5,0.125,TITLE,0.0,20)
0080 CALL SYMBCL(0.5,4.5,0.125,TITLE,0.0,20)
0081 GO TO 400
0082 CONTINUE
0083 CALL PLCT(XLEN+5.0,0.0,999)
0084 FORMAT(//4X,'NO. ',3X,'CURRENT(AMP)',15X,'HEAT FLUX',16X,'WALL SU
1PERHEAT(C)',3X,'RESISTANCE OF WIRE (OHM)',3X,'WIRE TEMP.(C)')
0085 FORMAT(32X,'BTU/FT**2HR',5X,'KCAL/M**2HR')

```

## Appendix A (continued)

PAGE 0003

```

FORTRAN IV G LEVEL 21      MAIN      DATE = 77175      10/48/18
0C86      5000  FCRMAT(3X,12,6X,E13.6,7X,E13.6,3X,E13.6,5X,E13.6,9X,E13.6,12X,E13
1.6)
0C87      6000  FCRMAT(7A4)
0C88      7000  FCRPMAT(12)
0C89      8000  FCRMAT(313)
0C90      9000  FCRMAT(2X,'RUN NJ.',2X,313/)
0C91      10000 FCRMAT(514)
0C92      11000 FCRMAT(1H1)
0C93      12000 FCRMAT(F4.1)
0C94      13000 FCRPMAT(1X,6E13.6,1X,214)
0C95      14000 FCRMAT(3X,12,14X,F6.4,2CX,F6.4)
0C96      15000 FCRMAT(1X,'DATA PCINT',2X,'V. ACROSS SHUNT RESISTOR',2X,'V. ACROSS
1S TEST WIRE'//)
0C97      16000 FCRMAT(2X,'WATER TEMPERATURE =',2X,F4.1,'C'//)
0C98      17000 FCRMAT(2X,'SYSTEM PRESSURE =',2X,F4.0,1X,'TORR'//)
0C99      18000 FCRMAT(2X,'TEST WIRE LENGTH =',2X,F5.3,1X,'INCH'//)
0100      19000 FCRMAT(2X,'SYSTEM RESISTANCE AT SYSTEM TEMPERATURE =',1X,F5.4,1X,
1.0PHM'//)
0101      20000 FCRMAT(///2X,'RESULTS OF CALCULATION'//)
0102      STOP
0103      END

```



## Appendix A (continued)

RUN NO. 101276 1

WATER TEMPERATURE = 83.0C

SYSTEM PRESSURE = 420. TORR

TEST WIRE LENGTH = 0.860 INCH

SYSTEM RESISTANCE AT SYSTEM TEMPERATURE = .2390 OHM

DATA POINT V. ACROSS SHUNT RESISTOR V. ACROSS TEST WIRE

1	0.0534	0.0583
2	0.1010	0.1111
3	0.2142	0.2357
4	0.4050	0.4520
5	0.6390	0.7280
6	0.8640	0.9350
7	0.5380	1.1010
8	0.9690	1.1650
9	0.5510	1.1930
10	0.5580	3.0600
11	0.8130	3.0900
12	1.5290	1.2470
13	0.7800	2.7800
14	0.7470	2.4100
15	0.8350	3.3400
16	0.8670	3.6000
17	0.8820	3.8000

## RESULTS OF CALCULATION

NO.	CURRENT (AMP)	HEAT FLUX BTU/FT**2HR	KCAL/M**2HR	WALL SUPERHEAT (C)	RESISTANCE OF WIRE (OHM)	WIRE TEMP. (C)
1	0.236283E 00	0.472249E C3	0.128102E 04	0.119165E 02	0.232544E 00	0.949165E 02
2	0.44903E 00	0.170252E C4	0.461935E 04	0.147537E 02	0.234406E 00	0.977937E 02
3	0.547738E 00	0.766209E C4	0.207842E 05	0.149233E 02	0.234491E 00	0.979233E 02
4	0.179204E J1	0.278055E C5	0.754252E C5	0.204016E 02	0.238033E 00	0.103402E 03
5	0.282743E 01	0.707452E C5	0.191903E C6	0.285356E 02	0.243284E 00	0.111536E 03
6	0.355752E 01	0.114458E C6	0.313430E C6	0.368393E 02	0.248630E 00	0.119839E 03
7	0.415044E 01	0.157326E C6	0.426761E C6	0.40494E 02	0.251079E 00	0.123649E 03
8	0.423761E C1	0.172203E C6	0.467118E C6	0.506951E 02	0.257519E 00	0.133695E 03
9	0.438456E 01	0.180358E C6	0.489239E C6	0.512473E 02	0.257873E 00	0.134247E 03
10	0.441593E 01	0.481455E C6	0.130599E C7	0.795313E 03	0.678752E 00	0.878313E 03
11	0.359735E 01	0.357653E C6	0.107867E C7	0.116045E 04	0.844773E 00	0.124345E 04
12	0.455309E J1	0.195822E C6	0.531187E C6	0.543903E 02	0.259686E 00	0.137080E 03
13	0.345133E 01	0.342854E C6	0.930026E C6	0.103625E 04	0.791253E 00	0.111925E 04
14	0.330521E C1	0.284113E C6	0.770686E C6	0.870118E 03	0.714936E 00	0.953118E 03
15	0.369469E C1	0.441826E C6	0.119850E C7	0.127108E 04	0.889806E 00	0.135408E 04
16	0.363628E C1	0.494759E C6	0.134208E C7	0.135996E 04	0.924214E 00	0.144296E 04

## Appendix A (continued)

RUN NC. 150776 4

WATER TEMPERATURE = 53.5C

SYSTEM PRESSURE = 600. TORR

TEST WIRE LENGTH = 0.760 INCH

SYSTEM RESISTANCE AT SYSTEM TEMPERATURE = .2190 CHW

DATA PCINT V. ACROSS SHUNT RESISTOR V. ACROSS TEST WIRE

1	0.0574	0.0581
2	0.0658	0.0668
3	0.0712	0.0722
4	0.0815	0.0828
5	0.0925	0.0939
6	0.1067	0.1084
7	0.1214	0.1235
8	0.1345	0.1368
9	0.1439	0.1465
10	0.1627	0.1660
11	0.1717	0.1754
12	0.1931	0.1977
13	0.2131	0.2185
14	0.2378	0.2448
15	0.2470	0.2545
16	0.2575	0.2656
17	0.2805	0.2904
18	0.3440	0.3581
19	0.3645	0.3811
20	0.3859	0.4055
21	0.4133	0.4360
22	0.4429	0.4658
23	0.4700	0.5000
24	0.4925	0.5258
25	0.5001	0.5360
26	0.5257	0.5660
27	0.5312	0.5867
28	0.5429	0.5800
29	0.5735	0.6147
30	0.5974	0.6350
31	0.6136	0.6510
32	0.6374	0.6790
33	0.6240	0.7070
34	0.6875	0.7350
35	0.7524	0.8060
36	0.7754	0.8300
37	0.7891	0.8460
38	0.8116	0.8730
39	0.9138	0.9790
40	0.9240	0.9910
41	0.9407	1.0080
42	0.9420	1.0060
43	0.9514	1.0150
44	0.9590	1.0290
45	0.9827	1.0520
46	0.7810	2.2600

## Appendix A (continued)

RESULTS OF CALCULATION						
AC.	CURRENT (AMP)	HEAT FLUX	WALL SUPERHEAT(C)	RESISTANCE OF WIRE (OHM)	WIRE TEMP.(C)	
		BTU/FT**2HR	KCAL/M**2HR			
1	0.25382E 00	0.565352E 03	0.154453E C4	0.170738E 02	0.214447E 00	0.110574E 03
2	0.291150E 00	0.750605E 03	0.203609E 04	0.182629E 02	0.215125E 00	0.111763E 03
3	0.315044E 00	0.877794E 03	0.238110E 04	0.178052E 02	0.214865E 00	0.111305E 03
4	0.363619E 00	0.115244E 04	0.312611E 04	0.185641E 02	0.215295E 00	0.112064E 03
5	0.409292E 00	0.148325E 04	0.407346E 04	0.182384E 02	0.215111E 00	0.111738E 03
6	0.472124E 00	0.151526E 04	0.535808E 04	0.185549E 02	0.215291E 00	0.112055E 03
7	0.537168E 00	0.256368E 04	0.654609E 04	0.190386E 02	0.215600E 00	0.112599E 03
8	0.555133E 00	0.314247E 04	0.852427E 04	0.190189E 02	0.215555E 00	0.112519E 03
9	0.636726E 00	0.360071E 04	0.916729E 04	0.194027E 02	0.215774E 00	0.112903E 03
10	0.717912E 00	0.461368E 04	0.125151E 05	0.202810E 02	0.216274E 00	0.113781E 03
11	0.758734E 00	0.514503E 04	0.139564E 05	0.207845E 02	0.216561E 00	0.114284E 03
12	0.854425E 00	0.652251E 04	0.176940E 05	0.216869E 02	0.217074E 00	0.115187E 03
13	0.542532E 00	0.755663E 04	0.213832E 05	0.222913E 02	0.217417E 00	0.115791E 03
14	0.105721E 01	0.555018E 04	0.269909E 05	0.239172E 02	0.218343E 00	0.117417E 03
15	0.109252E 01	0.107453E 05	0.291477E 05	0.242884E 02	0.218553E 00	0.117788E 03
16	0.113538E 01	0.116915E 05	0.317143E 05	0.247208E 02	0.218800E 00	0.118221E 03
17	0.124292E 01	0.135465E 05	0.378323E 05	0.256619E 02	0.219334E 00	0.119162E 03
18	0.152212E 01	0.210711E 05	0.571574E 05	0.285114E 02	0.220954E 00	0.122011E 03
19	0.161283E 01	0.237675E 05	0.644717E 05	0.303270E 02	0.221983E 00	0.123827E 03
20	0.170708E 01	0.267760E 05	0.726326E 05	0.325238E 02	0.223231E 00	0.126024E 03
21	0.182875E 01	0.308494E 05	0.836822E 05	0.340631E 02	0.224103E 00	0.127565E 03
22	0.155973E 01	0.356341E 05	0.566811E 05	0.363815E 02	0.225417E 00	0.129882E 03
23	0.207945E 01	0.402527E 05	0.109190E 06	0.376156E 02	0.226116E 00	0.131116E 03
24	0.217923E 01	0.443661E 05	0.120348E 06	0.391270E 02	0.226971E 00	0.132627E 03
25	0.221283E 01	0.4559360E 05	0.124606E 06	0.407931E 02	0.227914E 00	0.134293E 03
26	0.232611E 01	0.459360E 05	0.138355E 06	0.427420E 02	0.229016E 00	0.136242E 03
27	0.235044E 01	0.510045E 05	0.139855E 06	0.388156E 02	0.226794E 00	0.132316E 03

## Appendix A (continued)

28	0.242221E 01	0.535499E 05	0.146345E 06	0.394169E 02	0.227135E 00	0.132917E 03
29	0.253761E 01	C.6C4128E 05	0.163876E 06	0.408144E 02	0.227928E 00	0.134314E 03
30	0.264336E 01	0.645745E C5	0.176250E C6	0.372614E 02	0.225915E 00	0.130761E 03
31	0.271504E 01	0.684099E 05	0.185568E 06	0.364671E 02	0.225466E C0	0.129567E 03
32	0.282335E 01	0.741389E C5	0.201109E C6	0.381897E 02	0.226440E 00	0.131690E 03
33	0.286106E 01	0.758587E 05	0.205774E 06	0.653521E 02	0.241751E 00	0.158852E 03
34	0.304274E 01	C.8658C8E 05	0.234859E 06	0.357190E 02	0.227305E 00	0.133219E 03
35	0.329292E 01	0.103921E C6	0.231895E 06	0.405765E 02	0.227790E 00	0.134076E 03
36	0.343357E 01	0.110281E C6	0.259143E 06	0.402473E 02	0.227604E 00	0.133747E 03
37	0.349159E 01	C.1144C4E C6	0.310333E 06	0.409214E 02	0.227987E 00	0.134421E 03
38	0.359115E 01	0.121447E C6	0.329436E 06	0.423395E 02	0.228788E 00	0.135840E 03
39	0.404336E 01	C.1533C4E C6	0.415853E 06	0.406192E 02	0.227816E 00	0.134119E 03
40	0.403853E 01	0.156926E C6	0.425677E 06	0.410829E 02	0.228078E 00	0.134583E 03
41	0.416239E C1	0.162494E C6	0.440780E 06	0.406954E 02	0.227859E 00	0.134195E 03
42	0.415814E 01	0.162875E C6	0.441817E 06	0.405307E 02	0.227765E 00	0.134031E 03
43	0.420973E 01	0.166130E C6	0.450645E 06	0.405002E 02	0.227748E 00	0.134000E 03
44	0.424335E 01	0.169120E C6	0.458755E 06	0.412751E 02	0.228187E 00	0.134775E 03
45	0.424823E 01	C.177148E C6	0.480530E C6	0.402898E 02	0.227628E 00	0.133790E 03
46	0.345575E 01	0.314433E C6	0.852930E 06	0.878389E 03	0.635672E 00	0.936165E 03
47	C.333J53E C1	C.293824E C6	0.797027E C6	0.842665E 03	0.588763E 00	0.852958E 03
48	0.328319E 01	0.261226E C6	0.708602E 06	0.755458E 03	0.624643E 00	0.936165E 03
49	0.321631E 01	C.240182E C6	0.651519E 06	0.703404E 03	0.547569E 00	0.796704E 03
50	0.320354E C1	0.231304E C6	0.627436E C6	0.667245E 03	0.563902E 00	0.760745E 03
51	0.305310E 01	0.183012E C6	0.496439E 06	0.516511E 03	0.476955E 00	0.610011E 03
52	0.253717E 01	0.156737E C6	0.425165E 06	0.445717E 03	0.424263E 00	0.539217E 03
53	0.253717E 01	0.604656E C5	0.164019E 06	0.413086E 02	0.228205E 00	0.134309E 03
54	0.374336E 01	0.133563E C6	0.363387E 06	0.484872E 02	0.232260E 00	0.141987E 03
55	0.391372E 01	C.146916E C6	0.398523E 06	0.498443E 02	0.233026E 00	0.143344E 03
56	0.428628E 01	0.175439E C6	0.476980E 06	0.485558E 02	0.232524E 00	0.142456E 03
57	0.366314E C1	0.384633E C6	0.104336E 07	0.101356E 04	0.694496E 00	0.110706E 04
58	0.370736E 01	C.395456E C6	0.1C8343E C7	0.104236E 04	0.705762E 00	0.113586E 04
59	0.375664E 01	0.421549E C6	0.114349E C7	0.109433E 04	0.725714E 00	0.118783E 04
60	0.377976E 01	C.436427E C6	0.118385E 07	0.113918E 04	0.742552E 00	0.123268E 04
61	0.384071E 01	0.455249E C6	0.124576E C7	0.117675E 04	0.756382E 00	0.127025E 04
62	0.356503E C1	0.511868E 06	0.138649E 07	0.126938E 04	0.789414E 00	0.136289E 04
63	0.402655E 01	C.537723E C6	0.145320E 07	0.130808E 04	0.803767E 00	0.140158E 04
64	0.408503E 01	0.562327E 06	0.152537E 07	0.135103E 04	0.817292E 00	0.144459E 04
65	0.419227E 01	0.612254E C6	0.166091E 07	0.144291E 04	0.847217E 00	0.153641E 04
66	0.431416E 01	0.665149E C6	0.181513E 07	0.152753E 04	0.873465E 00	0.162103E 04

## Appendix A (continued)

RUN NO. 270776 5

WATER TEMPERATURE = 86.5C

SYSTEM PRESSURE = 500. TORR

TEST WIRE LENGTH = 0.800 INCH

SYSTEM RESISTANCE AT SYSTEM TEMPERATURE = .2450 OHM

DATA PCINT V. ACROSS SHUNT RESISTOR V. ACROSS TEST WIRE

1	0.0484	0.0550
2	0.0556	0.0632
3	0.0625	0.0705
4	0.0926	0.1053
5	0.0593	0.1128
6	0.1198	0.1367
7	0.1282	0.1582
8	0.1558	0.1782
9	0.1733	0.1923
10	0.1831	0.2098
11	0.2054	0.2360
12	0.2225	0.2560
13	0.2468	0.2830
14	0.2712	0.3140
15	0.2956	0.3435
16	0.3265	0.3804
17	0.3881	0.4570
18	0.4145	0.4670
19	0.4443	0.5210
20	0.4788	0.5650
21	0.5210	0.6100
22	0.5683	0.6654
23	0.5986	0.7025
24	0.6345	0.7450
25	0.6817	0.8005
26	0.6554	0.8220
27	0.7172	0.8410
28	0.7450	0.8750
29	0.7519	0.8850
30	0.7250	0.9100
31	0.7541	0.9370
32	0.8091	0.9570
33	0.8214	0.9715
34	0.8457	1.0030
35	0.8682	1.0310
36	0.8860	1.0540
37	0.8085	1.0810
38	0.9271	1.1050
39	0.9491	1.1330
40	0.9668	1.1570
41	0.7150	2.0000
42	0.6810	1.7800
43	0.7650	2.4800
44	0.7450	2.2800
45	0.7290	2.1600
46	0.7140	2.0600

## Appendix A (continued)

NC.	CURRENT (AMP)	HEAT FLUX		WALL SUPERHEAT (C)	RESISTANCE OF WIRE (OHM)	WIRE TEMP. (C)
		BTL/FT**2HR	KCAL/M**2HR			
47	0.7040	C.4022C1E C3	0.100101E C4	0.196263E 02	0.224265E 00	0.108126E 03
48	0.6710	0.530940F 03	0.146023E 04	0.197495E 02	0.224338E 00	0.108249E 03
49	0.6570	0.665349E 03	0.181568E 04	0.189851E 02	0.223821E 00	0.107385E 03
50	0.7750	0.147339E 04	0.299672E 04	0.199217E 02	0.224442E 00	0.108422E 03
51	0.7870	0.168790E 04	0.457850E 04	0.207673E 02	0.224949E 00	0.109267E 03
52	0.8040	0.247583E C4	0.671593E 04	0.213975E 02	0.225328E 00	0.109898E 03
53	0.8380	0.330681E 04	0.897305E 04	0.227713E 02	0.226153E 00	0.111271E 03
54	0.8170	0.415873E 04	0.113895E 05	0.224149E 02	0.225939E 00	0.110915E 03
55	0.9290	0.515746E 04	0.140386E C5	0.225993E 02	0.226049E 00	0.111099E 03
56	0.8470	0.581097E 04	0.157628E C5	0.231893E 02	0.226402E 00	0.111689E 03
57	0.8650	0.733566E 04	0.158987E C5	0.243782E 02	0.227115E 00	0.112878E 03
58	0.8750	0.862149E 04	0.213066E 05	0.249739E 02	0.227473E 00	0.113474E 03
59	0.8900	0.108924E 05	0.295468E 05	0.259642E 02	0.228007E 00	0.114364E 03
60	0.8530	0.129009E 05	0.349950E C5	0.277119E 02	0.229113E 00	0.116212E 03
61	0.9070	0.153507E 05	0.417487E C5	0.293068E 02	0.230068E 00	0.117807E 03
62	0.9190	0.188326E C5	0.510853E 05	0.304565E 02	0.230755E 00	0.118957E 03
63	0.9280	0.269335E C5	0.730598E 05	0.351616E 02	0.233568E 00	0.123662E 03
64	0.9370	0.306444E 05	0.831261E 05	0.341697E 02	0.232976E 00	0.122670E 03
65	0.9480	0.351313E 05	0.952972E 05	0.333093E 02	0.232461E 00	0.121809E 03
66	0.9570	0.410926E 05	0.114468E C6	0.361074E 02	0.234134E 00	0.124607E 03
		0.482230E 05	0.130810E 06	0.326260E 02	0.232053E 00	0.121126E 03
		0.574219E 05	0.155763E 06	0.322493E 02	0.231828E 00	0.120749E 03
		0.638281E 05	0.173140E 06	0.336445E 02	0.232674E 00	0.122164E 03
		C.717541E 05	0.194640E 06	0.338848E 02	0.232805E 00	0.122385E 03
		C.826361E 05	0.224701E 06	0.339278E 02	0.232831E 00	0.122428E 03
		C.872800E 05	0.236756E 06	0.343166E 02	0.233063E 00	0.122817E 03
		C.915410E 05	0.248314E C6	0.333031E 02	0.232458E 00	0.121803E 03

RESULTS OF CALCULATION

## Appendix A (continued)

28	0.329546E 01	0.585598E 05	0.268428E 06	0.340135E 02	0.232883E 00	0.122514E 03
29	0.332699E C1	0.101044E C6	0.274292E C6	0.349688E 02	0.233452E C0	0.123469E 03
30	0.320765E 01	0.101051E 06	0.274111E C6	0.646708E 02	0.251115E 00	0.153171E 03
31	0.351372E C1	0.113024E 06	0.306593E C6	0.360767E 02	0.234116E 00	0.124577E 03
32	0.353309E 01	0.117657E C6	0.319155E C6	0.371538E 02	0.234758E 00	0.125654E 03
33	0.363451E 01	0.121254E 06	0.328914E C6	0.371332E 02	0.234745E 00	0.125632E 03
34	0.374204E C1	0.126539E 06	0.349758E C6	0.383678E 02	0.235482E 00	0.126869E 03
35	0.384159E 01	0.136088E 06	0.369153E C6	0.389398E 02	0.235824E 00	0.127440E 03
36	0.382035E 01	0.142011E 06	0.385219E C6	0.397375E 02	0.236300E 00	0.128237E 03
37	0.401041E 01	0.149352E 06	0.405132E C6	0.398355E 02	0.236358E 00	0.128335E 03
38	0.412215E 01	0.155830E 06	0.422704E C6	0.405603E 02	0.236813E 00	0.129096E 03
39	0.419956E 01	0.163605E 06	0.443795E C6	0.413083E 02	0.237237E 00	0.129809E 03
40	0.427739E C1	0.170245E C6	0.461906E C6	0.424324E 02	0.237908E 00	0.130932E 03
41	0.316372E 01	0.234640E 06	0.636593E C6	0.721216E 03	0.596614E 00	0.809716E 03
42	0.313727E 01	0.158175E 06	0.537569E C6	0.634465E 03	0.559166E 00	0.722965E 03
43	0.338498E 01	0.213671E 06	0.850864E C6	0.545079E 03	0.700100E 00	0.103358E 04
44	0.325645E C1	0.280362E C6	0.759695E C6	0.851203E 03	0.659097E 00	0.939703E 03
45	0.322555E 01	0.255202E C6	0.703111E C6	0.802275E 03	0.637076E 00	0.890775E 03
46	0.315927E 01	0.241782E 06	0.659856E C6	0.763895E 03	0.619451E 00	0.852395E 03
47	0.311534E C1	0.225172E C6	0.613801E C6	0.708107E 03	0.593441E 00	0.796607E 03
48	0.296903E C1	0.191949E 06	0.520682E C6	0.631790E 03	0.556865E 00	0.723290E 03
49	0.280763E 01	0.174532E 06	0.473436E C6	0.573393E 03	0.528146E 00	0.661893E 03
50	0.348239E 01	0.320263E 06	0.868737E C6	0.536635E 03	0.696479E 00	0.102513E 04
51	0.345409E 06	0.345409E C6	0.936956E C6	0.101226E 04	0.728437E 00	0.110076E 04
52	0.355752E 01	0.376614E C6	0.100533E C7	0.106294E 04	0.749899E 00	0.115054E 04
53	0.357522E C1	0.375367E C6	0.102907E C7	0.108759E 04	0.759006E 00	0.117558E 04
54	0.361506E C1	0.406027E 06	0.110139E C7	0.117747E 04	0.794545E 00	0.126597E 04
55	0.365314E 01	0.410309E C6	0.111300E C7	0.113951E 04	0.779847E 00	0.122811E 04
56	0.374779E 01	0.443750E C6	0.120372E C7	0.121258E 04	0.807942E 00	0.130108E 04
57	0.382743E 01	0.472249E C6	0.128102E C7	0.125661E 04	0.824417E 00	0.134511E 04
58	0.367169E 01	0.486575E C6	0.131988E C7	0.127298E 04	0.830120E 00	0.136058E 04
59	0.389381E 01	0.502943E 06	0.136433E C7	0.132233E 04	0.849333E 00	0.141083E 04
60	0.395133E C1	0.531720E 06	0.144234E C7	0.138658E 04	0.870940E 00	0.147508E 04
61	0.401327E 01	0.557002E 06	0.151092E C7	0.142592E 04	0.884403E 00	0.151442E 04
62	0.406135E 01	0.565839E 06	0.154580E C7	0.142256E 04	0.883263E 00	0.151106E 04
63	0.410620E 01	0.585469E 06	0.158814E C7	0.143660E 04	0.888006E 00	0.152510E 04
64	0.414602E 01	0.602285E 06	0.163376E C7	0.146095E 04	0.896048E 00	0.154915E 04
65	0.419469E 01	0.625458E 06	0.168673E C7	0.150044E 04	0.909113E 00	0.158894E 04
66	0.423451E 01	0.651091E 06	0.176615E C7	0.156151E 04	0.928596E 00	0.165001E 04





## Appendix A (continued)

1	0.325221E 00	0.523453E 03	0.250507E 04	0.179989E 02	0.223289E 00	0.106499E 03
2	0.393708E 00	0.133311E 04	0.361620E 04	0.180727E 02	0.223333E 00	0.106573E 03
3	0.498253E 00	0.247762E 04	0.672079E 04	0.699276E 02	0.266007E 00	0.178428E 03
4	0.547345E 00	0.266717E 04	0.723479E 04	0.253146E 02	0.227678E 00	0.113815E 03
5	0.635283E 00	0.354939E 04	0.962803E 04	0.195249E 02	0.224204E 00	0.139025E 03
6	0.701327E 00	0.432478E 04	0.117314E 05	0.206198E 02	0.224861E 00	0.109120E 03
7	0.851770E 00	0.638536E 04	0.173249E 05	0.205795E 02	0.225077E 00	0.109480E 03
8	0.575221E 00	0.838407E 04	0.227426E 05	0.215913E 02	0.225444E 00	0.110091E 03
9	0.118628E 01	0.124899E 05	0.338300E 05	0.241386E 02	0.226972E 00	0.112639E 03
10	0.136283E 01	0.168581E 05	0.457293E 05	0.327425E 02	0.232122E 00	0.121242E 03
11	0.162766E 01	0.232482E 05	0.630630E 05	0.291043E 02	0.229047E 00	0.117604E 03
12	0.210000E 01	0.405355E 05	0.109557E 06	0.376675E 02	0.235065E 00	0.126168E 03
13	0.259159E 01	0.487286E 05	0.132181E 06	0.414182E 02	0.237302E 00	0.129918E 03
14	0.276726E 01	0.657213E 05	0.189128E 06	0.339430E 02	0.232841E 00	0.122443E 03
15	0.309159E 01	0.874465E 05	0.237207E 06	0.358411E 02	0.233975E 00	0.124341E 03
16	0.334735E 01	0.102666E 06	0.278493E 06	0.364285E 02	0.234325E 00	0.124929E 03
17	0.344292E 01	0.108594E 06	0.294545E 06	0.363246E 02	0.234263E 00	0.124825E 03
18	0.357611E 01	0.117100E 06	0.317646E 06	0.361654E 02	0.234168E 00	0.124655E 03
19	0.364391E 01	0.121942E 06	0.330779E 06	0.373464E 02	0.234873E 00	0.125846E 03
20	0.368363E 01	0.124522E 06	0.337777E 06	0.370314E 02	0.234685E 00	0.125531E 03
21	0.375531E 01	0.129752E 06	0.352073E 06	0.381754E 02	0.235368E 00	0.126675E 03
22	0.383009E 01	0.136977E 06	0.371563E 06	0.36706E 02	0.232678E 00	0.122171E 03
23	0.385664E 01	0.144064E 06	0.393789E 06	0.381294E 02	0.235340E 00	0.126629E 03
24	0.415221E 01	0.158707E 06	0.430510E 06	0.392518E 02	0.235413E 00	0.126752E 03
25	0.434912E 01	0.172600E 06	0.470907E 06	0.370803E 02	0.234714E 00	0.125580E 03
26	0.450752E 01	0.186382E 06	0.505579E 06	0.368813E 02	0.234595E 00	0.125381E 03
27	0.359735E 01	0.357388E 06	0.970807E 06	0.561850E 03	0.707252E 00	0.105035E 04
28	0.303629E 01	0.205555E 06	0.557696E 06	0.621785E 03	0.551991E 00	0.710285E 03
29	0.30385E 01	0.180513E 06	0.489660E 06	0.536577E 03	0.509917E 00	0.625477E 03
30	0.256460E 01	0.165962E 06	0.450189E 06	0.463917E 03	0.482912E 00	0.572417E 03
31	0.292478E 01	0.154565E 06	0.420359E 06	0.445967E 03	0.463277E 00	0.534467E 03
32	0.251062E 01	0.151953E 06	0.412187E 06	0.437196E 03	0.458701E 00	0.525696E 03
33	0.309646E 01	0.912358E 05	0.247486E 06	0.515723E 02	0.243347E 00	0.140072E 03
34	0.353761E 01	0.118750E 06	0.322230E 06	0.505611E 02	0.242746E 00	0.139061E 03

## Appendix A (continued)

RUN NO. 310776 7

WATER TEMPERATURE = 88.5C

SYSTEM PRESSURE = 500. TCRR

TEST WIRE LENGTH = 0.720 INCH

SYSTEM RESISTANCE AT SYSTEM TEMPERATURE = .2120 OHM

DATA POINT V. ACROSS SHUNT RESISTOR V. ACROSS TEST WIRE

1	0.0745	0.0720
2	0.1048	0.1030
3	0.1631	0.1635
4	0.1589	0.1970
5	0.2370	0.2354
6	0.2540	0.2940
7	0.3637	0.3681
8	0.4370	0.4446
9	0.4780	0.4854
10	0.5693	0.5805
11	0.6526	0.7073
12	0.7478	0.7645
13	0.8136	0.8315
14	0.8941	0.9135
15	0.9325	0.9631
16	0.5610	0.5900
17	0.8270	2.5340
18	0.7575	2.0440
19	0.7000	1.6540
20	0.6560	1.3500

## RESULTS OF CALCULATION

NO.	CURRENT (AMP)	HEAT FLUX BTU/FT**2HR	KCAL/M**2HR	WALL SUPERHEAT(C)	RESISTANCE OF WIRE (OHM)	WIRE TEMP.(C)
1	0.329646E 00	0.947336E 03	0.256974E 04	0.174295E 02	0.200651E 00	0.105929E 03
2	0.463717E 03	0.188087E 04	0.510205E 04	0.186667E 02	0.201320E 00	0.107167E 03
3	0.721631E 00	0.457444E C4	0.124080E C5	0.202070E 02	0.202153E 00	0.108708E 03
4	0.883389E 00	0.683292E 04	0.185350E 05	0.218556E 02	0.203043E 00	0.110356E 03
5	0.104867E 01	0.973163E 04	0.263991E 05	0.230295E 02	0.203676E 00	0.111529E 03
6	0.137788E 01	0.150878E 05	0.404270E C5	0.258581E 02	0.205202E 00	0.114358E 03
7	0.160629E 01	0.233973E 05	0.634674E C5	0.309317E 02	0.207938E 00	0.119432E 03
8	0.193363E 01	0.339729E C5	0.921549E C5	0.331561E 02	0.209132E 00	0.121656E 03
9	0.211504E 01	0.405629E 05	0.110031E C6	0.323534E 02	0.208700E 00	0.120853E 03
10	0.251903E 01	0.577592E 05	0.156786E C6	0.341145E 02	0.209648E 00	0.122614E 03
11	0.308460E 01	0.856858E 05	0.232442E C6	0.347667E 02	0.209998E 00	0.123267E 03
12	0.330855E 01	0.100012E C6	0.271292E C6	0.352321E 02	0.210249E 00	0.123732E 03
13	0.363000E 01	0.118345E C6	0.321022E C6	0.350912E 02	0.210174E 00	0.123591E 03

## Appendix A (continued)

14	0.355619E 01	0.142876E 06	0.287564E 06	0.349656E 02	0.210105E 00	0.123466E 03
15	0.412611E 01	0.157270E 06	0.426611E 06	0.396399E 02	0.212618E 00	0.128140E 03
16	0.425221E 01	0.166562E 06	0.451816E 06	0.385300E 02	0.212022E 00	0.127030E 03
17	0.365929E 01	0.390775E 06	0.106301E 07	0.105571E 04	0.671685E 00	0.114421E 04
18	0.335177E 01	0.287508E 06	0.779855E 06	0.840854E 03	0.589029E 00	0.929354E 03
19	0.309735E 01	0.213913E 06	0.580261E 06	0.659416E 03	0.513207E 00	0.747916E 03
20	0.290265E 01	0.162639E 06	0.441176E 06	0.504909E 03	0.444293E 00	0.593409E 03

# Appendix A (continued)

RUN NO. 10876 8

WATER TEMPERATURE = 82.7C

SYSTEM PRESSURE = 400. TCRR

TEST WIRE LENGTH = 0.800 INCH

SYSTEM RESISTANCE AT SYSTEM TEMPERATURE = .2030 OHM

DATA POINT V. ACROSS SPUNT RESISTOR V. ACROSS TEST WIRE

1	0.0675	0.0672
2	0.0932	0.0670
3	0.1225	0.1149
4	0.1780	0.1676
5	0.2320	0.2195
6	0.2581	0.2845
7	0.3524	0.3756
8	0.4484	0.4375
9	0.5703	0.5672
10	0.6170	0.6140
11	0.7070	0.7000
12	0.8110	0.8130
13	0.8780	0.8930
14	0.9170	0.9290
15	0.9270	0.9360
16	0.9480	0.9500
17	0.9330	2.5910
18	0.7600	2.0700
19	0.6770	1.5250

## RESULTS OF CALCULATION

NO.	CURRENT (AMP)	HEAT FLUX BTU/FT**2HR	KCAL/M**2HR	WALL SUPERHEAT (C)	RESISTANCE OF WIRE (OHM)	WIRE TEMP. (C)
1	0.258673E 00	0.759832E 03	0.205941E 04	0.142481E 02	0.217544E 00	0.969481E 02
2	0.412399E 00	0.144243E 04	0.391274E 04	0.131893E 02	0.216906E 00	0.953893E 02
3	0.542035E 00	0.250357E 04	0.679119E 04	0.148715E 02	0.217919E 00	0.975715E 02
4	0.787611E 00	0.530582E 04	0.143926E 05	0.162289E 02	0.218736E 00	0.989289E 02
5	0.102655E 01	0.905574E 04	0.245646E 05	0.179373E 02	0.219764E 00	0.100637E 03
6	0.131903E 01	0.150780E 05	0.409006E 05	0.210404E 02	0.221630E 00	0.103740E 03
7	0.173628E 01	0.264727E 05	0.718058E 05	0.259303E 02	0.224568E 00	0.108631E 03
8	0.193407E 01	0.348569E 05	0.945529E 05	0.260629E 02	0.226447E 00	0.111763E 03
9	0.252345E 01	0.574471E 05	0.155831E 06	0.361829E 02	0.230712E 00	0.118833E 03
10	0.273009E 01	0.672784E 05	0.182499E 06	0.364007E 02	0.230842E 00	0.119101E 03
11	0.312832E 01	0.879016E 05	0.238442E 06	0.344964E 02	0.229703E 00	0.117196E 03
12	0.358850E 01	0.117072E 06	0.317569E 06	0.391705E 02	0.232498E 00	0.121870E 03
13	0.368496E 01	0.139164E 06	0.377456E 06	0.447030E 02	0.235802E 00	0.127403E 03
14	0.405752E 01	0.151220E 06	0.410200E 06	0.431892E 02	0.234858E 00	0.125889E 03

## Appendix A (continued)

15	0.410177E 01	C.154034E 06	0.417833E 06	0.419104E 02	0.234135E 00	0.124610E 03
16	0.419469E 01	0.159910E 06	0.433773E 06	0.390356E 02	0.232417E 00	0.121736E 03
17	0.368564E 01	0.376589E 06	0.102153E 07	0.571533E 03	0.708901E 00	0.105423E 04
18	0.336283E 01	0.274824E 06	0.745488E 06	0.774035E 03	0.621493E 00	0.856736E 03
19	0.299557E 01	0.180716E 06	0.490213E 06	0.552930E 03	0.515025E 00	0.635630E 03

## Appendix A (continued)

RUN NO. 1C876 9

WATER TEMPERATURE = 76.0C

SYSTEM PRESSURE = 300. TCRR

TEST WIRE LENGTH = 0.780 INCH

SYSTEM RESISTANCE AT SYSTEM TEMPERATURE = .2020 C/H

DATA POINT V. ACROSS SHUNT RESISTOR V. ACROSS TEST WIRE

1	0.0720
2	0.0766
3	0.1167
4	0.1854
5	0.2436
6	0.3326
7	0.4027
8	0.5063
9	0.6067
10	0.6929
11	0.7630
12	0.8410
13	0.9050
14	0.9590
15	0.9300
16	0.5830
17	0.8490
18	0.7210
19	0.6580
20	0.8750
21	0.8750
22	0.8990

## RESULTS OF CALCULATION

NO.	CURRENT (AMP)	FEAT FLUX BTU/FT**2HR	KCAL/M**2HR	WALL SUPERHEAT (C)	RESISTANCE OF WIRE (OHM)	WIRE TEMP. (C)
1	0.33938E 00	0.568399E 03	0.262688E 04	0.176871E 02	0.210189E 00	0.936871E 02
2	0.547748E 00	0.253687E 04	0.688151E 04	0.187251E 02	0.210799E 00	0.947251E 02
3	0.984371E 00	0.664519E 04	0.183257E 05	0.207630E 02	0.211997E 00	0.967630E 02
4	0.113163E 01	0.105598E 05	0.297295E 05	0.218709E 02	0.212646E 00	0.978709E 02
5	0.152124E 01	0.200841E 05	0.544801E 05	0.282670E 02	0.216398E 00	0.104267E 03
6	0.182522E 01	0.291750E 05	0.751509E 05	0.316712E 02	0.218391E 00	0.107671E 03
7	0.225664E 01	0.453646E 05	0.123056E 06	0.380481E 02	0.222121E 00	0.114948E 03
8	0.269327E 01	0.648055E 05	0.175802E 06	0.400277E 02	0.223277E 00	0.116029E 03
9	0.309584E 01	0.848976E 05	0.230293E 06	0.383581E 02	0.222305E 00	0.114358E 03
10	0.344650E 01	0.107175E 06	0.250722E 06	0.428431E 02	0.224921E 00	0.118843E 03
11	0.369469E 01	0.123351E 06	0.334711E 06	0.436400E 02	0.225384E 00	0.119640E 03

## Appendix A (continued)

12	0.397788E 01	G.142958E 06	0.387787E 06	0.434408E 02	0.225269E 00	0.119441E 03
13	0.406155F 01	0.148229E 06	0.402086E 06	0.412762E 02	0.224007E 00	0.117276E 03
14	0.411504E 01	0.152292E 06	0.413108E 06	0.416872E 02	0.224247E 00	0.117687E 03
15	0.420335E 01	C.158400E 06	0.425676E 06	0.404480E 02	0.223523E 00	0.116448E 03
16	0.434955E 01	0.168905E 06	0.458170E 06	0.388861E 02	0.222611E 00	0.114886E 03
17	0.375664E 01	C.455238E 06	0.123488E 07	0.127057E 04	0.804333E 00	0.134657E 04
18	0.319727E 01	0.252421F 06	0.684719E 06	0.808575E 03	0.618398E 00	0.884575E 03
19	0.291150E 01	0.183614E 06	0.498072E 06	0.638282E 03	0.540092E 00	0.714282E 03
20	0.365044E 01	0.406828E 06	0.110356E 07	0.115442E 04	0.761299E 00	0.123042E 04
21	0.387168E 01	0.486531E 06	0.131976E 07	0.128438E 04	0.809294E 00	0.136038E 04
22	0.397788E 01	0.520736E 06	0.141255E 07	0.131611E 04	0.820561E 00	0.139211E 04

## Appendix A (continued)

RUN NO. 30177 1

WATER TEMPERATURE = 63.0C

SYSTEM PRESSURE = 200. TORR

TEST WIRE LENGTH = 0.860 INCH

SYSTEM RESISTANCE AT SYSTEM TEMPERATURE = .217C CHM

DATA PCINT V. ACROSS SHUNT RESISTOR V. ACROSS TEST WIRE

1	0.0500	0.0500
2	0.0860	0.0860
3	0.1550	0.1550
4	0.2900	0.2940
5	0.3580	0.4080
6	0.6640	0.7100
7	0.7670	0.8600
8	0.8550	0.5350
9	0.8960	1.0070
10	0.8940	1.0030
11	0.7650	2.6000
12	0.7110	2.0100
13	0.7500	2.5800
14	0.8280	3.2700
15	0.8520	3.5800

## RESULTS OF CALCULATION

NO.	CURRENT (AMP)	BTU/FT**2HR	HEAT FLUX KCAL/M**2HR	WALL SUPERHEAT(C)	RESISTANCE OF WIRE (OHM)	WIRE TEMP.(C)
1	0.221239E 03	0.393045E 03	0.106617E 04	0.137803E 02	0.223759E 00	0.767803E 02
2	0.263531E 03	0.116278E 04	0.315417E 04	0.137803E 02	0.220759E 00	0.767803E 02
3	0.683341E 00	0.377716E 04	0.102459E 05	0.137803E 02	0.220759E 00	0.767803E 02
4	0.128319E 01	0.134387E 05	0.363725E 05	0.185690E 02	0.223877E 00	0.815690E 02
5	0.176104E 01	0.255445E 05	0.692921E 05	0.225081E 02	0.226438E 00	0.855081E 02
6	0.253905E 01	0.742328E 05	0.201364E 06	0.378995E 02	0.236416E 00	0.100899E 03
7	0.339381E 01	0.103970E 06	0.292030E 06	0.561129E 02	0.248162E 00	0.119113E 03
8	0.37819E 01	0.125939E 06	0.341623E 06	0.463996E 02	0.241906E 00	0.109400E 03
9	0.392335E 01	0.139672E 06	0.378874E 06	0.587204E 02	0.249838E 00	0.121720E 03
10	0.39575E 01	0.141338E 06	0.383394E 06	0.563489E 02	0.248314E 00	0.119349E 03
11	0.33456E 01	0.217946E 06	0.862459E 06	0.992978E 03	0.762864E 00	0.105598E 04
12	0.314602E 01	0.228129E 06	0.618922E 06	0.725176E 03	0.633662E 00	0.788176E 03
13	0.349557E 01	0.376579E 06	0.102151E 07	0.118642E 04	0.847266E 00	0.124942E 04
14	0.368372E 01	0.43224E 06	0.117516E 07	0.128475E 04	0.887295E 00	0.134775E 04
15	0.376991E 01	0.488215E 06	0.132433E 07	0.143406E 04	0.944384E 00	0.149706E 04



## Appendix A (continued)

RUN NO. 30177 2

WATER TEMPERATURE = 63.0C

SYSTEM PRESSURE = 200. TORR

TEST WIRE LENGTH = 0.860 INCH

SYSTEM RESISTANCE AT SYSTEM TEMPERATURE = .2170 OHM

DATA POINT V. ACROSS SHUNT RESISTOR V. ACROSS TEST WIRE

1	0.0450	0.0450
2	0.0870	0.0870
3	0.1550	0.1550
4	0.2740	0.2770
5	0.3620	0.4000
6	0.6700	0.7100
7	0.7680	0.8340
8	0.8530	0.9240
9	0.5450	1.0250
10	1.0150	1.1100

## RESULTS OF CALCULATION

NO.	CURRENT (AMP)	HEAT FLUX BTL/FT**2HR	KCAL/M**2HR	WALL SUPERHEAT (C)	RESISTANCE OF WIRE (OHM)	WIRE TEMP. (C)
1	0.199115E 00	0.318366E 03	0.863600E 03	0.137803E 02	0.220759E 00	0.767803E 02
2	0.384956E 00	0.118558E 04	0.322755E 04	0.137803E 02	0.220759E 00	0.767803E 02
3	0.695841E 00	0.377716E 04	0.102459E 05	0.137803E 02	0.220759E 00	0.767803E 02
4	0.121239E 01	0.115355E 05	0.323765E 05	0.175794E 02	0.223234E 00	0.805794E 02
5	0.173451E 01	0.246635E 05	0.669021E 05	0.208660E 02	0.223372E 00	0.838660E 02
6	0.256460E 01	0.748886E 05	0.203143E 06	0.345561E 02	0.234252E 00	0.975561E 02
7	0.339823E 01	0.100889E 06	0.273672E 06	0.437266E 02	0.240181E 00	0.106727E 03
8	0.377434E 01	0.124141E 06	0.336744E 06	0.427788E 02	0.239571E 00	0.105779E 03

## Appendix A (continued)

RUN NO. 270277 1

WATER TEMPERATURE = 59.0C

SYSTEM PRESSURE = 760. TORR

TEST WIRE LENGTH = 0.800 INCH

SYSTEM RESISTANCE AT SYSTEM TEMPERATURE = .2340 OHM

DATA POINT V. ACROSS SHUNT RESISTOR V. ACROSS TEST WIRE

1	0.0440	0.047C
2	0.0540	0.1010
3	0.1860	0.2000
4	0.2570	0.3200
5	0.3540	0.4270
6	0.4880	0.534C
7	0.5850	0.6400
8	0.6850	0.7600
9	0.7840	0.8660
10	0.8270	0.9250
11	0.9020	1.008C
12	0.9430	1.0610
13	0.9580	1.0900
14	0.8200	2.70CC
15	0.8570	2.8800

## RESULTS OF CALCULATION

NO.	CURRENT (AMP)	HEAT FLUX BTL/FT**2HR	KCAL/M**2HR	WALL SUPERHEAT (C)	RESISTANCE OF WIRE (OHM)	WIRE TEMP. (C)
1	0.194690E 00	0.335247E 03	0.909390E 03	0.123297E 02	0.226187E 00	0.111330E 03
2	0.415929E 00	0.153969E 04	0.417657E C4	0.146580E 02	0.227607E 00	0.113698E 03
3	0.823009E 00	0.603322E 04	0.163657E C5	0.150019E 02	0.227788E 00	0.114002E 03
4	0.131416E 01	0.154160E 05	0.418174E 05	0.158216E 02	0.228279E 00	0.114822E 03
5	0.174336E 01	0.272957E C5	0.740531E C5	0.182026E 02	0.229707E 00	0.117203E 03
6	0.215929E 01	0.423127E 05	0.114777E 06	0.221722E 02	0.232081E 00	0.121172E 03
7	0.258850E C1	0.607909E 05	0.164901E 06	0.220801E 02	0.232025E 00	0.121080E 03
8	0.303057E 01	0.846066E 05	0.229504E 06	0.275351E 02	0.235522E 00	0.126935E 03
9	0.346903E 01	0.110309E 06	0.259223E 06	0.260786E 02	0.236415E 00	0.125079E 03
10	0.365929E C1	0.128387E C6	0.337411E C6	0.213490E 02	0.237559E 00	0.130349E 03
11	0.399115E 01	0.147832E 06	0.401009E 06	0.209764E 02	0.237336E 00	0.129976E 03
12	0.417257E 01	0.162749E C6	0.441472E 06	0.338620E 02	0.239057E 00	0.132862E 03
13	0.423894E 01	0.169577E 06	0.461078E 06	0.386687E 02	0.241917E 00	0.137669E 03
14	0.362832E 01	0.375233E 06	0.101786E 07	0.100293E 04	0.728924E 00	0.110193E 04
15	0.379204E 01	0.418486E 06	0.113518E C7	0.104016E 04	0.744264E 00	0.113918E 04

# Appendix A (continued)

RUN NO. 91276 1

WATER TEMPERATURE = 98.0C

SYSTEM PRESSURE = 760. TCRR

TEST WIRE LENGTH = 0.920 INCH

SYSTEM RESISTANCE AT SYSTEM TEMPERATURE = .2590 OHM

DATA POINT V. ACROSS SHUNT RESISTOR V. ACROSS TEST WIRE

1	0.3017	0.3466
2	0.3990	0.4640
3	0.4590	0.5840
4	0.5910	0.7000
5	0.6710	0.8010
6	0.8090	0.9770
7	0.9680	1.1130
8	0.9760	1.2080
9	1.0130	1.2570
10	1.0400	1.2990
11	1.0650	1.3350
12	1.0750	1.3660
13	1.0810	1.3750
14	1.1090	1.4100
15	0.9080	3.5000
16	0.8220	2.8000
17	0.8050	2.0800
18	0.9230	3.7100
19	0.9370	3.6400
20	0.9500	3.5800

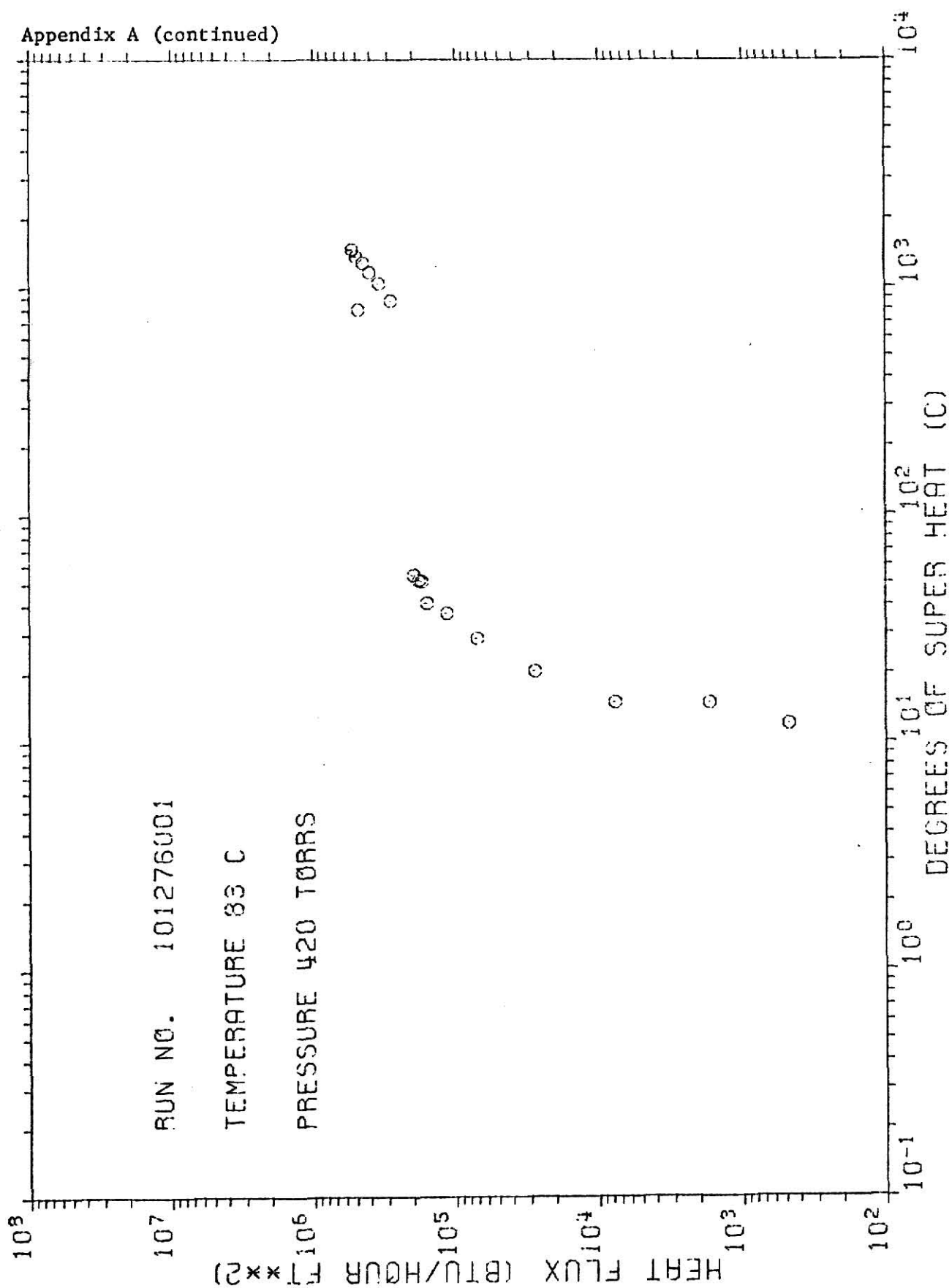
## RESULTS OF CALCULATION

NC.	CURRENT (AMP)	HEAT FLUX BTU/FT**2HR	KCAL/M**2HR	WALL SUPERHEAT (C)	RESISTANCE OF WIRE (OHM)	WIRE TEMP. (C)
1	0.133496E 01	0.152421E 05	0.413457E 05	0.513467E 00	0.251536E 00	0.989135E 02
2	0.176549E 01	0.269561E 05	0.732295E 05	0.551564E 01	0.254715E 00	0.103516E 03
3	0.220756E 01	0.425022E 05	0.115291E 06	0.794492E 01	0.256399E 00	0.105945E 03
4	0.261504E 01	0.603595E 05	0.163731E 06	0.125584E 02	0.255584E 00	0.110558E 03
5	0.256903E 01	0.784370E 05	0.212768E 06	0.156089E 02	0.261687E 00	0.113609E 03
6	0.357965E 01	0.115385E 06	0.313004E 06	0.201778E 02	0.264834E 00	0.118178E 03
7	0.401770E 01	0.147604E 06	0.400390E 06	0.261299E 02	0.268926E 00	0.124130E 03
8	0.431858E 01	0.172250E 06	0.467245E 06	0.300603E 02	0.271623E 00	0.128060E 03
9	0.448230E 01	0.186046E 06	0.504668E 06	0.311025E 02	0.272338E 00	0.129102E 03
10	0.460177E 01	0.197425E 06	0.535536E 06	0.337967E 02	0.274184E 00	0.131797E 03
11	0.473009E 01	0.206553E 06	0.565721E 06	0.337264E 02	0.274137E 00	0.131726E 03
12	0.475664E 01	0.214703E 06	0.582404E 06	0.409453E 02	0.279079E 00	0.138945E 03
13	0.478318E 01	0.217330E 06	0.589530E 06	0.413688E 02	0.279367E 00	0.139369E 03

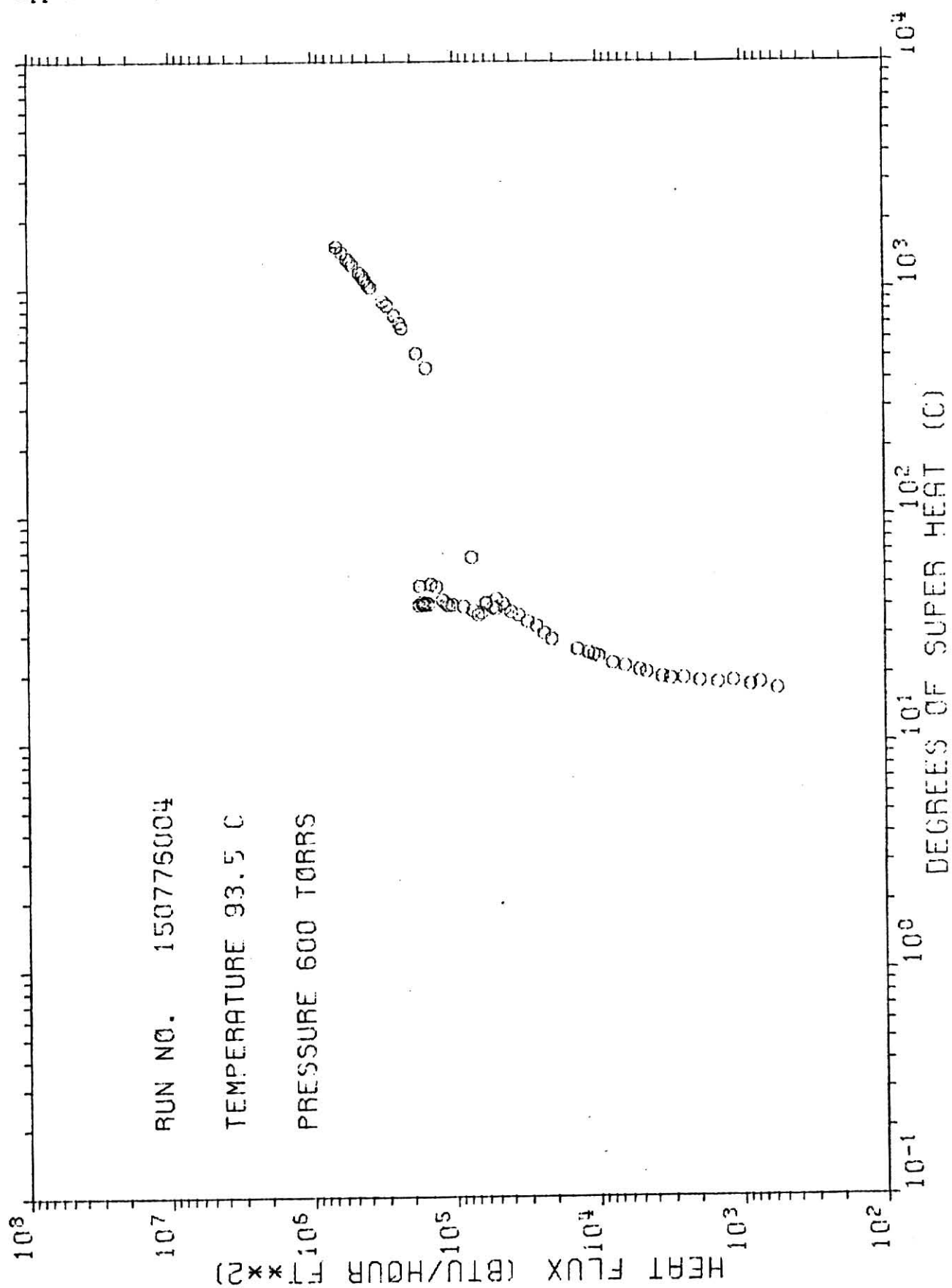
## Appendix A (continued)

14	0.460701E 01	0.228632E 06	0.620187E 06	0.411829E 02	0.279242E 00	0.139183E 03
15	0.470177E 01	0.473638E 06	0.123455E 07	0.105644E 04	0.863047E 00	0.115444E 04
16	0.503717E 01	0.342631E 06	0.929448E 06	0.845072E 03	0.761731E 00	0.947072E 03
17	0.356105E 01	0.248425E 06	0.673979E 06	0.509332E 03	0.575852E 00	0.607332E 03
18	0.404407E 01	0.510609E 06	0.138508E 07	0.113788E 04	0.900309E 00	0.123586E 04
19	0.414402E 01	0.536610E 06	0.145561E 07	0.117785E 04	0.919091E 00	0.127585E 04
20	0.420334E 01	0.563993E 06	0.152990E 07	0.122525E 04	0.938723E 00	0.132325E 04

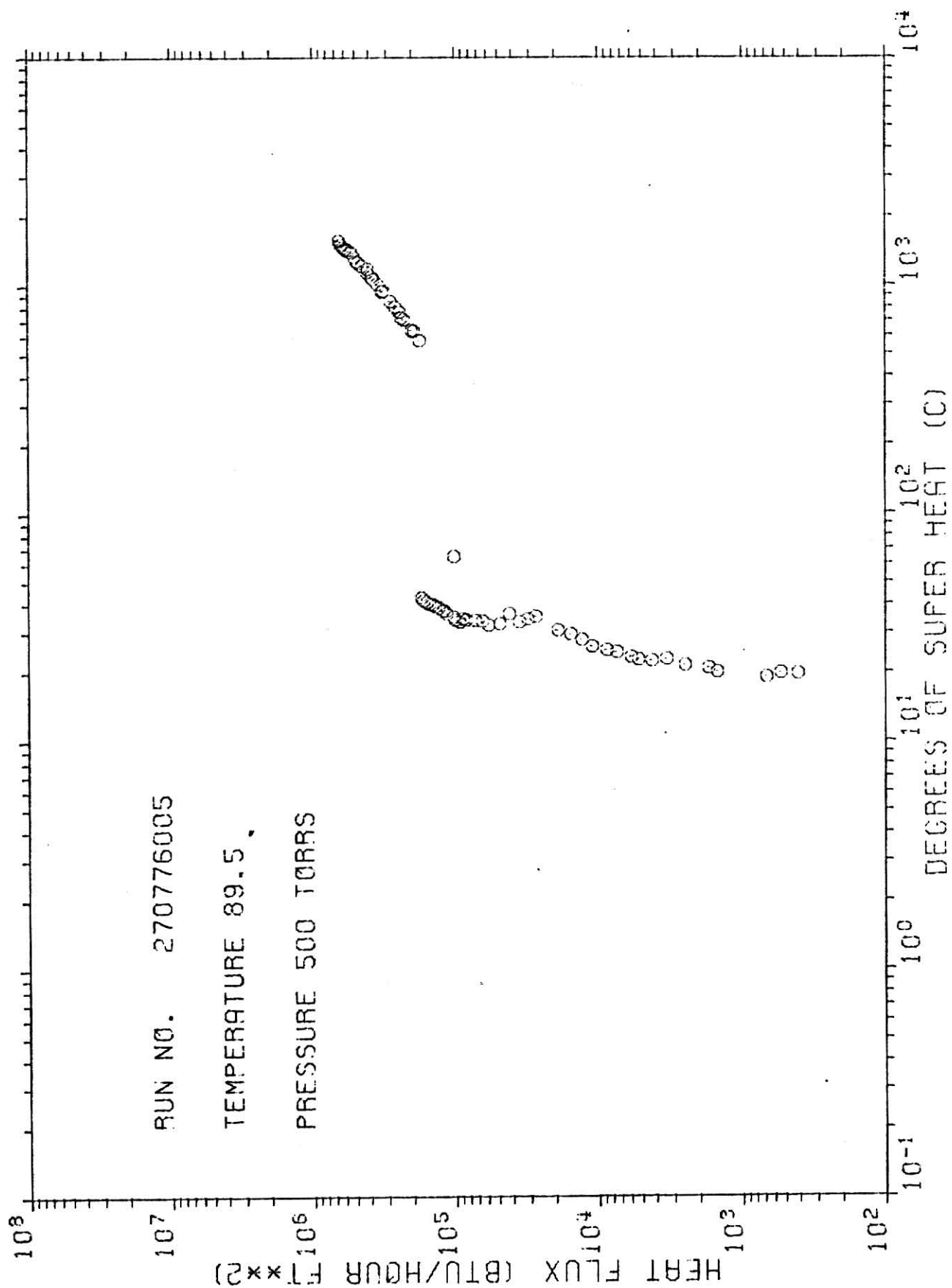
## Appendix A (continued)



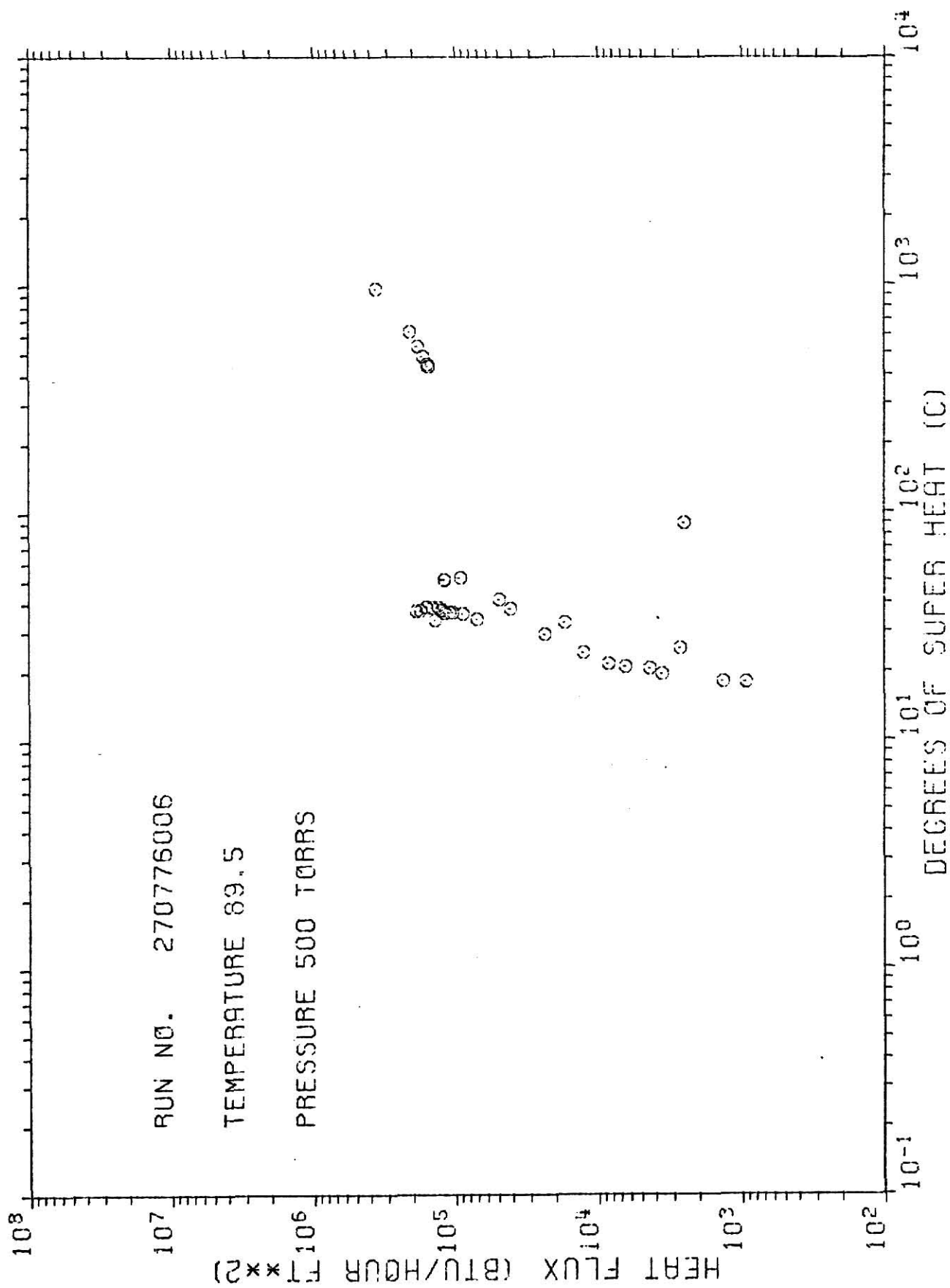
## Appendix A (continued)



## Appendix A (continued)

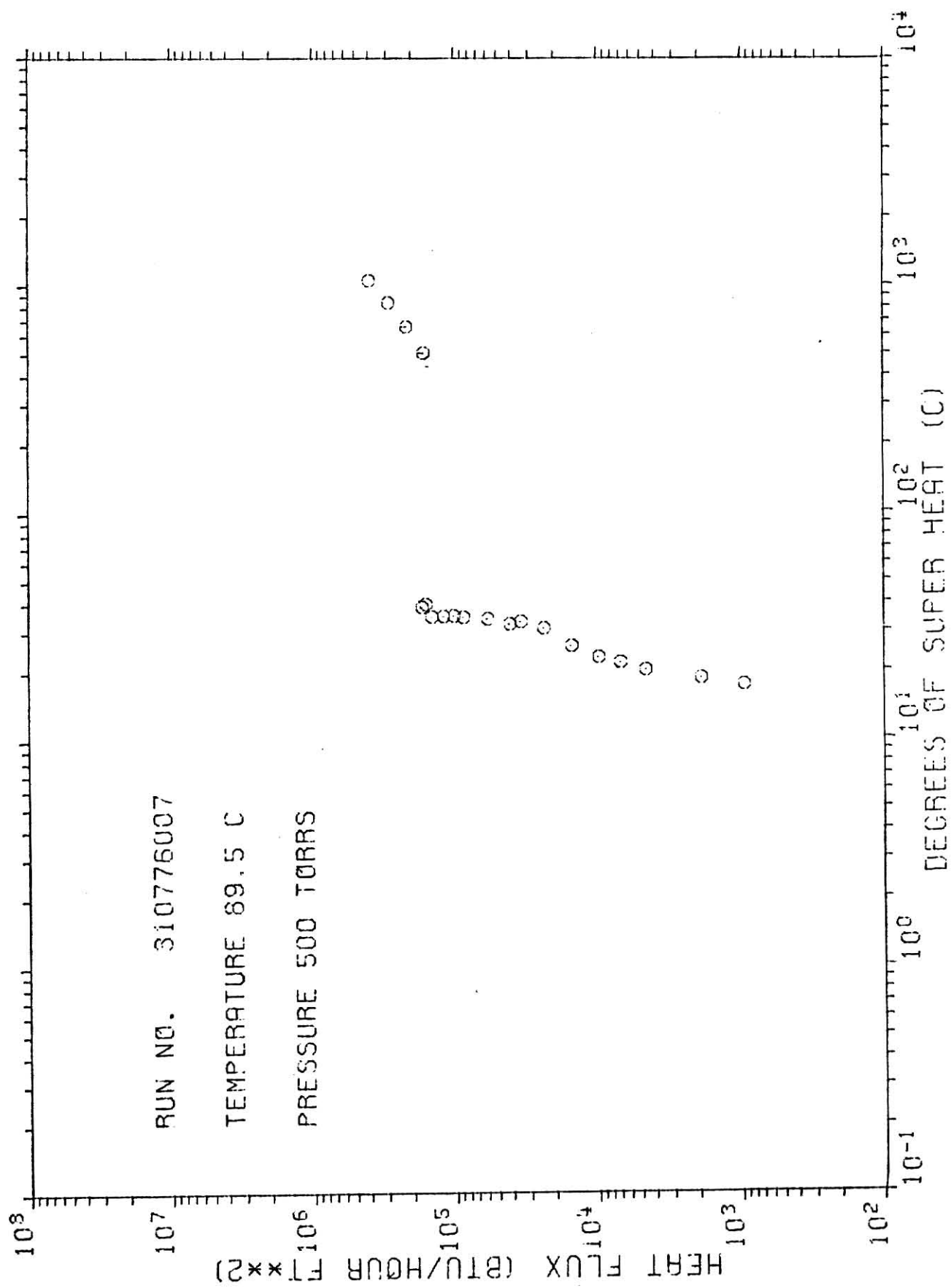


## Appendix A (continued)

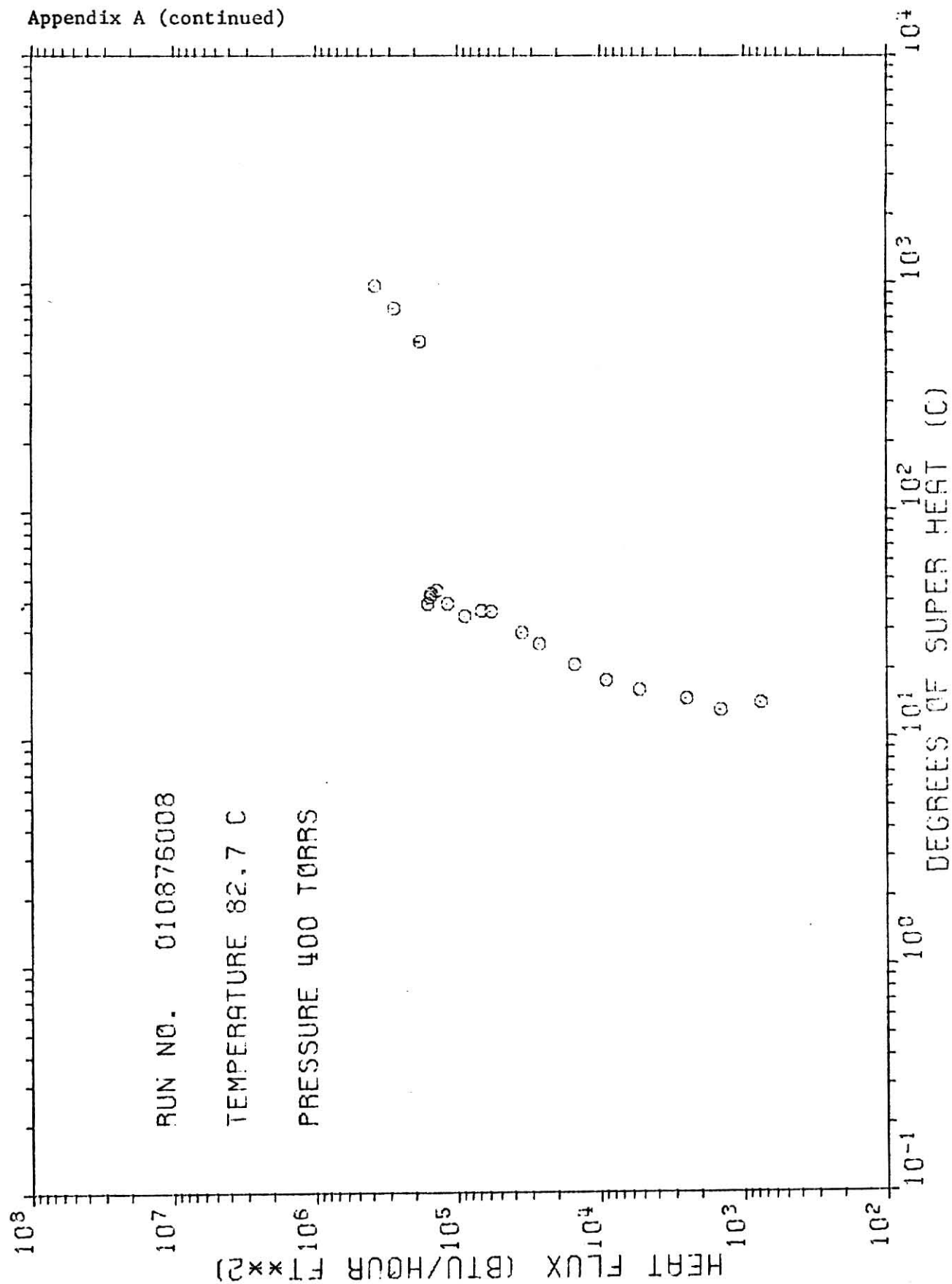




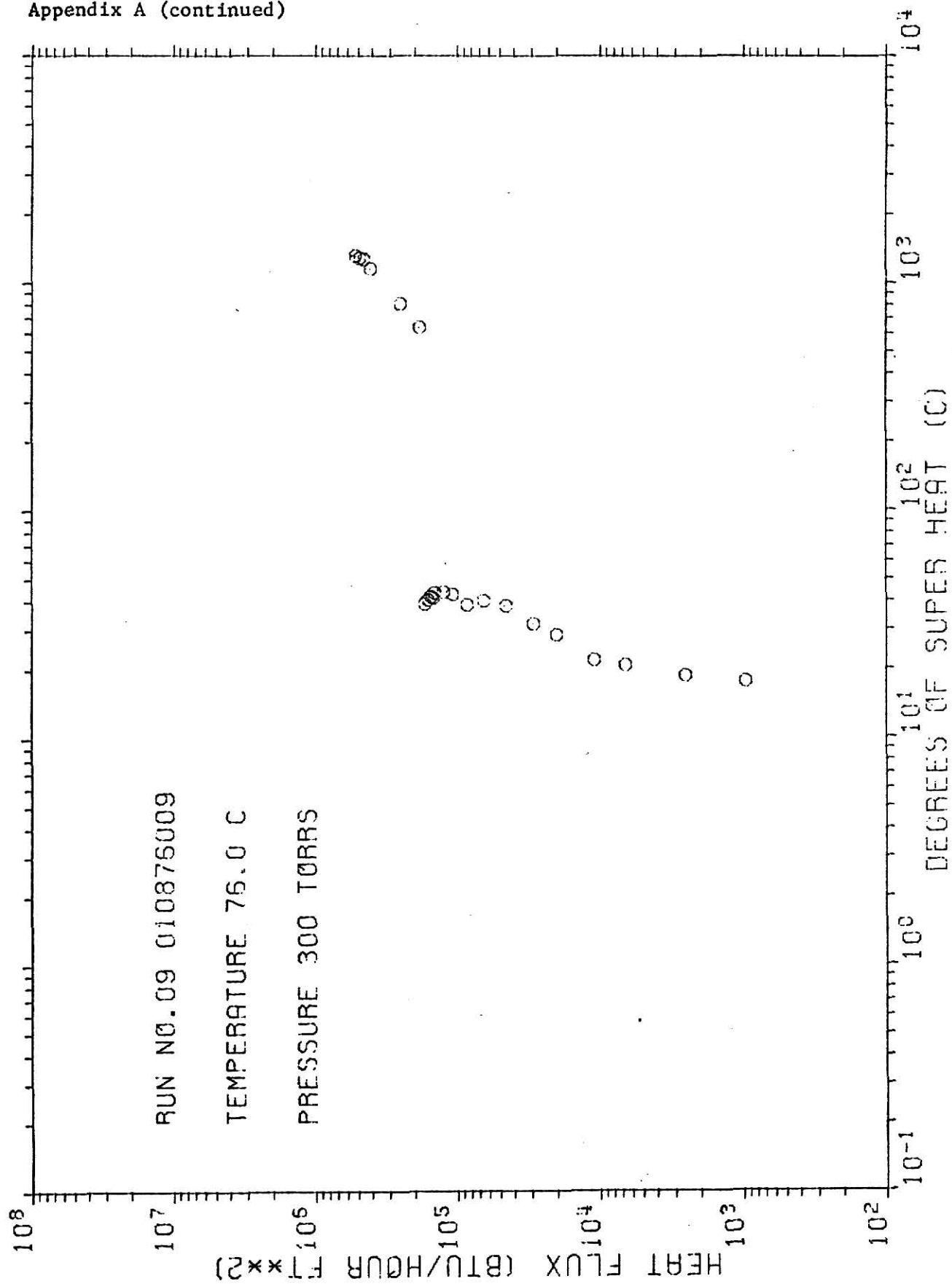
## Appendix A (continued)



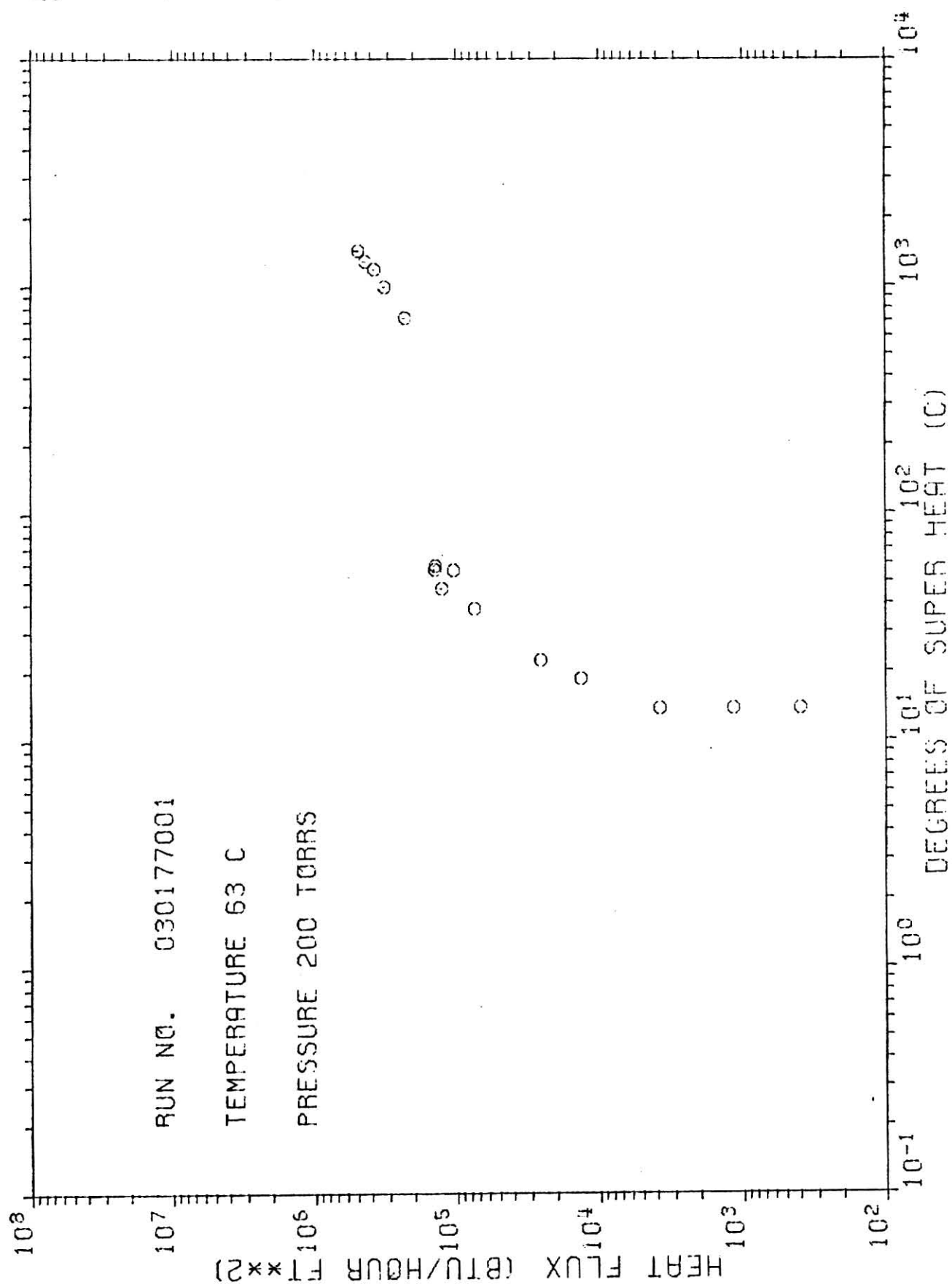
## Appendix A (continued)

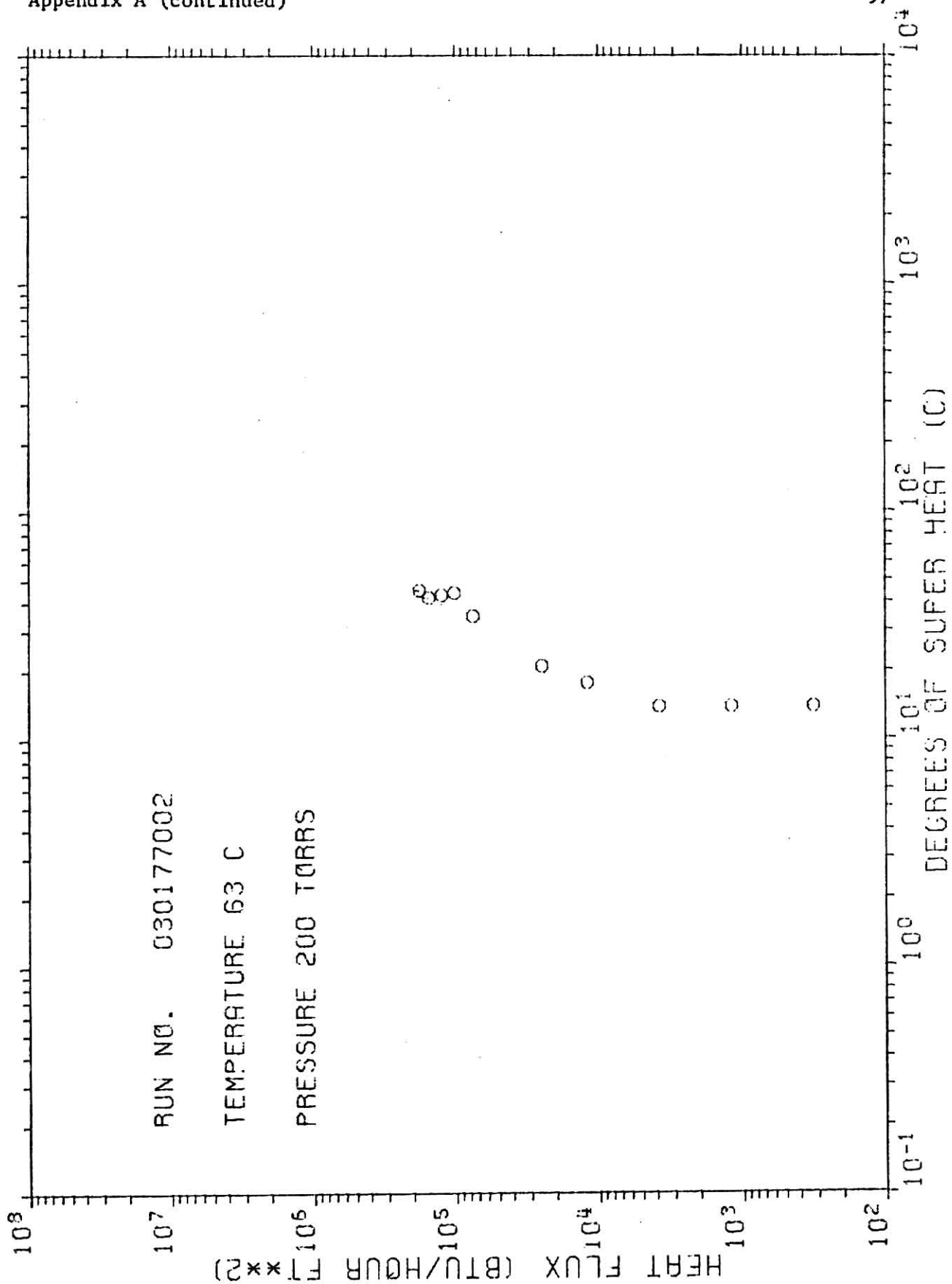


## Appendix A (continued)

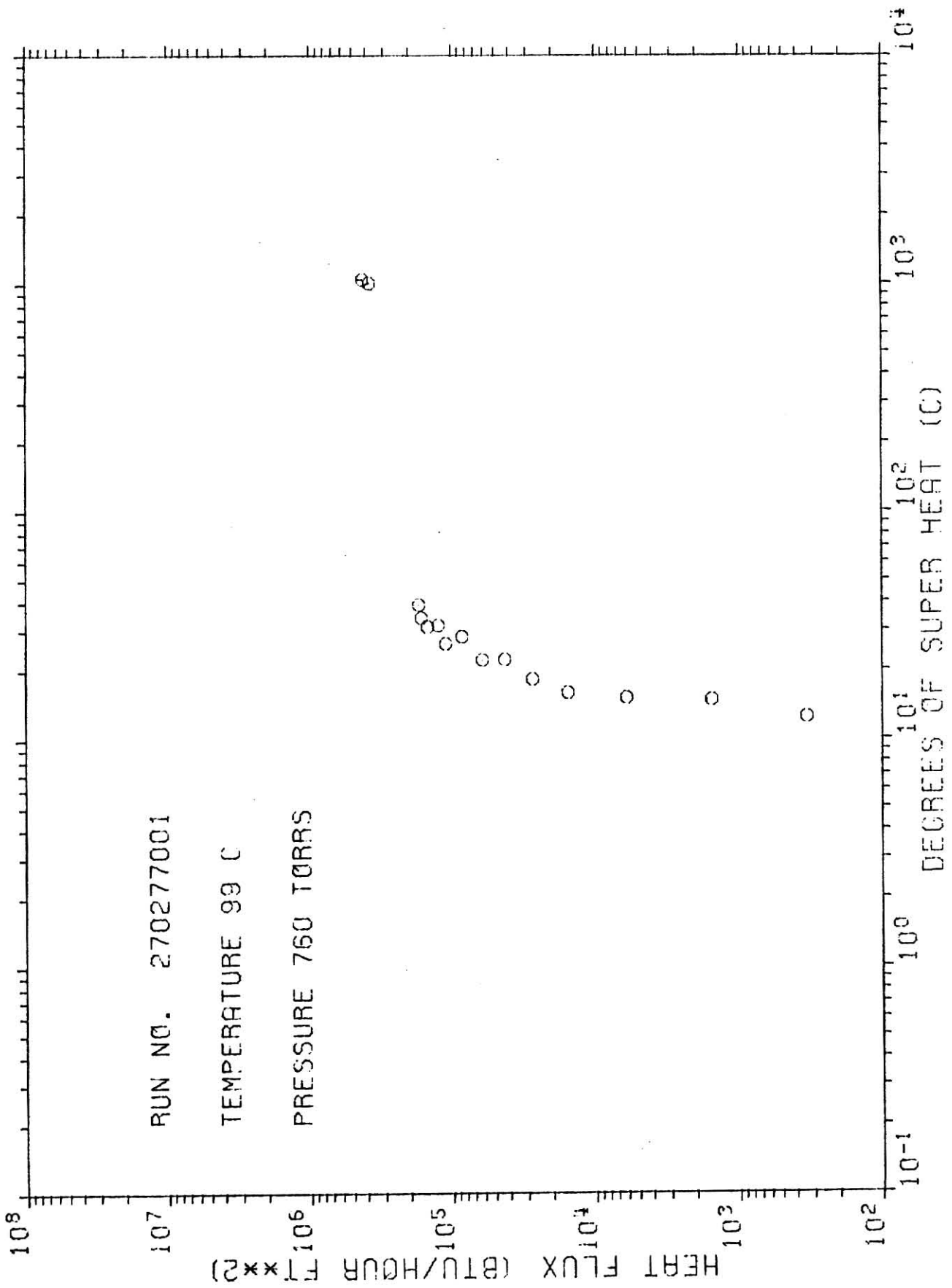


## Appendix A (continued)





Appendix A (continued)





## Appendix B (continued)

PDA NO.	INITIAL HEAT FLUX		WATER TEMP.	INITIAL WIRE TEMP.		INITIAL WIRE TEMP. DROP
	(KCAL/HP **2)	(BTU/FT**2 HR)	(C)	(C)	(C)	(C)
83	0.289017E 06	0.106561E 06	70.00	141.40	7.94	
83	0.295545E 06	0.110444E 06	84.00	150.20	13.68	
89	0.293842E 06	0.108340E 06	79.00	148.24	12.55	
80	0.291878E 06	0.107615E 06	74.00	145.42	8.42	
93	0.299017E 06	0.106541E 06	70.00	141.40	8.51	
84	0.290766E 06	0.107021E 06	69.50	143.10	14.12	
60	0.394346E 06	0.143395E 06	75.00	169.59	19.23	
61	0.390912E 06	0.145109E 06	77.00	169.07	7.09	
62	0.391844E 06	0.144473E 06	79.00	166.01	8.16	
64	0.354575E 06	0.145627E 06	82.00	170.46	10.10	
78	0.553473E 06	0.204045E 06	79.00	167.18	10.16	
79	0.551273E 06	0.203256E 06	74.50	172.13	12.14	
80	0.565476E 06	0.209966E 06	69.00	173.17	11.03	
81	0.525982E 06	0.193930E 06	50.00	150.37	8.50	
55	0.244266E 06	0.900609E 05	88.00	81.27	12.52	
54	0.243077E 06	0.896225E 05	85.00	78.70	15.95	
53	0.245890E 06	0.906555E 05	84.00	81.63	1.94	
56	0.246784E 06	0.90891E 05	90.00	82.99	13.80	
45	0.391547E 06	0.144363E 06	84.00	166.82	18.34	
65	0.396326E 06	0.146126E 06	86.00	172.02	16.51	
67	0.370133E 06	0.136468E 06	88.00	143.85	16.17	
63	0.366477E 06	0.146391E 06	90.00	171.46	12.89	
62	0.395875E 06	0.150680E 06	86.00	184.30	9.78	
56	0.388257E 06	0.143165E 06	82.50	161.34	16.48	
57	0.394543E 06	0.141781E 06	90.00	157.45	15.67	
82	0.550179E 06	0.206538E 06	83.50	172.42	24.09	
83	0.546455E 06	0.201479E 06	86.00	162.01	9.83	



## Appendix B (continued)

85	0.541851E 06	0.159780E 06	50.00	158.61	13.49
87	0.543234E 06	0.200290E 06	88.00	159.61	1.86
100	0.547489E 06	0.201859E 06	91.00	158.83	6.86
101	0.507739E 06	0.187203E 06	85.00	141.04	7.54
102	0.527588E 06	0.194669E 06	92.00	151.29	6.52
103	0.493047E 06	0.182524E 06	90.00	128.93	11.82
105	0.550590E 06	0.203150E 06	88.00	168.04	2.19

BOILING HEAT TRANSFER PHENOMENA  
DURING RAPID DECOMPRESSION

by

Shin-Ping Kung

B.S., National Tsing Hua University, 1972

---

AN ABSTRACT OF A MASTER'S THESIS

submitted in partial fulfillment of the  
requirement for the degree

MASTER OF SCIENCE

Department of Nuclear Engineering

KANSAS STATE UNIVERSITY

Manhattan, Kansas

1977

## ABSTRACT

Results of an experimental study of the temporal behavior of the transient behavior of local boiling under rapid decompression are presented. Specifically, the heat transfer from a thin wire heating element to water during and shortly after the decompression is discussed. The fast pressure transient is observed to cause an initial heater temperature drop and delay the boiling transition in both totally subcooled depressurization and depressurization with flashing. Flashing, which has been considered responsible for the enhanced heat transfer during and after a pressure transient, is found to be of questionable importance in this experiment, since at this rapid decompression rate, flashing does not become significant until the decompression is complete.